Persoonia 48, 2022: 54–90
www.ingentaconnect.com/content/nhn/pimj

RESEARCH ARTICLE

ISSN (Online) 1878-9080
https://doi.org/10.3767/persoonia.2022.48.02

Eight new *Halophytophthora* species from marine and brackish-water ecosystems in Portugal and an updated phylogeny for the genus

C. Maia[1], M. Horta Jung[2,3], G. Carella[4], I. Milenković[2], J. Janoušek[2], M. Tomšovský[2], S. Mosca[5], L. Schena[5], A. Cravador[6], S. Moricca[4], T. Jung[2,3,*]

Key words

breeding system
ecological role
evolution
lifestyle
oomycetes
Peronosporaceae
Phytophthora

Abstract During an oomycete survey in December 2015, 10 previously unknown *Halophytophthora* taxa were isolated from marine and brackish water of tidal ponds and channels in saltmarshes, lagoon ecosystems and river estuaries at seven sites along the Algarve coast in the South of Portugal. Phylogenetic analyses of LSU and ITS datasets, comprising all described *Halophytophthora* species, the 10 new *Halophytophthora* taxa and all relevant and distinctive sequences available from GenBank, provided an updated phylogeny of the genus *Halophytophthora* s.str. showing for the first time a structure of 10 clades designated as Clades 1–10. Nine of the 10 new *Halophytophthora* taxa resided in Clade 6 together with *H. polymorphica* and *H. vesicula*. Based on differences in morphology and temperature-growth relations and a multigene (LSU, ITS, *Btub*, *hsp90*, *rpl10*, *tigA*, *cox1*, *nadh1*, *rps10*) phylogeny, eight new *Halophytophthora* taxa from Portugal are described here as *H. brevisporangia*, *H. celeris*, *H. frigida*, *H. lateralis*, *H. lusitanica*, *H. macrosporangia*, *H. sinuata* and *H. thermoambigua*. Three species, *H. frigida*, *H. macrosporangia* and *H. sinuata*, have a homothallic breeding system while the remaining five species are sterile. Pathogenicity and litter decomposition tests are underway to clarify their pathological and ecological role in the marine and brackish-water ecosystems. More oomycete surveys in yet undersurveyed regions of the world and population genetic or phylogenomic analyses of global populations are needed to clarify the origin of the new *Halophytophthora* species.

Citation: Maia C, Horta Jung M, Carella G, et al. 2022. Eight new Halophytophthora species from marine and brackish-water ecosystems in Portugal and an updated phylogeny for the genus. Persoonia 48: 54–90. https://doi.org/10.3767/persoonia.2022.48.02.
Effectively published online: 20 March 2022 [Received: 4 November 2021; Accepted: 25 January 2022].

INTRODUCTION

The aquatic genus *Halophytophthora* is a sister genus to *Phytophthora* and *Nothophytophthora* within the *Peronosporaceae*, class *Oomycota*, kingdom *Straminipila*. The first species, originally described as *Phytophthora vesicula*, was discovered in 1969 in a marine habitat near Vancouver (Anastasiou & Churchland 1969). In 1990, Ho & Jong transferred *P. vesicula* together with eight other marine *Phytophthora* species, i.e., *P. avicennae*, *P. bahamensis*, *P. batemanensis*, *P. epistomium*, *P. mycoparasitica*, *P. operculata*, *P. polymorphica* and *P. spinosa* (Fell & Master 1975, Pegg & Alcorn 1982, Gerrettson-Cornell & Simpson 1984), to the newly established genus *Halophytophthora*. Between 1990 and 2003 a further six *Halophytophthora* species were described, including *H. elongata*, *H. exoprolifera*, *H. kandeliae*, *H. masteri*, *H. porrigovesica* and *H. tartarea* (Ho et al. 1991, 1992, 2003, Nakagiri et al. 1994, 2001). However, recent phylogenetic studies revealed the polyphyletic nature of *Halophytophthora* (Lara & Belbahri 2011, Nigrelli & Thines 2013, Jung et al. 2017d) causing a reassignment of numerous *Halophytophthora* species to other genera. *Halophytophthora kandeliae* was transferred to *Phytopythium* (Thines 2014), *H. tartarea* to *Salisapilia* (Hulvey et al. 2010), *H. spinosa* to *Salispina* (Li et al. 2016) and *H. operculata* to *Calycofera*, a genus established to accommodate this species (Bennett et al. 2017a). Furthermore, *H. exoprolifera* was shown to belong to a yet undescribed sister genus of *Halophytophthora* s.str. (Jung et al. 2017d). Recently, Bennet & Thines (2019) revised *Salisapilia* and included another five *Halophytophthora* species, *H. bahamensis*, *H. elongata*, *H. epistomia*, *H. masteri* and *H. mycoparasitica*. Currently, *Halophytophthora* s.str. comprises seven described species, *H. avicennae*, *H. batemanensis*, *H. fluviatilis*, *H. insularis*, *H. polymorphica*, *H. souzae* and *H. vesicula* (Yang & Hong 2014, Jung et al. 2017d, Bennet & Thines 2019, Jesus et al. 2019), and the informally designated taxa *Halophytophthora* sp. Zostera (Govers et al. 2016), *Halophytophthora* sp. 1 and 2 (Nigrelli & Thines 2013), and *Halophytophthora* sp-1 and sp-3 (Man in 't Veld et al. 2019) from the North Sea, *Halophytophthora* sp. 1 and 2 from Georgia, USA (Hulvey et al. 2010) and *Halophytophthora* sp-4 from Southern France (Man in 't Veld et al. 2019). The phylogenetic position and taxonomic status of *H. porrigovesica*, originally described

[1] Centre of Marine Sciences (CCMAR), University of Algarve, 8005-139 Faro, Portugal.
[2] Mendel University in Brno, Faculty of Forestry and Wood Technology, Department of Forest Protection and Wildlife Management, Phytophthora Research Centre, 613 00 Brno, Czech Republic; corresponding author e-mail: thomas.jung@mendelu.cz, dr.t.jung@gmail.com.
[3] Phytophthora Research and Consultancy, 83131 Nußdorf, Germany.
[4] University of Florence, Department of Agri-Food Production and Environmental Sciences, Plant Pathology and Entomology Division, 50144 Florence, Italy.
[5] Dipartimento di Agraria, Università Mediterranea di Reggio Calabria, 89122 Reggio Calabria, Italy.
[6] Mediterranean Institute for Agriculture, Environment and Development (MED), University of Algarve, 8005-139 Faro, Portugal.

from mangrove stands in Japan and Thailand (Nakagiri et al. 2001), is unclear.

Although *Halophytophthora* species are mainly found in marine, mangrove and estuarine habitats, from the tropics to the south-eastern bight of the North Sea (Nigrelli & Thines 2013), they are well adapted to a wide range of temperature and salinity with some species occurring in low salinity and even freshwater habitats (Nakagiri 2000, Reeser et al. 2011, Hüberli et al. 2013, Yang & Hong 2014, Caballol et al. 2021). *Halophytophthora* species share many features of their morphology and lifecycle with *Phytophthora* (Sullivan et al. 2018). In contrast to *Phytophthora*, which comprises primary plant pathogens (Erwin & Ribeiro 1996, Lamour 2013, Jung et al. 2018), *Halophytophthora* species are usually considered as saprophytes, playing an important role in decomposition and secondary production (Nakagiri 2000). However, recent studies (Govers et al. 2016, Man in 't Veld et al. 2019) suggested that several marine *Phytophthora* and *Halophytophthora* species, including *Halophytophthora* sp. Zostera, might be involved in the widespread decline of the seagrass *Zostera marina* (eelgrass), an important marine foundation species that has been suffering from recurring wasting disease outbreaks since 1930 (Muehlstein et al. 1988). Almost 99 % of tested *Z. marina* seeds were infected, resulting in reduced germination rates and devastating consequences for restauration efforts (Govers et al. 2016).

Fig. 1 Sampling sites along the Algarve coast in the South of Portugal; a. tidal zone of the Rio Séqua near the estuary in Tavira; b–d. Parque Natural da Ria Formosa; b. saltmarsh near Almancil during high tide with flooded tidal channels and ponds; c. tidal channel in a saltmarsh near Santa Luzia during low tide, with baiting raft; d. saltwater pond in a saltmarsh near Quelfes during low tide, with baiting raft; e. marine lagoon in Ria de Alvor, with baiting raft (arrow) floating among the marine algal vegetation; f. baiting raft tied to an iron stick in the estuary of the Rio Guadiana near Sapal de Castro Marim.

Despite being known since more than 50 years, knowledge on the diversity, distribution and ecology of *Halophytophthora* species is still scarce. Therefore, in December 2015, a survey was carried out in marine and brackish-water ecosystems along the Algarve coast in the South of Portugal which unveiled a high diversity of *Halophytophthora* species, most of them new to science.

In this study, morphological and physiological characteristics were used in combination with DNA sequence data from six nuclear and three mitochondrial gene regions to characterise and officially describe eight new *Halophytophthora* species from the Algarve as *H. brevisporangia* sp. nov., *H. celeris* sp. nov., *H. frigida* sp. nov., *H. lateralis* sp. nov., *H. lusitanica* sp. nov., *H. macrosporangia* sp. nov., *H. sinuata* sp. nov. and *H. thermoambigua* sp. nov.

MATERIAL AND METHODS

Sampling and Halophytophthora isolation

Sampling was performed in December 2015 at seven different marine and brackish-water sites, including tidal ponds and channels in saltmarshes which did not dry out during low tides, lagoons and river estuaries (Fig. 1), along the Algarve coast in the South of Portugal using a leaf baiting method adopted from Jung et al. (2017a). Fly mesh and styrofoam were used to create 25 × 30 cm baiting-bag rafts able to float on the water surface. Unwounded leaves of *Ceratonia siliqua*, *Quercus suber*, *Q. rubra* and *Citrus* spp. were placed inside the rafts and used as baits. Two rafts were placed on each site and collected after three to six days. The leaves were washed with distilled water, blotted dry and 2 × 2 mm pieces of discoloured and/or necrotic tissues were plated onto selective PARPNH agar (V8 juice agar (V8A) amended with 10 µg/mL pimaricin, 200 µg/mL ampicillin, 10 µg/mL rifampicin, 25 µg/mL pentachloronitrobenzene, 50 µg/mL nystatin and 50 µg/mL hymexazol) and incubated at 20 °C in the dark (Jung et al. 1996). After 16 to 48 h, Petri dishes were observed under the dissecting microscope and axenic cultures obtained by transferring single hyphal tips to V8 juice agar (V8A; 16 g agar, 3 g $CaCO_3$, 100 mL Campbell's V8 juice, 900 mL distilled water). Stock cultures were maintained on carrot juice seawater agar (sCA; 16 g agar, 3 g $CaCO_3$, 100 mL carrot juice, 450 mL distilled water, 450 mL seawater) at 4–8 °C in the dark.

DNA isolation, amplification and sequencing

For *Halophytophthora* and *Phytophthora* isolates obtained in this study and several additional *Phytophthora* and *Nothophytophthora* isolates used in the phylogenetic analyses the internal transcribed spacer region (ITS1-5.8S-ITS2) of the ribosomal RNA gene (ITS) and the 5' terminal domain of the large subunit (LSU) of the nuclear ribosomal RNA gene were amplified and sequenced. In addition, for all isolates of the new *Halophytophthora* species used in the phylogenetic analyses (Table 1) four additional nuclear loci, i.e., heat shock protein 90 (*hsp90*), β-tubulin (*Btub*), 60S ribosomal protein L10 (*rpl10*) and *tigA* (a locus containing two genes, a triosephosphate isomerase and glyceraldehyde-3-phosphate dehydrogenase, fused into a single transcriptional unit), and the three mitochondrial genes cytochrome-c oxidase 1 (*cox1*), subunit 1 of NADH dehydrogenase (*nadh1*) and 40S ribosomal protein S10 (*rps10*) were amplified and sequenced.

DNA was extracted from mycelium scraped from 1–3-wk-old V8A cultures, placed into 2 mL homogenisation tubes (MP Biomedicals, Irvine, USA) and disrupted using a Precellys Evolution instrument (Bertin Technologies, Montigny-le-Bretonneux, France). 300 µL of lysis buffer (Lamour & Finley 2006) supplemented by 3 µL of RNase A (New England Biolabs, Ipswich, USA) was added to each sample and incubated at 65 °C for 20 min (Lamour & Finley 2006). Each sample was centrifuged at 20 000 g for 3 min and the supernatant transferred to a fresh tube. Each sample was then mixed with 150 µL of 5 M potassium acetate, stored at -20 °C for at least 30 min followed by 30 min of centrifugation at 20 000 g (Lamour & Finley 2006). The supernatant was transferred to a 2 mL tube and further purified using Monarch® PCR & DNA Cleanup Kit (New England Biolabs, Ipswich, USA) following the manufacturer´s protocol. DNA was eluted with 80 µL of pre-warmed elution buffer and concentration was estimated by spectrophotometry using QUICKDROP (Molecular Devices, San Jose, USA). DNA was preserved at -80 °C for long-term storage.

PCR amplifications were performed using a LightCycler 480 II instrument (Roche, Basel, Switzerland) and PCR conditions were optimised for each locus. Primers were synthetized by Elizabeth Pharmacon spol. s.r.o. (Brno, Czech Republic) and their annealing temperatures were estimated using Tm calculator (http://tmcalculator.neb.com/#!/main) and adjusted empirically, according to observed PCR amplification rates. Table 2 provides a comprehensive overview of the PCR methodology and primers used.

PCR products were visualised by gel electrophoresis (300V; 5 min) using 2 % agarose gel stained by DNA Stain G (SERVA, Heidelberg, Germany). All amplicons were purified and sequenced in both directions by Eurofins Genomics GmbH (Cologne and Ebersberg, Germany) using the amplification primers except for the *tigA* and LSU amplicons which required two additional primers (Table 2).

Electropherograms were quality checked and forward and reverse reads were compiled using Geneious Prime® v. 2021.2.2 (Biomatters Ltd., Auckland, New Zealand). Pronounced double peaks were considered as heterozygous positions and labelled according to the IUPAC coding system. All sequences generated in this study were deposited in GenBank and accession numbers are given in Table 1.

Phylogenetic analysis

In the past decade LSU and/or ITS sequences of numerous unidentified *Halophytophthora* isolates and taxa have been submitted to GenBank. To provide an updated phylogenetic structure of the genus *Halophytophthora* s.str. and resolve the phylogenetic positions of the 10 new *Halophytophthora* taxa from Portugal within the genus, two datasets comprising all relevant and distinctive (i) LSU and (ii) ITS sequences available from GenBank and respective sequences from the new Portuguese taxa were analysed. In the LSU analysis representative species of related genera in the *Peronosporaceae*, *Pythiaceae* and *Salisapiliaceae* were included and *Aphanomyces euteiches* (CBS 156.73) used as outgroup taxon (dataset: 59 isolates and 1 289 characters). In the ITS analysis *Phytophthora castanetorum* (CBS 142.299) and *P.* × *cambivora* (CBS 141.218) were used as outgroup taxa (dataset: 63 isolates and 1 254 characters).

To study the relative phylogenetic positions of the nine new *Halophytophthora* taxa from Portugal for which living isolates were available and related *Halophytophthora* species, i.e., *H. avicennae*, *H. fluviatilis* and *H. polymorphica*, (iii) a full 9-partition dataset (9 loci: ITS-LSU-*rpl10-Btub-hsp90-tigA-cox1-nadh1-rps10*) was analysed with *P. castanetorum* (CBS 142.299) and *P.* × *cambivora* (CBS 141.218) as outgroup taxa (dataset: 60 isolates and 8 759 characters).

The sequences of the loci used in the analyses were aligned using the MAFFT v. 7 (Katoh & Standley 2013) plugin within the Geneious software by the E-INS-I strategy (ITS) or the G-INS-I

Table 1 Details of oomycete isolates included in this study. GenBank numbers for sequences obtained in the present study are printed in *italics*.

Species	Isolate numbers[a]		Origin			GenBank accession numbers					
	International collections	Local collections	Source	Location; year[f]	Collector; reference	LSU	ITS	*coxI*	*Btub hsp90*	*tigA* 60S *rpl10*	*nadh1* 40S *rps10*
Halophytophthora avicennae[b]	CBS 188.85; ATCC 64709	DAR 50187	Fallen *Avicennia marina* leave in Clyde River estuary	Bateman's Bay, AU; 1982	J. Simpson; Gerrettson-Cornell & Simpson 1984	AY598668	HQ643147	HQ708219	*OK091259* *OK091315*	n.a. *OK091426*	KY788594 *OK091535*
H. avicennae	–	BD88	Baiting; brackish river water, Ribeira de Odelouca	Silves, PT; 2014	T. Jung; this study	n.a.	*OK040996*	*OK091587*	n.a.	n.a.	n.a.
H. avicennae	–	BD629	Baiting; Rio Séqua estuary, Ria Formosa	Tavira, PT; 2015	T. Jung; this study	n.a.	*OK040997*	n.a.	n.a.	n.a.	n.a.
H. avicennae[b,c,d]	–	BD633	Baiting; Rio Séqua estuary, Ria Formosa	Tavira, PT; 2015	T. Jung; this study	*OK033574*	*OK033632*	*OK091197*	*OK091252* *OK091308*	*OK091363* *OK091419*	n.a. *OK091528*
H. avicennae	–	BD635	Baiting; Rio Séqua estuary, Ria Formosa	Tavira, PT; 2015	T. Jung; this study	*OK033575*	*OK033633*	*OK091198*	*OK091253* *OK091309*	*OK091364* *OK091420*	n.a. *OK091529*
H. avicennae[b,c,d]	–	BD636	Baiting; Rio Séqua estuary, Ria Formosa	Tavira, PT; 2015	T. Jung; this study	n.a.	*OK040998*	n.a.	n.a.	n.a.	n.a.
H. avicennae[b,c,d]	–	BD670	Baiting; coastal lagoon, Ria de Alvor	Alvor, PT; 2015	T. Jung; this study	*OK033576*	*OK033634*	*OK091199*	*OK091254* *OK091310*	*OK091365* *OK091421*	n.a. *OK091530*
H. avicennae	–	BD671	Baiting; coastal lagoon, Ria de Alvor	Alvor, PT; 2015	T. Jung; this study	n.a.	*OK040999*	n.a.	n.a.	n.a.	n.a.
H. avicennae[b,c]	–	BD682	Baiting; coastal lagoon, Ria Formosa	Almancil, PT; 2015	T. Jung; this study	*OK033577*	*OK033635*	*OK091200*	*OK091255* *OK091311*	*OK091366* *OK091422*	n.a. *OK091531*
H. avicennae[b,c]	–	BD687	Baiting; tidal pond in salt marsh, Ria Formosa	Almancil, PT; 2015	T. Jung; this study	OK033578	*OK033636*	*OK091201*	*OK091256* *OK091312*	*OK091367* *OK091423*	n.a. *OK091532*
H. avicennae	–	BD689	Baiting; estuary of Rio Guadiana	Castro Marim, PT; 2015	T. Jung; this study	n.a.	*OK041001*	n.a.	n.a.	n.a.	n.a.
H. avicennae[b,c]	–	BD690	Baiting; estuary of Rio Guadiana	Castro Marim, PT; 2015	T. Jung; this study	*OK033579*	*OK033637*	*OK091202*	*OK091257* *OK091313*	*OK091368* *OK091424*	n.a. *OK091533*
H. avicennae[b,c]	–	BD697	Baiting; estuary of Rio Guadiana	Castro Marim, PT; 2015	T. Jung; this study	*OK033580*	*OK033638*	*OK091203*	*OK091258* *OK091314*	*OK091369* *OK091425*	n.a. *OK091534*
H. batemanensis[b], ex-type	CBS 679.84; WPC P11617; IMI 327602; NBRC 32616	DAR 41559	Fallen *Avicennia marina* leave in Clyde River estuary	Bateman's Bay, AU; 1982	J. Simpson; Gerrettson-Cornell & Simpson 1984	HQ665286	HQ643148	HQ171166	KY788513 n.a.	n.a.	n.a.
H. brevisporangia[b,c,d], ex-type	CBS 147238	BD662	Baiting; tidal pond in salt marsh, Ria Formosa	Quelfes, PT; 2015	T. Jung; this study	*OK033583*	*OK033641*	*OK091206*	*OK091262* *OK091318*	*OK091372* *OK091429*	*OK091481* *OK091538*
H. brevisporangia[b,c]	–	BD644	Baiting; tidal channel in salt marsh, Ria Formosa	Santa Luzia, PT; 2015	T. Jung; this study	*OK033581*	*OK033639*	*OK091204*	*OK091260* *OK091316*	*OK091370* *OK091427*	*OK091479* *OK091536*
H. brevisporangia[b,c,d]	–	BD658	Baiting; tidal pond in salt marsh, Ria Formosa	Quelfes, PT; 2015	T. Jung; this study	*OK033582*	*OK033640*	*OK091205*	*OK091261* *OK091317*	*OK091371* *OK091428*	*OK091480* *OK091537*
H. brevisporangia[b,c,d]	CBS 147239	BD695	Baiting; estuary of Rio Guadiana	Castro Marim, PT; 2015	G. Carella; this study	*OK033584*	*OK033642*	*OK091207*	*OK091263* *OK091319*	*OK091373* *OK091430*	*OK091482* *OK091539*
H. brevisporangia[b]	–	BD887	Baiting; tidal channel in salt marsh, Ria Formosa	Santa Luzia, PT; 2015	T. Jung; this study	*OK033585*	*OK033643*	*OK091208*	*OK091264* *OK091320*	*OK091374* *OK091431*	*OK091483* *OK091540*
H. celeris[b,c,d], ex-type	CBS 147240	BD885	Baiting; tidal channel in salt marsh, Ria Formosa	Santa Luzia, PT; 2015	T. Jung; this study	*OK033587*	*OK033645*	*OK091210*	*OK091266* *OK091322*	*OK091376* *OK091433*	*OK091485* *OK091542*

Table 1 (cont.)

Species	Isolate numbers[a]		Origin			GenBank accession numbers					
	International collections	Local collections	Source	Location; year[f]	Collector; reference	LSU	ITS	*coxI*	*Btub hsp90*	*tigA* 60S *rpl10*	*nadh1* 40S *rps10*
H. celeris[b,c,d]	CBS 147241	BD646	Baiting; tidal channel in salt marsh, Ria Formosa	Santa Luzia, PT; 2015	T. Jung; this study	*OK033586*	*OK033644*	*OK091209*	*OK091265* *OK091321*	*OK091375* *OK091432*	*OK091484* *OK091541*
H. celeris[b,c,d]	–	BD886	Baiting; tidal channel in salt marsh, Ria Formosa	Santa Luzia, PT; 2015	T. Jung; this study	*OK033588*	*OK033646*	*OK091211*	*OK091267* *OK091323*	*OK091377* *OK091434*	*OK091486* *OK091543*
H. celeris[b]	–	BD985	Baiting; tidal channel in salt marsh, Ria Formosa	Santa Luzia, PT; 2015	T. Jung; this study	*OK033589*	*OK033647*	*OK091212*	*OK091268* *OK091324*	*OK091378* *OK091435*	*OK091487* *OK091544*
H. celeris[b]	–	BD987	Baiting; tidal channel in salt marsh, Ria Formosa	Santa Luzia, PT; 2015	T. Jung; this study	*OK033590*	*OK033648*	*OK091213*	*OK091269* *OK091325*	*OK091379* *OK091436*	*OK091488* *OK091545*
H. fluviatilis[b], ex-type	ATCC MYA-4961	57A9	Baiting; Flint Run Stream	Virginia, US; 2011	X. Yang; Yang & Hong 2014	KX252673	KF734963	n.a.	KX252669 KX252672	KX252674 KX252668	n.a.
H. fluviatilis[b]	–	59J1	Baiting; Rappahannock River	Virginia, US; 2012	X. Yang; Yang & Hong 2014	n.a.	KF734968	n.a.	n.a.	n.a.	n.a.
H. frigida[b,c,d], ex-type	CBS 147235	BD655	Baiting; tidal pond in salt marsh, Ria Formosa	Santa Luzia, PT; 2015	T. Jung; this study	*OK033594*	*OK033652*	*OK091217*	*OK091273* *OK091329*	*OK091383* *OK091440*	*OK091492* *OK091549*
H. frigida[b,c,d]	–	BD641	Baiting; tidal channel in salt marsh, Ria Formosa	Santa Luzia, PT; 2015	T. Jung; this study	*OK033591*	*OK033649*	*OK091214*	*OK091270* *OK091326*	*OK091380* *OK091437*	*OK091489* *OK091546*
H. frigida[b,c,d]	–	BD647	Baiting; tidal pond in salt marsh, Ria Formosa	Santa Luzia, PT; 2015	T. Jung; this study	*OK033592*	*OK033650*	*OK091215*	*OK091271* *OK091327*	*OK091381* *OK091438*	*OK091490* *OK091547*
H. frigida[b,c,d]	CBS 147236	BD650	Baiting; tidal pond in salt marsh, Ria Formosa	Santa Luzia, PT; 2015	T. Jung; this study	*OK033593*	*OK033651*	*OK091216*	*OK091272* *OK091328*	*OK091382* *OK091439*	*OK091491* *OK091548*
H. frigida[c,d]	–	BD654	Baiting; tidal pond in salt marsh, Ria Formosa	Santa Luzia, PT; 2015	T. Jung; this study	n.a.	*OK041002*	*OK091589*	n.a.	n.a.	n.a.
H. frigida[b,c]	–	BD675	Baiting; coastal lagoon, Ria de Alvor	Alvor, PT; 2015	T. Jung; this study	*OK033595*	*OK033653*	*OK091218*	*OK091274* *OK091330*	*OK091384* *OK091441*	*OK091493* *OK091550*
H. frigida[b,c]	–	BD676	Baiting; coastal lagoon, Ria de Alvor	Alvor, PT; 2015	T. Jung; this study	*OK033596*	*OK033654*	*OK091219*	*OK091275* *OK091331*	*OK091385* *OK091442*	*OK091494* *OK091551*
H. insularis[b], ex-type	CCIBt 4114		Submerged leaf of *Laguncularia racemosa*; Perequê river	Ilha do Cardoso, BR; 2012	A.V. Marano, A.L. Jesus & C.L.A. Pires-Zottarelli; Jesus et al. 2019	KY327272	KY320204	n.a.	n.a.	n.a.	n.a.
H. insularis[b]	–	AJM 74	Submerged leaf of *Laguncularia racemosa*; Perequê river	Ilha do Cardoso, BR; 2012	A.V. Marano, A.L. Jesus & C.L.A. Pires-Zottarelli; Jesus et al. 2019	KY327270	KY320202	KY327277	n.a.	n.a.	n.a.
H. lateralis[b,c,d], ex-type	CBS 147233	BD657	Baiting; tidal pond in salt marsh, Ria Formosa	Quelfes, PT; 2015	T. Jung; this study	*OK033597*	*OK033655*	*OK091220*	*OK091276* *OK091332*	*OK091386* *OK091443*	*OK091495* *OK091552*
H. lateralis[b,c,d]	–	BD660	Baiting; tidal pond in salt marsh, Ria Formosa	Quelfes, PT; 2015	T. Jung; this study	*OK033598*	*OK033656*	*OK091221*	*OK091277* *OK091333*	*OK091387* *OK091444*	*OK091496* *OK091553*
H. lateralis[b,c,d]	–	BD665	Baiting; tidal pond in salt marsh, Ria Formosa	Quelfes, PT; 2015	T. Jung; this study	*OK033599*	*OK033657*	*OK091222*	*OK091278* *OK091334*	*OK091388* *OK091445*	*OK091497* *OK091554*
H. lateralis[b,c,d]	CBS 147234	BD680	Baiting; coastal lagoon, Ria Formosa	Almancil, PT; 2015	T. Jung; this study	*OK033600*	*OK033658*	*OK091223*	*OK091279* *OK091335*	*OK091389* *OK091446*	*OK091498* *OK091555*
H. lusitanica[b,c,d], ex-type	CBS 147231	BD686	Baiting; tidal pond in salt marsh, Ria Formosa	Almancil, PT; 2015	T. Jung; this study	*OK033605*	*OK033663*	*OK091228*	*OK091284* *OK091340*	*OK091394* *OK091451*	*OK091503* *OK091560*

Table 1 (cont.)

Species	Isolate numbers[a]		Origin			GenBank accession numbers					
	International collections	Local collections	Source	Location; year[f]	Collector; reference	LSU	ITS	*coxI*	*Btub hsp90*	*tigA* 60S *rpl10*	*nadh1* 40S *rps10*
H. lusitanica[b,c,d]	CBS 147232	BD628	Baiting; Rio Séqua estuary, Ria Formosa	Tavira, PT; 2015	T. Jung; this study	*OK033601*	*OK033659*	*OK091224*	*OK091280* *OK091336*	*OK091390* *OK091447*	*OK091499* *OK091556*
H. lusitanica[c,d]	–	BD632	Baiting; Rio Séqua estuary, Ria Formosa	Tavira, PT; 2015	T. Jung; this study	n.a.	*OK041003*	*OK091590*	n.a.	n.a.	n.a.
H. lusitanica[b,c,d]	–	BD634	Baiting; Rio Séqua estuary, Ria Formosa	Tavira, PT; 2015	T. Jung; this study	*OK033602*	*OK033660*	*OK091225*	*OK091281* *OK091337*	*OK091391* *OK091448*	*OK091500* *OK091557*
H. lusitanica	–	BD638	Baiting; Rio Séqua estuary, Ria Formosa	Tavira, PT; 2015	T. Jung; this study	n.a.	*OK041004*	n.a.	n.a.	n.a.	n.a.
H. lusitanica[b,c]	–	BD679	Baiting; coastal lagoon, Ria Formosa	Almancil, PT; 2015	T. Jung; this study	*OK033603*	*OK033661*	*OK091226*	*OK091282* *OK091338*	*OK091392* *OK091449*	*OK091501* *OK091558*
H. lusitanica[b,c,d]	–	BD681	Baiting; coastal lagoon, Ria Formosa	Almancil, PT; 2015	T. Jung; this study	*OK033604*	*OK033662*	*OK091227*	*OK091283* *OK091339*	*OK091393* *OK091450*	*OK091502* *OK091559*
H. lusitanica	–	BD934	Baiting; estuary of Rio Guadiana	Castro Marim, PT; 2015	T. Jung; this study	n.a.	*OK041005*	*OK091591*	n.a.	n.a.	n.a.
H. macrosporangia[b,c,d], ex-type	CBS 147290	BD639	Baiting; tidal channel in salt marsh, Ria Formosa	Santa Luzia, PT; 2015	T. Jung; this study	*OK033606*	*OK033664*	*OK091229*	*OK091285* *OK091341*	*OK091395* *OK091452*	*OK091504* *OK091561*
H. macrosporangia[b,d]	CBS 147291	BD642	Baiting; tidal channel in salt marsh, Ria Formosa	Santa Luzia, PT; 2015	T. Jung; this study	*OK033607*	*OK033665*	*OK091230*	*OK091286* *OK091342*	*OK091396* *OK091453*	*OK091505* *OK091562*
H. macrosporangia[b,c,d]	–	BD643	Baiting; tidal channel in salt marsh, Ria Formosa	Santa Luzia, PT; 2015	T. Jung; this study	*OK033608*	*OK033666*	*OK091231*	*OK091287* *OK091343*	*OK091397* *OK091454*	*OK091506* *OK091563*
H. macrosporangia[c,d]	–	BD645	Baiting; tidal channel in salt marsh, Ria Formosa	Santa Luzia, PT; 2015	T. Jung; this study	n.a.	*OK041006*	*OK091592*	n.a.	n.a.	n.a.
H. macrosporangia[b,c,d]	–	BD649	Baiting; tidal pond in salt marsh, Ria Formosa	Santa Luzia, PT; 2015	T. Jung; this study	*OK033609*	*OK033667*	*OK091232*	*OK091288* *OK091344*	*OK091398* *OK091455*	*OK091507* *OK091564*
H. macrosporangia[b,c,d]	–	BD659	Baiting; tidal pond in salt marsh, Ria Formosa	Quelfes, PT; 2015	T. Jung; this study	*OK033610*	*OK033668*	*OK091233*	*OK091289* *OK091345*	*OK091399* *OK091456*	*OK091508* *OK091565*
H. macrosporangia[b,c,d]	–	BD664	Baiting; tidal pond in salt marsh, Ria Formosa	Quelfes, PT; 2015	T. Jung; this study	*OK033611*	*OK033669*	*OK091234*	*OK091290* *OK091346*	*OK091400* *OK091457*	*OK091509* *OK091566*
H. polymorphica[b], ex-type	CBS 680.84; NBRC 32619; ATCC 56966	DAR 41562	Fallen *Eucalyptus* sp. leave in Clyde River estuary	Bateman's Bay, AU; 1982	J. Simpson; Gerrettson-Cornell & Simpson 1984	AY598669	HQ643313	HQ708363	*OK091291* n.a.	*OK091401* *OK091458*	n.a. *OK091567*
H. polymorphica[b]	CCIBt 4112	AJM 33	Submerged leaves of *Laguncularia racemosa;* Perequê river	Ilha do Cardoso, BR; 2012	A.L. Jesus, A.V. Marano & C.L.A. Pires-Zottarelli; Jesus et al. 2019	KT455404	KT455391	KT897699	n.a.	n.a.	n.a.
H. sinuata[b,c,d], ex-type	CBS 147237	BD656	Baiting; tidal pond in salt marsh, Ria Formosa	Santa Luzia, PT; 2015	T. Jung; this study	*OK033613*	*OK033671*	*OK091236*	*OK091293* *OK091348*	*OK091403* *OK091460*	*OK091511* *OK091569*
H. sinuata[b,c,d]	–	BD640	Baiting; tidal channel in salt marsh, Ria Formosa	Santa Luzia, PT; 2015	T. Jung; this study	*OK033612*	*OK033670*	*OK091235*	*OK091292* *OK091347*	*OK091402* *OK091459*	*OK091510* *OK091568*
H. sinuata[b,c,d]	–	BD941	Baiting; tidal channel in salt marsh, Ria Formosa	Santa Luzia, PT; 2015	T. Jung; this study	*OK033614*	*OK033672*	*OK091237*	*OK091294* *OK091349*	*OK091404* *OK091461*	*OK091512* *OK091570*
H. sinuata[b,c,d]	–	BD942	Baiting; tidal channel in salt marsh, Ria Formosa	Santa Luzia, PT; 2015	T. Jung; this study	*OK033615*	*OK033673*	*OK091238*	*OK091295* *OK091350*	*OK091405* *OK091462*	*OK091513* *OK091571*
H. sinuata[b,c,d]	CBS 147292	BD943	Baiting; tidal channel in salt marsh, Ria Formosa	Santa Luzia, PT; 2015	T. Jung; this study	*OK033616*	*OK033674*	*OK091239*	*OK091296* *OK091351*	*OK091406* *OK091463*	*OK091514* *OK091572*

Table 1 (cont.)

Species	Isolate numbers[a]		Origin			GenBank accession numbers					
	International collections	Local collections	Source	Location; year[f]	Collector; reference	LSU	ITS	*coxI*	*Btub* *hsp90*	*tigA* 60S *rpl10*	*nadh1* 40S *rps10*
H. sinuata[c]	–	BD944	Baiting; tidal pond in salt marsh, Ria Formosa	Santa Luzia, PT; 2015	T. Jung; this study	n.a.	*OK041007*	*OK091593*	n.a.	n.a.	n.a.
H. souzae[b], ex-type	CCIBt 4113		Submerged leaf of *Laguncularia racemosa*; Perequê river	Ilha do Cardoso, BR; 2012	A.L. Jesus, A.V. Marano & C.L.A. Pires-Zottarelli; Jesus et al. 2019	KY327269	KY320200	KY327275	n.a.	n.a.	n.a.
H. souzae[b]	–	AJM 23	Submerged leaf of *Laguncularia racemosa*; Perequê river	Ilha do Cardoso, BR; 2012	A.L. Jesus, A.V. Marano & C.L.A. Pires-Zottarelli; Jesus et al. 2019	KY327268	KY320199	KY327274	n.a.	n.a.	n.a.
H. thermoambigua[b,c,d], ex-type	CBS 147229	BD651	Baiting; tidal pond in salt marsh, Ria Formosa	Santa Luzia, PT; 2015	T. Jung; this study	*OK033622*	*OK033680*	*OK091244*	*OK091300* *OK091355*	*OK091411* *OK091469*	*OK091520* *OK091577*
H. thermoambigua[b,c]	–	BD91	Baiting; brackish river water, Ribeira de Odelouca	Silves, PT; 2014	T. Jung; this study	*OK033617*	*OK033675*	*OK091240*	n.a.	*OK091407* *OK091464*	*OK091515* *OK091573*
H. thermoambigua[b,c]	–	BD93	Baiting; brackish river water, Ribeira de Odelouca	Silves, PT; 2014	T. Jung; this study	*OK033618*	*OK033676*	*OK091241*	n.a.	*OK091408* *OK091465*	*OK091516* *OK091574*
H. thermoambigua[b]	–	BD630	Baiting; Rio Séqua estuary, Ria Formosa	Tavira, PT; 2015	T. Jung; this study	*OK033619*	*OK033677*	*OK091242*	*OK091297* *OK091352*	*OK091409* *OK091466*	*OK091517* *OK091575*
H. thermoambigua[c]	–	BD631	Baiting; Rio Séqua estuary, Ria Formosa	Tavira, PT; 2015	T. Jung; this study	n.a.	*OK041008*	n.a.	n.a.	n.a.	n.a.
H. thermoambigua[b,c,d]	CBS 147230	BD637	Baiting; Rio Séqua estuary, Ria Formosa	Tavira, PT; 2015	T. Jung; this study	*OK033620*	*OK033678*	*OK091243*	*OK091298* *OK091353*	*OK091410* *OK091467*	*OK091518* *OK091576*
H. thermoambigua[b]	–	BD648	Baiting; tidal pond in salt marsh, Ria Formosa	Santa Luzia, PT; 2015	T. Jung; this study	*OK033621*	*OK033679*	n.a.	*OK091299* *OK091354*	n.a. *OK091468*	*OK091519* n.a.
H. thermoambigua[b,e]	–	BD668	Baiting; coastal lagoon, Ria de Alvor	Alvor, PT; 2015	T. Jung; this study	*OK033623*	*OK033681*	*OK091245*	*OK091301* *OK091356*	*OK091412* *OK091470*	*OK091521* *OK091578*
H. thermoambigua	–	BD669	Baiting; coastal lagoon, Ria de Alvor	Alvor, PT; 2015	T. Jung; this study	n.a.	*OK041009*	n.a.	n.a.	n.a.	n.a.
H. thermoambigua[c]	–	BD673	Baiting; coastal lagoon, Ria de Alvor	Alvor, PT; 2015	T. Jung; this study	n.a.	*OK041010*	n.a.	n.a.	n.a.	n.a.
H. thermoambigua[b,c]	–	BD674	Baiting; coastal lagoon, Ria de Alvor	Alvor, PT; 2015	T. Jung; this study	*OK033624*	*OK033682*	*OK091246*	*OK091302* *OK091357*	*OK091413* *OK091471*	*OK091522* *OK091579*
H. thermoambigua	–	BD683	Baiting; tidal pond, Ria Formosa	Almancil, PT; 2015	T. Jung; this study	n.a.	*OK041011*	n.a.	n.a.	n.a.	n.a.
H. thermoambigua	–	BD684	Baiting; tidal pond, Ria Formosa	Almancil, PT; 2015	T. Jung; this study	n.a.	*OK041012*	n.a.	n.a.	n.a.	n.a.
H. thermoambigua[b]	–	BD685	Baiting; tidal pond, Ria Formosa	Almancil, PT; 2015	T. Jung; this study	*OK033625*	*OK033683*	*OK091247*	*OK091303* *OK091358*	*OK091414* *OK091472*	*OK091523* *OK091580*
H. thermoambigua	–	BD692	Baiting; estuary of Rio Guadiana	Castro Marim, PT; 2015	T. Jung; this study	n.a.	*OK041013*	n.a.	n.a.	n.a.	n.a.
H. thermoambigua[b]	–	BD693	Baiting; estuary of Rio Guadiana	Castro Marim, PT; 2015	T. Jung; this study	*OK033626*	*OK033684*	*OK091248*	*OK091304* *OK091359*	*OK091415* *OK091473*	*OK091524* *OK091581*
H. thermoambigua	–	BD696	Baiting; estuary of Rio Guadiana	Castro Marim, PT; 2015	T. Jung; this study	n.a.	*OK041014*	n.a.	n.a.	n.a.	n.a.
H. thermoambigua[b,c]	–	BD698	Baiting; estuary of Rio Guadiana	Castro Marim, PT; 2015	T. Jung; this study	*OK033627*	*OK033685*	*OK091249*	*OK091305* *OK091360*	*OK091416* *OK091474*	*OK091525* *OK091582*

Table 1 (cont.)

Species	Isolate numbers[a]		Origin			GenBank accession numbers					
	International collections	Local collections	Source	Location; year[f]	Collector; reference	LSU	ITS	*coxI*	*Btub* *hsp90*	*tigA* 60S *rpl10*	*nadh1* 40S *rps10*
H. vesicula[b], ex-type	CBS 393.81; NBRC 32216	–	Baiting; Horseshoe Bay	British Columbia; CA; 1968	C.J. Anastasiou; Anastasiou & Churchland 1969	JX436352	JF750389	MG019397	n.a.	n.a.	n.a.
H. '*vesicula*'[b]	CBS 152.96	–	*Rhizophora mangle* submerged, decaying leaves	Florida, Miami, US; 1985	n.a.	HQ232463	HQ232472	n.a.	n.a.	n.a.	n.a.
H. '*vesicula*'[b]	CCIBt 4142	AJM 124	Submerged leaf of *Laguncularia racemosa*; Perequê river	Ilha do Cardoso, BR; 2013	A.L. Jesus, A.V. Marano & C.L.A. Pires-Zottarelli; Jesus et al. 2019	KT455407	KT455395	n.a.	n.a.	n.a.	n.a.
H. '*vesicula*'[b]	CCIBt 4143	AJM 126	Submerged leaf of *Laguncularia racemosa*; Perequê river	Ilha do Cardoso, BR; 2013	A.L. Jesus, A.V. Marano & C.L.A. Pires-Zottarelli; Jesus et al. 2019	KT455408	KT455396	n.a.	n.a.	n.a.	n.a.
H. '*vesicula*'[b]	CCIBt 4144	AJM 133	Submerged leaf of *Laguncularia racemosa*; Perequê river	Ilha do Cardoso, BR; 2013	A.L. Jesus, A.V. Marano & C.L.A. Pires-Zottarelli; Jesus et al. 2019	KT455409	KT455397	n.a.	n.a.	n.a.	n.a.
H. '*vesicula*'[b]	CCIBt 4146	AJM 137	Submerged leaf of *Rhizophora mangle*, Perequê river	Ilha do Cardoso, BR; 2013	A.L. Jesus, A.V. Marano & C.L.A. Pires-Zottarelli; Jesus et al. 2019	KT455411	n.a.	n.a.	n.a.	n.a.	n.a.
H. '*vesicula*'[b]	–	IMB147	Mangrove fallen yellowish green leaves	Haomeili, TW; 2012	n.a.	n.a.	KM205201	n.a.	n.a.	n.a.	n.a.
H. sp. Portugal_9[b]	–	BD694	Baiting; estuary of Rio Guadiana	Castro Marim, PT; 2015	T. Jung; this study	n.a.	*OK041015*	n.a.	n.a.	n.a.	n.a.
H. sp. thermoambigua-like[b]	–	BD652	Baiting; tidal pond in salt marsh, Ria Formosa	Santa Luzia, PT; 2015	T. Jung; this study	*OK033628*	*OK033686*	*OK091250*	*OK091306* *OK091361*	*OK091417* *OK091475*	*OK091526* *OK091583*
H. sp. thermoambigua-like[b]	–	BD653	Baiting; tidal pond in salt marsh, Ria Formosa	Santa Luzia, PT; 2015	T. Jung; this study	*OK033629*	*OK033687*	*OK091251*	*OK091307* *OK091362*	*OK091418* *OK091476*	*OK091527* *OK091584*
H. sp.1 KC-2014[b]	–	1104-4-5A	Washington state stream	Washington, US; 2001	n.a.	n.a.	KF889754	n.a.	n.a.	n.a.	n.a.
H. sp.2 KC-2014[b]	–	1110-2-5A	Washington state stream	Washington, US; 2001	n.a.	n.a.	KF889755	n.a.	n.a.	n.a.	n.a.
H. sp. 1 LT6430[b]	–	LT6430	Marsh grass (*Spartina alterniflora*) leaf litter	Saint Simon's Island, Georgia, USA; 2009	J. Hulvey; Hulvey et al. 2010	HQ232456	HQ232465	KJ654026	n.a.	n.a.	n.a.
H. sp. 2 LT6465[b]	–	LT6465	Marsh grass (*Spartina alterniflora*) leaf litter	Sapelo Island, Georgia, USA; 2009	J. Hulvey; Hulvey et al. 2010	HQ232460	HQ232469	n.a.	n.a.	n.a.	n.a.
H. sp-1[b]	CBS 140651		*Zostera marina* (seeds)	Sylt, DE; 2014	K. Rosendahl; Man In't Veld et al. 2019		KX364106	n.a.	n.a.	n.a.	n.a.
H. sp-3[b]	CBS 140657		*Zostera marina* (seeds)	Sylt, DE; 2014	K. Rosendahl; Man in 't Veld et al. 2019		KX364108	n.a.	n.a.	n.a.	n.a.
H. sp-4[b]	–	PD6234625	*Zostera marina* (seeds), Thau lagoon	FR; 2015	K. Rosendahl; Man in 't Veld et al. 2019	n.a.	KX364110	n.a.	n.a.	n.a.	n.a.
H. sp. 1 EMTD7[b]	CBS 133933	EMTD7	Leaf litter and organic debris	Schleswig-Holstein, DE; 2010	M. Thines; Nigrelli & Thines 2013	n.a.	JX910903	n.a.	n.a.	n.a.	n.a.
H. sp. 1 EMTD10[b]	CBS 133859	EMTD10	Leaf litter and organic debris	Schleswig-Holstein, DE; 2010	M. Thines; Nigrelli & Thines 2013	n.a.	JX910917	n.a.	n.a.	n.a.	n.a.
H. sp. 2 EMTD12[b]	–	EMTD12	Leaf litter and organic debris	Schleswig-Holstein, DE; 2010	M. Thines; Nigrelli & Thines 2013	n.a.	JX910916	n.a.	n.a.	n.a.	n.a.
H. sp. 2 EMTS19[b]	CBS 133863	EMTS19	Leaf litter and organic debris	Schleswig-Holstein, DE; 2010	M. Thines; Nigrelli & Thines 2013	n.a.	JX910916	n.a.	n.a.	n.a.	n.a.

Table 1 (cont.)

Species	Isolate numbers[a]		Origin			GenBank accession numbers					
	International collections	Local collections	Source	Location; year[f]	Collector; reference	LSU	ITS	*coxI*	*Btub* *hsp90*	*tigA* 60S *rpl10*	*nadh1* 40S *rps10*
H. sp. isolate BBGYB1[b]	–	USTCMS 4125	n.a.	PH	n.a.	n.a.	MT178024	n.a.	n.a.	n.a.	n.a.
H. sp. isolate BBGYB2B[b]	–	USTCMS 4136	n.a.	PH	n.a.	MT178010	MT178029	n.a.	n.a.	n.a.	n.a.
H. sp. isolate BBGYB5[b]	–	USTCMS 4129	n.a.	PH	n.a.	MT178016	n.a.	n.a.	n.a.	n.a.	n.a.
H. sp. isolate BCCYBL1[b]	–	USTCMS 4158	n.a.	PH	n.a.	MT178013	MT178042	n.a.	n.a.	n.a.	n.a.
H. sp. isolate BCCYGL1[b]	–	USTCMS 4159	n.a.	PH	n.a.	MT178003	n.a.	n.a.	n.a.	n.a.	n.a.
H. sp. isolate CLE33[b]	–	CLE33	*Zostera marina*	California, US	n.a.	MN944508	n.a.	n.a.	n.a.	n.a.	n.a.
H. sp. isolate DGPBL2[b]	–	USTCMS 4161	n.a.	PH	n.a.	MT177998	MT178039	n.a.	n.a.	n.a.	n.a.
H. sp. isolate DGPYB2[b]	–	USTCMS 4162	n.a.	PH	n.a.	MT178018	MT178041	n.a.	n.a.	n.a.	n.a.
H. sp. isolate PNGLYBE[b]	–	USTCMS 4123	n.a.	PH	n.a.	MT177993	MT178043	n.a.	n.a.	n.a.	n.a.
H. sp. isolate PQ1YB[b]	–	USTCMS 4108	n.a.	PH	n.a.	MT178019	n.a.	n.a.	n.a.	n.a.	n.a.
H. sp. isolate PSQNBL3[b]	–	USTCMS 4153	n.a.	PH	n.a.	MT177995	n.a.	n.a.	n.a.	n.a.	n.a.
H. sp. isolate PSQNBL4[b]	–	USTCMS 4152	n.a.	PH	n.a.	MT178000	n.a.	n.a.	n.a.	n.a.	n.a.
H. sp. isolate PSQNYB1[b]	–	USTCMS 4154	n.a.	PH	n.a.	MT178004	MT178037	n.a.	n.a.	n.a.	n.a.
H. sp. isolate PSQNYB2[b]	–	USTCMS 4155	n.a.	PH	n.a.	MT177996	n.a.	n.a.	n.a.	n.a.	n.a.
H. sp. isolate PSQNYL1[b]	–	USTCMS 4156	n.a.	PH	n.a.	MT178014	MT178037	n.a.	n.a.	n.a.	n.a.
H. sp. isolate PSQNYL2[b]	–	USTCMS 4157	n.a.	PH	n.a.	MT178002	MT178031	n.a.	n.a.	n.a.	n.a.
H. sp. isolate TBJBL1.3[b]	–	USTCMS 4110	n.a.	PH	n.a.	MT178017	MT178022	n.a.	n.a.	n.a.	n.a.
H. sp. isolate TTLBL3.2A[b]	–	USTCMS 4116	n.a.	PH	n.a.	MT178015	MT178033	n.a.	n.a.	n.a.	n.a.
H. sp. isolate TTLBL4.2[b]	–	USTCMS 4118	n.a.	PH	n.a.	MT178001	MT178034	n.a.	n.a.	n.a.	n.a.
H. sp. isolate TWBL1[b]	–	USTCMS 4160	n.a.	PH	n.a.	MT178007	MT178038	n.a.	n.a.	n.a.	n.a.
H. sp. NBRC 32444[b]	NBRC 32444; ATCC 90462	AN-1063	Fallen leaf, *Bruguiera gymnorrhyza*	JP	n.a.; Rahman et al. 2014	n.a.	AB688423	AB688315	n.a.	n.a.	n.a.
H. sp. NBRC 32445[b]	NBRC 32445	AN-1132	Fallen leaf, *Rhizophora stylosa*	JP	n.a.	n.a.	AB688424	AB688316	n.a.	n.a.	n.a.
H. sp. Zostera[b]	CBS 140648	–	*Zostera marina* (seeds)	Sylt, DE; 2014	K. Rosendahl; Govers et al. 2016		KT986007	n.a.	n.a.	n.a.	n.a.
Phytophthora condilina	–	BD661	Baiting; tidal pond in salt marsh, Ria Formosa	Quelfes, PT; 2015	T. Jung; Botella & Jung 2021	n.a.	MW830150	*OK091594*	n.a.	n.a.	MW836949 n.a.
P. condilina	–	BD677	Baiting; coastal lagoon, Ria de Alvor	Alvor, PT; 2015	T. Jung; this study	n.a.	*OK041016*	*OK091595*	n.a.	n.a.	n.a.
P. gonapodyides	–	BD666	Baiting; tidal pond in salt marsh, Ria Formosa	Quelfes, PT; 2015	T. Jung; this study	n.a.	*OK041017*	n.a.	n.a.	n.a.	n.a.
P. inundata	–	BD672	Baiting; coastal lagoon, Ria de Alvor	Alvor, PT; 2015	T. Jung; this study	n.a.	*OK041018*	n.a.	n.a.	n.a.	n.a.
P. plurivora	–	BD691	Baiting; estuary of Rio Guadiana	Castro Marim, PT; 2015	T. Jung; this study	n.a.	*OK041019*	n.a.	n.a.	n.a.	n.a.
P. pseudocryptogea	–	BD688	Baiting; tidal pond, Ria Formosa	Almancil, PT; 2015	T. Jung; this study	n.a.	*OK041020*	n.a.	n.a.	n.a.	n.a.
P. sp. Clade06a New PT	–	BD678	Baiting; coastal lagoon, Ria Formosa	Almancil, PT; 2015	T. Jung; this study	n.a.	n.a.	*OK091596*	*OK091597* n.a.	n.a.	*OK091598* *OK091599*
P. castanetorum[b], ex-type	CBS 142299	BD292	*Castanea sativa*	Monchique, PT; 2015	T. Jung; Jung et al. 2017b	*OK033631*	MF036182	MZ736427	MZ736453 MF036240	MZ736480 *OK091478*	MF036292 *OK091586*

Table 1 (cont.)

Species	Isolate numbers[a]		Origin			GenBank accession numbers					
	International collections	Local collections	Source	Location; year[f]	Collector; reference	LSU	ITS	*coxI*	*Btub* *hsp90*	*tigA* 60S *rpl10*	*nadh1* 40S *rps10*
P. × *cambivora*[b], ex-type	CBS 141218	TJ197; IT 5-3	*Quercus pubescens*	Sicily, IT; 2013	T. Jung; Jung et al. 2017c	*OK033630*	KU899179	MZ736422	KU899255 KU899412	MZ736475 *OK091477*	KU899497 *OK091585*
Nothophytophthora amphigynosa[b], ex-type	CBS 142348	BD268	Stream baiting; atlantic forest	Sintra, PT; 2015	T. Jung; Jung et al. 2017d	*OK047740*	KY788382	–	–	–	–
N. intricata[b], ex-type	CBS 142354	TJ275; RK113-1s	*Aesculus hippocastanum*	Wiesbaden, DE; 2011	T. Jung; Jung et al. 2017d	*OK047739*	KY788413	–	–	–	–
'*Halophytophthora' exoprolifera*[b], ex-paratype	CBS 252.93; ATCC 76607	AN-1065	*Bruguiera gymnorrhyza*, submerged yellow leaf	Okinawa, JP; 1988	A. Nakagiri; Ho et al. 1992	HQ665174	HQ643132	–	–	–	–
'*Halophytophthora' porrigovesica*[b]	WPC P15166; NBRC 33162	MT-95	Submerged decaying leaf of *Avicennia alba* in a mangrove	Ranong, TH; 1999	A. Nakagiri; Nakagiri et al. 2001	n.a.	GU258844	n.a.	n.a.	n.a.	n.a.
Calycofera operculata[b], ex-type	CBS 241.83; ATCC 44952; IMI 249911	–	Decaying leaf, *Avicennia marina*	Moreton Bay, Queens Island, AU	K.G. Pegg & J.L. Alcorn; n.a.	JX115217	KJ128038	–	–	–	–
Phytopythium mirpurense[b]	CBS 124524	DAOM 238992; LEV 3078	Water pond	Sindh, Mirpurkhas, PK; 2006	A.M. Lodhi; n.a.	KJ831614	KJ831614	–	–	–	–
Ph. ostracodes[b]	CBS 768.73	–	Clay soil	Ibiza, ES; 1972	A.J. van der Plaats-Niterink; n.a.	HQ665295	AY598663	–	–	–	–
Pythium angustatum[b]	CBS 522.74	–	Soil	Oostelijk Flevoland, NL; 1971	A.J. van der Plaats-Niterink; n.a.	AY598623	HQ643437	–	–	–	–
Py. myriotylum[b]	CBS 254.70	MUCL 16166	*Arachis hypogaea*	IL	Z.R. Frank; n.a.	AY598678	AY598678	–	–	–	–
Elongisporangium anandrum[b]	CBS 285.31	–	*Rheum rhaponticum*	n.a.	C. Drechsler; n.a.	HQ665185	HQ643435	–	–	–	–
E. dimorphum[b], ex-type	CBS 406.72; ATCC 22843	–	*Pinus taeda*, dead root	Louisiana, US; 1971	F.F. Hendrix Jr. & W.A. Campbell; n.a.	HQ665229	HQ643525	–	–	–	–
Globisporangium paroecandrum[b]	CBS 157.64	BPIC 1297	Loamy nursery soil	South Australia, Adelaide, AU; 1962	O. Vaartaja; n.a.	AY598644	AY598644	–	–	–	–
G. spinosum	CBS 275.67	–	Compost	Baarn, Cantonspark, NL	A.J. van der Plaats-Niterink; n.a.	HQ665181	HQ643793	–	–	–	–
Salisapilia epistomium[b], ex-type	CBS 590.85; ATCC 28923; IMI 330183	–	Decaying leaf	Florida, Miami, Bear Cut, US; 1970	I.M. Master & J.W. Fell; Bennett & Thines 2019	HQ665279	HQ643220	–	–	–	–
S. nakagiriі[b], ex-type	CBS 127947	LT6456	Leaf litter of marsh grass (*Spartina alternifolia*)	Georgia, Sapelo Island, US; 2009	J. Hulvey; Hulvey et al. 2010	HQ232458	HQ232467	–	–	–	–
Aphanomyces euteiches[b]	CBS 156.73; IMI 170485	–	*Pisum sativum*, root	NO	L. Sundheim; n.a.	HQ665132	HQ643117	–	–	–	–

n.a. = not available.

[a] Abbreviations of isolates and culture collections: ATCC = American Type Culture Collection, Manassas, USA; CBS = Centraalbureau voor Schimmelcultures, Utrecht, Netherlands; IMI = CABI Bioscience, UK; PD = Phytophthora Database (http://www.phytophthoradb.org); WPC = World Phytophthora Collection, University of California Riverside, USA; other isolate names and numbers are as given by the collectors and on GenBank, respectively.

[b] Isolates used in the phylogenetic studies.

[c] Isolates used in the morphological studies.

[d] Isolates used in the temperature-growth studies.

[e] Isolate only used for sporangial measurements.

[f] Abbreviations of country names: AU = Australia; BR = Brazil; CA = Canada; DE = Germany; ES = Spain; FR = France; IL = Israel; IT = Italy; JP = Japan; NL = Netherlands; NO = Norway; PH = Philippines; PK = Pakistan; PT = Portugal; TH = Thailand; TW = Taiwan; US = United States of America.

Table 2 Overview of PCR conditions and details of primers used for amplification and sequencing of oomycete isolates.

Locus	Primer names	Primer sequences (5'-3')	Orientation	Annealing temperature (°C)	Extension time (s)	Reference for primer sequences
LSU[a,b]	CTB6	GCATATCAATAAGCGGAGG	Forward	53	20	Garbelotto et al. (1997);
	LR3[e]	CCGTGTTTCAAGACGGG	Reverse			Hopple & Vilgalys (1994)
	LR3R[e]	GTCTTGAAACACGGACC	Forward			
	LR7	TACTACCACCAAGATCT	Reverse			
ITS[a]	ITS1	TCCGTAGGTGAACCTGCGG	Forward	63	12	White et al. (1990);
	ITS4	TCCTCCGCTTATTGATATGC	Reverse			Cooke et al. (2000)
	ITS6[f]	GAAGGTGAAGTCGTAACAAGG	Forward			
btub[a]	TUBUF2	CGGTAACAACTGGGCCAAGG	Forward	68	12	Kroon et al. (2004)
	TUBUR1	CCTGGTACTGCTGGTACTCAG	Reverse			
hsp90[a]	HSP90_F1int	CAAGGTGATCCCGGACAAGGC	Forward	66	15	Blair et al. (2008)
	HSP90R1	ACACCCTTGACRAACGACAG	Reverse			
tigA[c]	Tig_FY	TCGTGGGCGGYAAYTGGAA	Forward	60	120	Blair et al. (2008)
	Tig_rev[e]	CCGAAKCCGTTGATRGCGA	Reverse			
	G3PDH_for[e]	TCGCYATCAACGGMTTCGG	Forward			
	G3PDH_rev	GCCCCACTCRTTGTCRTACCAC	Reverse			
rpl10[a]	60SL10_for	GCTAAGTGTTACCGTTTCCAG	Forward	64	7	Martin & Tooley (2003)
	60SL10_rev	ACTTCTTGGAGCCCAGCAC	Reverse			
cox1	OomCoxI-Levup[a]	TCAWCWMGATGGCTTTTTTCAAC	Forward	60	10	Robideau et al. (2011)
	OomCoxI-Levlo[a]	CYTCHGGRTGWCCRAAAAACCAAA	Reverse			
	COXF4N[c]	GTATTTCTTCTTTATTAGGTGC	Forward	50	65	Kroon et al. (2004)
	COXR4N[c]	CGTGAACTAATGTTACATATAC	Reverse			
nadh1[c]	NADHF1	CTGTGGCTTATTTTACTTTAG	Forward	50	65	Kroon et al. (2004)
	NADHR1	CAGCAGTATACAAAAACCAAC	Reverse			
rps10[d]	rps10_DB_FOR	GTTGGTTAGAGYARAAGACT	Forward	48	30	Foster et al. (2021)
	rps10_DB_REV	RTAYACTCTAACCAACTGAGT	Reverse			

[a] PCR protocol 1: 20 µL volume containing 10.4 µL H_2O, 4 µL Q5 Reaction Buffer (5X), 1 µL of each primer (10 µM), 0.4 µL deoxynucleotide (dNTP) mixture (Meridian Bioscience, Memphis, USA) (2.5 mM each), 0.2 µL of Q5 High-Fidelity DNA Polymerase (2 U/µL) (New England Biolabs, Ipswich, USA), and 3 µL of gDNA (3–60 ng). Initial denaturation for 30 s at 98 °C; 35 cycles consisting of 5 s at 98 °C, 20 s at optimised annealing temperature for each primer set, optimised length of extension at 72 °C; 2 min at 72 °C for final extension.

[b] Double concentration of Q5 polymerase.

[c] PCR protocol 2: 20 µL volume containing 10 µL H_2O, 4 µL PrimeSTAR GXL Buffer (5X), 0.8 µL of each primer, 1.6 µL dNTP mixture, 0.4 µL PrimeSTAR GXL DNA Polymerase (1.25 U/µL) (TaKaRa Bio, Kusatsu, Shiga, Japan), and 3 µL of gDNA. Initial denaturation for 5 s at 98 °C; 35 cycles consisting of 10 s at 98 °C, 15 s at optimised annealing temperature, optimised length of extension at 68 °C; 5 min at 68 °C for final extension.

[d] PCR protocol 3: 20 µL volume containing 6.2 µL H_2O, 10 µL One*Taq* Hot Start Quick-Load 2X Master Mix with Standard Buffer (New England Biolabs, Ipswich, USA) 0.4 µL of each primer, and 3 µL of gDNA. Initial denaturation for 5 s at 98 °C; 35 cycles consisting of 30 s at 98 °C, 30 s at optimised annealing temperature, optimised length of extension at 72 °C; 7 min at 72 °C for final extension.

[e] Primers used exclusively for sequencing.

[f] Two primer combinations were used: ITS1/ITS4 or ITS6/ITS4.

strategy (all other loci). The ITS alignments in this study were manually edited and adjusted.

Bayesian Inference (BI) analysis was performed using MrBayes v. 3.2.7 (Ronquist & Huelsenbeck 2003) into partitions with the GTR Gamma + I nucleotide substitution model. Four Markov chains were run for 10 M generations, sampling every 1 000 steps, and with a burn in at 6 000 trees. Maximum-Likelihood (ML) analyses were carried out using raxmlGUI v. 2.0 (Edler et al. 2021) with a GTR Gamma + I nucleotide substitution model. There were 10 runs of the ML and bootstrap (thorough bootstrap) analyses with 1 000 replicates used to test the support of the branches.

Phylogenetic trees were visualized in TreeGraph2 v. 2.15.0-887 beta (Stöver & Müller 2010) and/or MEGA X v. 10.2.6 (Kumar et al. 2018) and edited in figure editor programs.

All datasets and original trees deriving from BI and ML analyses were deposited in the Dryad Digital Repository (https://datadryad.org; https://doi.org/10.5061/dryad.gf1vhhmr2).

Morphology of asexual and sexual structures

Characteristic morphological features of sporangia, oogonia, oospores, antheridia, chlamydospores, hyphal swellings and aggregations of the eight new *Halophytophthora* species and *H. avicennae* were recorded and compared with each other.

Sporangia formation and zoospore release were induced using a modified protocol of Nakagiri et al. (1994), Jesus et al. (2016) and Jung et al. (2017c). Two 12–15 mm square discs were cut from the growing edge of a 2–5-d-old V8A colony and submerged in a 90 mm diam Petri dish in 50 % non-sterile seawater. The Petri dishes were incubated at 20 °C in natural light and the water was changed after c. 6 h. Shape and special features of sporangia and the formation of hyphal swellings and aggregations were recorded after 18–48 h depending on the isolate. For each isolate 50 fully mature sporangia and 20 encysted zoospores and exit pores, chosen at random, were measured at ×400 using a compound microscope (Axio Imager. Z2), a digital camera (AxioCam ICc3) and a biometric software (ZEN) (all Zeiss, Jena, Germany).

Gametangia formation (oogonia and antheridia) and their characteristic features were examined after 21–30 d growth at 20 °C in the dark on V8A. For each non-sterile isolate each 50 oogonia, oospores and antheridia chosen at random were measured under a compound microscope at ×400. The oospore wall index was calculated according to Dick (1990).

Colony morphology, growth rates and cardinal temperatures

Colony growth patterns of all eight *Halophytophthora* species were described from 7-d-old cultures grown at 20 °C in the dark in 90 mm plates on sCA, vegetable juice seawater agar (sV8A), and potato dextrose seawater agar (sPDA; Oxoid Ltd., UK) prepared like normal CA, V8A and PDA (Erwin & Ribeiro 1996, Jung & Burgess 2009, Jung et al. 2017c) but with 50 % seawater.

Temperature-growth relationships were determined by subculturing three to five representative isolates per *Halophytophthora* species onto 90 mm sV8A Petri dishes and incubating them for 24 h at 20 °C to stimulate onset of growth (Jung et al. 1999). Three replicate plates per isolate were subsequently incubated at 10, 15, 20, 25, 27.5, 30, 32.5 and 35 °C. Radial growth was recorded daily for 5 d or until the isolate almost reached the edge of the Petri dish, along two lines drawn to overlap in the centre of the inoculum plug at right angles. The mean growth rates (mm/d) were calculated and the cardinal temperatures established. Petri dishes showing no growth at 27.5, 30, 32.5 and 35 °C were re-incubated at 20 °C to check for viability and determine the lethal temperature (Jung et al. 2017d).

RESULTS

Phylogenetic analysis

For all three datasets the ML and BI analyses produced phylogenetic trees with similar topologies. Since the BI analyses provided higher support values than the ML analyses for the deeper nodes and partly also for the terminal nodes the BI trees are presented with both BI Posterior Probability values and ML bootstrap values included (Fig. 2–4, Dryad dataset: https://doi.org/10.5061/dryad.gf1vhhmr2). The LSU dataset included 22 isolates of nine new *Halophytophthora* taxa from Portugal and eight described *Halophytophthora* species, 21 unidentified *Halophytophthora* isolates and 15 isolates from representative species of other genera in the *Peronosporaceae*, *Pythiaceae* and *Salisapiliaceae*. In the LSU analysis *Halophytophthora* s.str. resided in sister position to *Phytophthora* and revealed a structure of eight phylogenetic clades which are designated here as Clades 1 to 8 (Fig. 2). Clade 1 comprised the ex-type isolate of *H. batemanensis* from New South Wales, Australia, 11 unidentified isolates from the Philippines which most likely belong to *H. batemanensis* (2–4 bp differences), three further isolates from the Philippines (DGPBL2, PSQNBL3 and PSQNYB2) belonging to an undescribed species, and a group of three isolates from Brazil (CCIBt4143 and CCIBt4146) and Florida (CBS 152.96) which were previously assigned to *H. vesicula* and constitute two or three new species. Clade 2 included two undescribed taxa from the Philippines and clustered in sister position to Clade 1 while Clades 3, 4, 5, 7 and 8 each contained only one species, *H. insularis*, *H. avicennae*, *H. fluviatilis*, *H. souzae* and the distinct undescribed *Halophytophthora* sp. PNGLYBE, respectively (Fig. 2). All nine new taxa from Portugal resided in Clade 6 together with the ex-type isolates of *H. vesicula* (CBS 393.81) and *H. polymorphica* (CBS 680.84), *Halophytophthora* sp. CLE33, an undescribed species from California related to *H. vesicula* and *H. lateralis* from Portugal, two new species related to *H. polymorphica*, *Halophytophthora* sp. PQ1YB from the Philippines and *Halophytophthora* '*polymorphica*' CCIBt 4112 from Brazil, and two other potentially new species from Georgia, USA, *Halophytophthora* sp. 1 LT6430 and *Halophytophthora* sp. 2 LT6445, both related to *H. brevisporangia* and *H. celeris* from Portugal. The LSU sequences of *H. vesicula* and *H. lateralis* were identical. Both the deepest and second deepest nodes within *Halophytophthora* s.str. were highly supported. A polytomy at the second deepest node indicated either an ancient radiation or a character conflict. '*Halophytophthora*' *exoprolifera* was basal to the *Halophytophthora-Phytophthora-Nothophytophthora* cluster (Fig. 2) and belongs to an undescribed genus.

The BI and ML analyses of the ITS dataset comprising 61 *Halophytophthora* s.str. isolates confirmed the LSU clade structure of the genus expanding it by two further clades designated here as Clades 9 and 10 (Fig. 3). Clade 1 again contained the *H. batemanensis* ex-type, 11 isolates from the Philippines and Japan which should be assigned to *H. batemanensis*, isolate DGPBL2 from the Philippines belonging to an undescribed species, and three isolates from Brazil (CCIBt 4142 and CCIBt 4144) and Florida (CBS 152.96) previously assigned to *H. vesicula* and representing one or two new species (Fig. 3). Different from the LSU analysis the distinct *Halophytophthora* sp. PNGLYBE from Clade 8 resided in sister position to the latter cluster from Clade 1. Clades 1 and 2, the latter represented by an undescribed species comprising isolate BCCYBL1 from the Philippines and isolate IMB147 from Taiwan which was previously assigned to *H. vesicula*, constituted sister clades as in the LSU analysis. *Halophytophthora avicennae* (Clade 4) and *H. fluviatilis* (Clade 5) formed a polytomy together with the common ancestor of Clades 1 and 2 (Fig. 3). This four-clades cluster formed another polytomy together with Clades 3, 6, 7, 10 and the common ancestor of Clades 7 and 9. Clade 9 included the undescribed *Halophytophthora* sp. 2 KC-2014 from a stream in Washington State, USA, and resided in sister position to the Clade 7 species *H. souzae* from Brazil whereas Clade 10 contained the undescribed taxon *Halophytophthora* sp. Portugal_9 (Fig. 3). As in the LSU phylogeny, Clade 6 comprised nine new species from Portugal, the ex-types of *H. vesicula* and *H. polymorphica*, an undescribed species represented by the Brazilian isolate CCiBt 4112, previously assigned to *H. polymorphica*, and 11 unidentified isolates (Fig. 3). *Halophytophthora* sp. 1 KC-2014 from a stream in Washington State, USA, belongs to a new species related to *H. lusitanica* (15 bp differences = 1.2 %) while the undescribed *Halophytophthora* sp-4 (isolate PD6234625) from the Thau lagoon in Southern France resided in a basal position to this cluster. The informally designated *Halophytophthora* sp. Zostera (isolate CBS 140648) was identical to *Halophytophthora* sp-3 (isolate CBS 140657) from *Z. marina* in the North Sea and most likely belongs to *H. lateralis* (1 bp difference) which clustered in sister position to *H. vesicula* differing from the latter at 39 positions (= 3.1 %). This cluster together with a cluster comprising *H. thermoambigua*, *H.* sp. thermoambigua-like, *H. polymorphica* and *Halophytophthora* '*polymorphica*' CCIBt 4112 constituted a distinct subclade designated here as Subclade 6a (Fig. 3). *Halophytophthora thermoambigua* and *H.* sp. thermoambigua-like are sister species differing in ITS at 7–9 positions. Subclade 6b contained a cluster comprising the sister species *H. frigida* and *H. sinuata* from Portugal and a larger cluster with an undescribed species from the German North Sea coast (*Halophytophthora* sp. 1 of Nigrelli & Thines 2013; isolates EMTD10 and EMTS19) residing in a basal position of a cluster containing *H. macrosporangia*, *H. brevisporangia* and *H. celeris* from Portugal and five unidentified isolates. Similar to the LSU analysis, *H.* sp. 2 LT6465 from Georgia, USA, constituted a new species basal to a cluster which included the two sister species *H. brevisporangia* and *H. celeris* from Portugal, *H.* sp. 1 LT6430 from Georgia and three isolates from the North Sea (CBS 140651, EMTD7 and EMTD12). With differences at 7–12 positions *H.* sp. 1 LT6430 from Georgia might belong to *H. brevisporangia* or to a closely related unknown species whereas the 5–6 polymorphisms differentiating isolates CBS 140651 (*Halophytophthora* sp-1), EMTD7 and EMTD12 (both *Halophytophthora* sp. 2 of Nigrelli

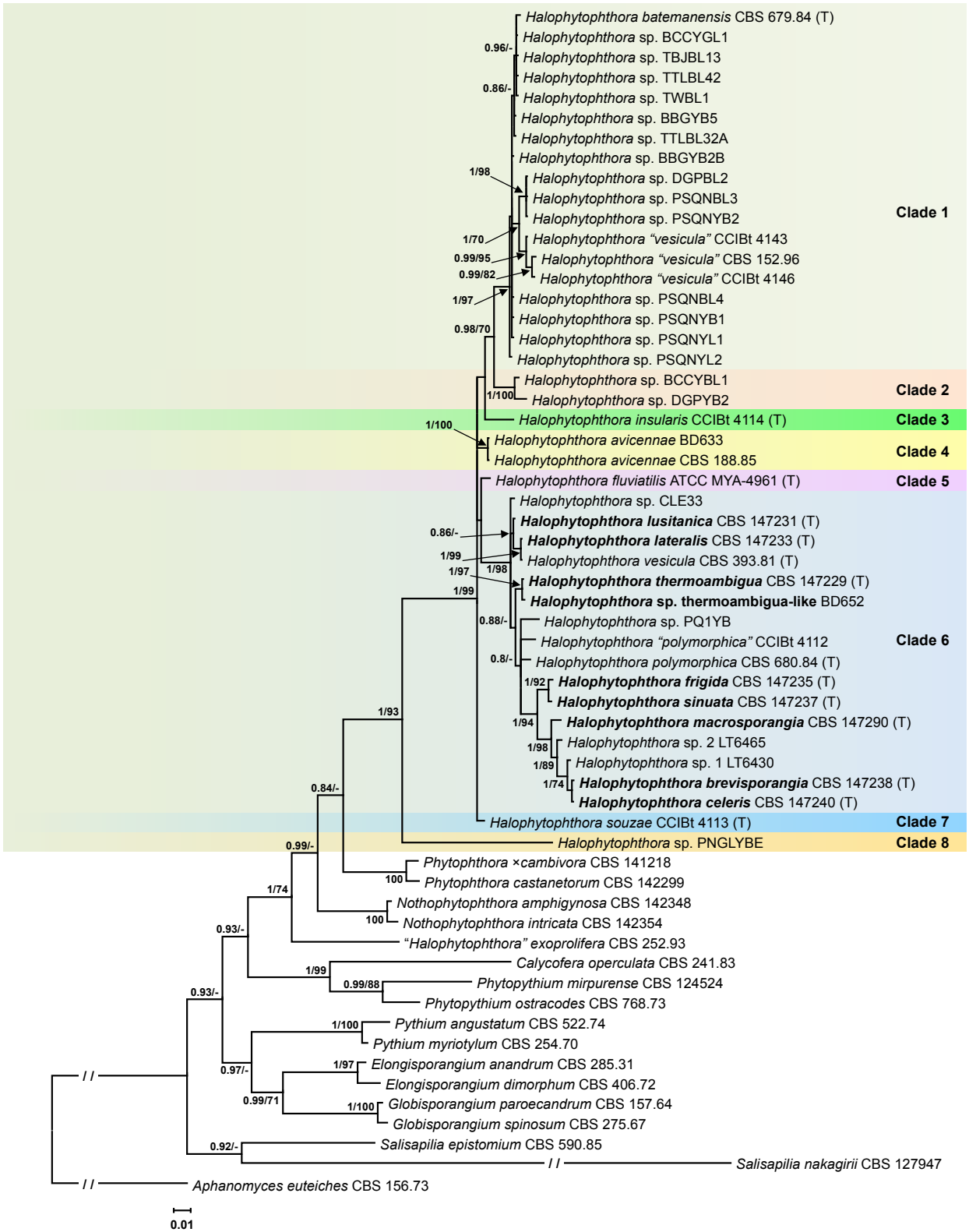

Fig. 2 Fifty percent majority rule consensus phylogram derived from Bayesian inference analysis of an LSU dataset of *Halophytophthora* s.str. and representative species from related genera in the *Peronosporaceae*, *Pythiaceae* and *Salisapiliaceae*. Bayesian posterior probabilities and ML bootstrap values (in %) are indicated but not shown below 0.80 and 70 %, respectively. *Aphanomyces euteiches* was used as outgroup taxon. Scale bar indicates 0.01 expected changes per site per branch.

& Thines 2013) from the Portuguese isolates of *H. celeris* are most likely within the variation of the latter species.

When the phylogeny of the nine new *Halophytophthora* taxa from Portugal within Clade 6 was analysed with the 9-partition dataset (ITS-LSU-*rpl10-Btub-hsp90-tigA-cox1-nadh1-rps10*), the Portuguese isolates formed nine fully supported distinct clades (Fig. 4). Within Subclade 6a, *H. lateralis* with *H. lusitanica* and *H. thermoambigua* with *H.* sp. thermoambigua-like clustered in sister position to each other with both clusters being well supported in both analyses and *H. polymorphica* residing in a basal position to them. Within Subclade 6b, *H. frigida* and *H. sinuata* clustered in sister position to each other while the sister species *H. brevisporangia* and *H. celeris* formed another cluster together with *H. macrosporangia* which resided in a basal position (Fig. 4). Across the 8 759 character multigene alignment there were 637 unique polymorphic sites (7.3 %) within Clade 6.

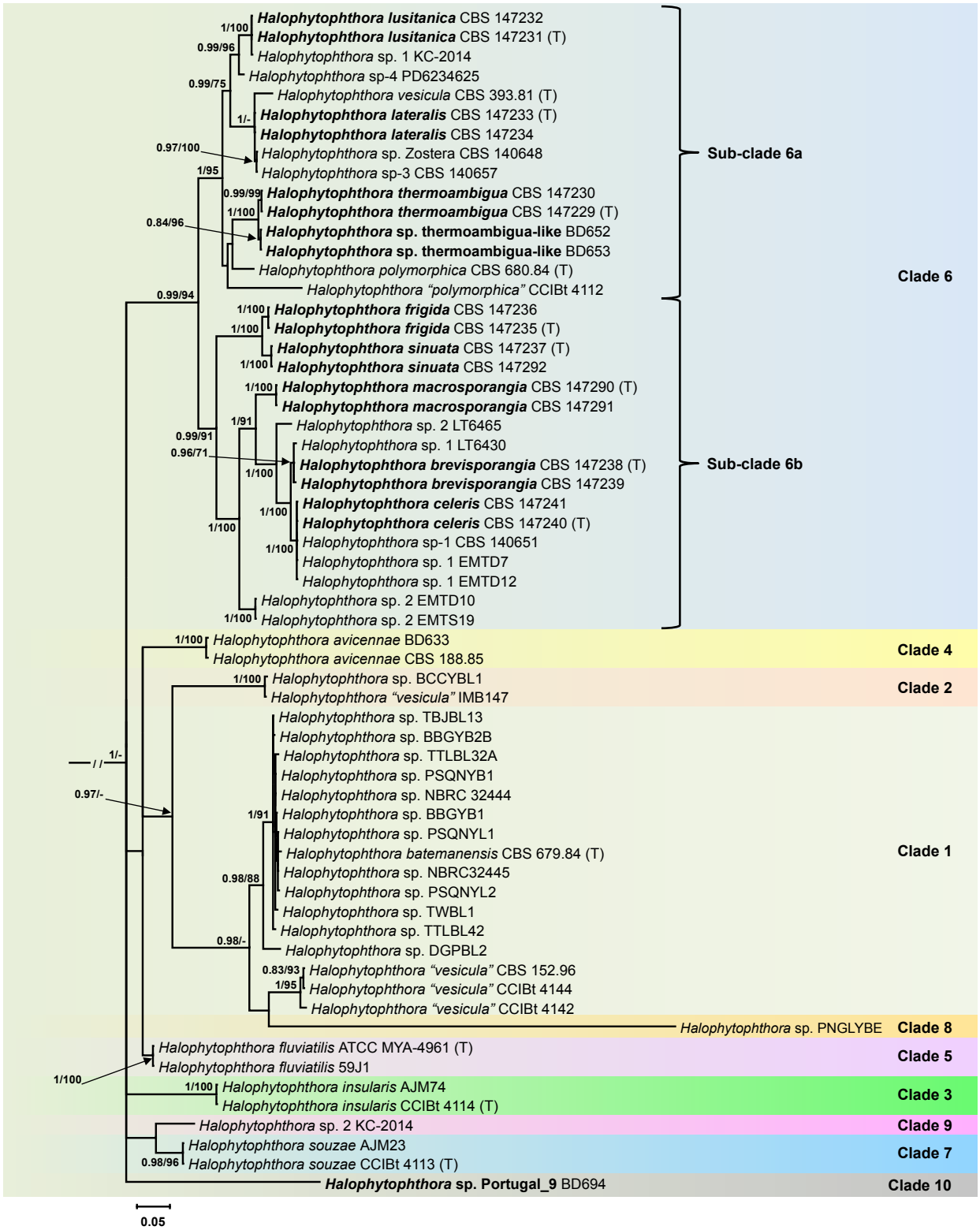

Fig. 3 Fifty percent majority rule consensus phylogram derived from Bayesian inference analysis of an ITS dataset of *Halophytophthora* s.str.. Bayesian posterior probabilities and ML bootstrap values (in %) are indicated but not shown below 0.80 and 70 %, respectively. *Phytophthora castanetorum* (CBS 142.299) and *P.* × *cambivora* (CBS 141.218) were used as outgroup taxa (not shown). Scale bar indicates 0.05 expected changes per site per branch.

Halophytophthora brevisporangia, *H. celeris*, *H. frigida*, *H. lateralis*, *H. lusitanica*, *H. macrosporangia*, *H. polymorphica*, *H. sinuata*, *H. thermoambigua* and *H.* sp. thermoambigua-like had 55–61, 32–36, 50–51, 68–69, 53–71, 76–82, 61, 52–63, 23–70 and 29–32 unique polymorphisms, respectively, and differed from each other at 82–501 positions corresponding to sequence similarities of 94.3–99.1 %. The sister species *H. lateralis* with *H. lusitanica*, *H. frigida* with *H. sinuata*, *H. brevisporangia* with *H. celeris*, and *H. thermoambigua* with *H.* sp. thermoambigua-like shared 12, 56, 63 and 38–41 unique polymorphisms and differed from each other at 267–283, 170–178, 82–90 and 106–125 positions, respectively, corresponding to sequence similarities of 96.8–96.9, 98–98.1, 98.6–98.8 and 99–99.1 %, respectively. The ITS alignment contained several indels of up to 29 characters length which were partly shared between the Clade 6 species and also with *H. fluviatilis* (Clade 5) but were absent in *H. avicennae* (Clade 4). In *hsp90* two isolates of *H. sinuata* (BD656 and BD943) had a 6 bp insertion at positions 433–438 whereas *H. brevifolia*, *H. celeris* and *H. fluviatilis* shared a 3 bp deletion at positions 497–499.

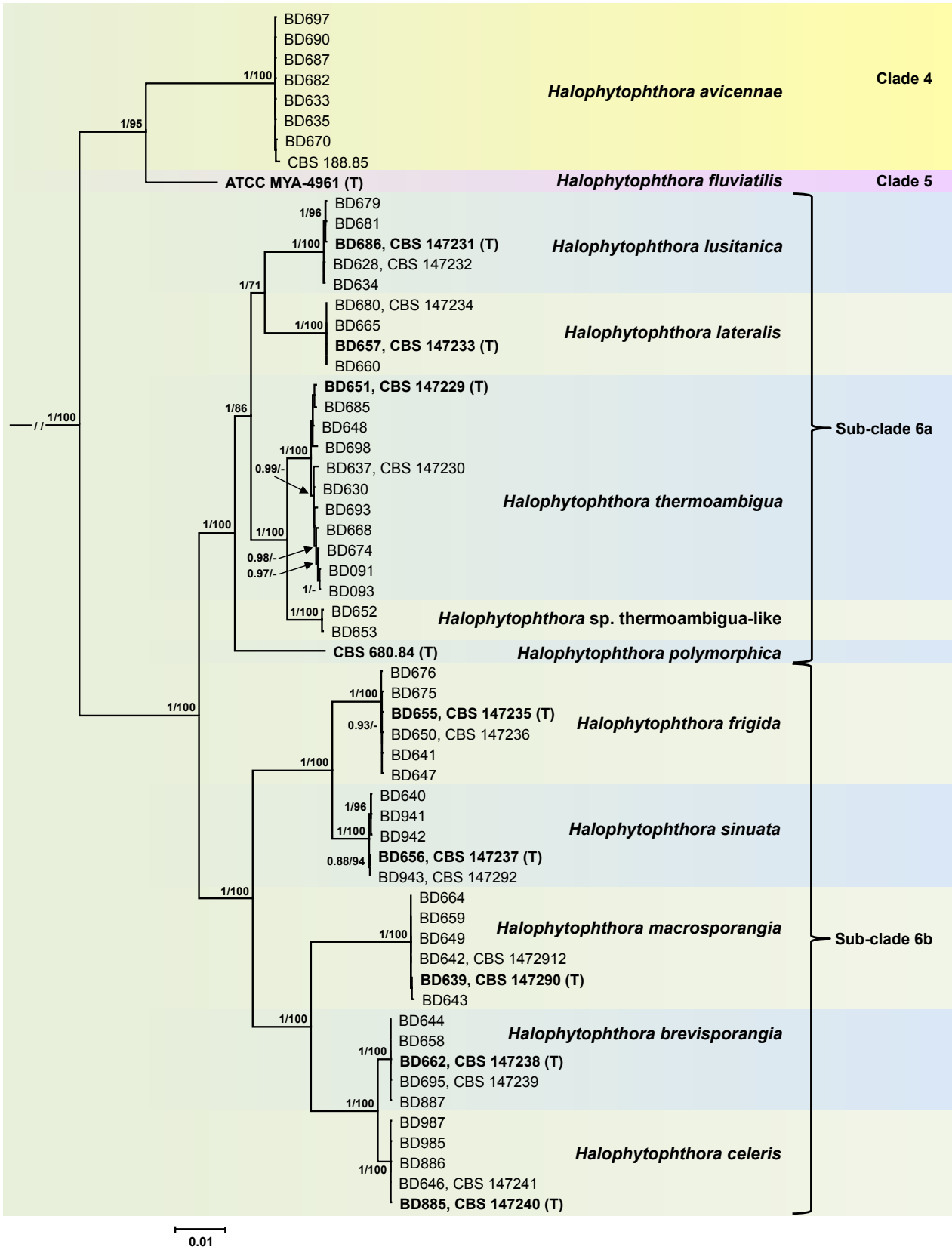

Fig. 4 Fifty percent majority rule consensus phylogram derived from Bayesian inference analysis of a concatenated nine-locus (ITS-LSU-*rpl10*-*Btub*-*hsp90*-*tigA*-*cox1*-*nadh1*-*rps10*) dataset of *Halophytophthora* s.str. Clades 4, 5 and 6. Bayesian posterior probabilities and ML bootstrap values (in %) are indicated but not shown below 0.80 and 70 %, respectively. *Phytophthora castanetorum* (CBS 142.299) and *P.* × *cambivora* (CBS 141.218) were used as outgroup taxa (not shown). Scale bar indicates 0.01 expected changes per site per branch.

Heterozygous positions were present in all three nuclear single-copy genes, *Btub*, *hsp90* and *tigA*, and in all Clade 6 species except of *H. frigida*. In the other nine species the frequencies of heterozygous sites varied considerably between and within species. While *H. lateralis*, *H. sinuata*, *H. polymorphica*, *H. macrosporangia*, *H.* sp. thermoambigua-like, *H. celeris* and *H. lusitanica* had in total only 2, 2, 3, 5, 6 and 13 heterozygous sites across the 3450 character alignment, *H. brevisporangia* and *H. thermoambigua* were heterozygous at 37 and 49 positions potentially indicating hybrid origin. Interestingly, the frequency of heterozygous sites varied considerably between individual isolates of *H. thermoambigua* with one isolate (BD637) being

Table 3 Morphological characters and dimensions (µm), cardinal temperatures (°C) and temperature-growth relations (mm/d) of eight new *Halophytophthora* species. Most discriminating characters are highlighted in **bold**.

	H. brevisporangia	*H. celeris*	*H. frigida*	*H. lateralis*	*H. lusitanica*	*H. macrosporangia*	*H. sinuata*	*H. thermoambigua*
No. of isolates	3[a]	3[a]	7[a]	4[a]	6[a]	7[a]	6[a]	11[a]
Sporangia	ovoid 86 %, obpyriform, (distorded, ellipsoid, obturbinate)	ovoid 60 %, obpyriform, (subglobose, limoniform)	obpyriform 83 %, ovoid, (distorted, obturbinate, limoniform, ellipsoid)	**ovoid 95 %** (subglobose, ovoid-obpyriform, distorted)	obpyriform 54 %, ovoid (ellipsoid, limoniform, obturbinate, distorted)	obpyriform 56 %, ovoid, (subglobose, distorted, peanut-shaped)	obpyriform 85 %, ovoid, (distorted, limoniform), **often asymmetric**	obpyriform 50 %, ovoid, (limoniform, ellipsoid, ampulliform, distorted)
l×b mean	**57.6±10.9** × **42.1±8.8**	**60.5±12.5** × **46.1±10.4**	80.4±19.3 × 50.1±13.8	75.9±16.1 × 52.4±12.5	84.0±15.8 × 54.3±10.6	**97.5±24.8** × **55.0±14.8**	74.1±19.5 × 44.0±12.6	75.3±15.7 × 48.1±9.7
range of isolate means	54.7–59.7 × 39.9–45.9	56.2–64.6 × 43.9–47.3	72.7–85.7 × 44.5–57.1	67.7–89.5 × 45.4–63.6	76.2–95.4 × 47.1–60.2	76.8–118.9 × 42.9–67.4	56.9–82.1 × 32.5–51.4	69.2–83.2 × 40.3–57.1
total range	31.2–101.4 × 20.9–78.8	29.4–92.8 × 20.8–78.0	32.4–150.7 × 18.8–98.1	41.6–122 × 22.8–100.3	40.5–162.5 × 25.4–86.3	58–186.7 × 32.3–106.3	28.1–129.2 × 19.8–89.5	43.4–185.3 × 25.3–83.9
l/b ratio	**1.4** ± **0.1**	**1.3** ± **0.1**	1.6 ± 0.3	1.5 ± 0.2	1.6 ± 0.3	**1.8** ± **0.4**	1.7 ± 0.3	1.6 ± 0.3
apex[b]	non-papillate, often pointed, **2 apices not observed**	non-papillate, often pointed, 2 apices rare	non-papillate, pointed to **protuberant**, some curved or 2 apices	non-papillate or **semi-papillate**, sometimes pointed or 2 apices	non-papillate or rarely semipapillate, sometimes 2 apices or curved	non-papillate, sometimes pointed or 2 apices	non-papillate, often pointed, sometimes 2 apices	non-papillate, pointed to **protuberant**, some curved, **2 apices common**
special features	basal plug frequent, lateral attachment occasionally	**protruding basal plugs,** sometimes intercalary or lateral attachment (13 %)	**frequently intercalary** or lateral attachment	**lateral attachment 41.5 %**, sometimes protruding basal plug	some with lateral attachment, hyphal beak or basal plug	sometimes lateral attachment, **small vacuoles**, **swelling close to base**	lateral attachment 31.4 %, often 1 or more **vacuoles**	some intercalary, **lateral attachment 38.4 %**, basal plug common
external proliferation	**common, lax sympodia**	rare	infrequent	infrequent	rare	infrequent	rare	infrequent
zoospore release	through semi-persistent elongated vesicle	through semi-persistent elongated vesicle	through semi-persistent elongated vesicle	through semi-persistent elongated vesicle	through semi-persistent elongated vesicle	through semi-persistent elongated vesicle	**direct** or through semi-persistent vesicle	through semi-persistent elongated vesicle
exitpores	9.8 ± 1.7	10.5 ± 1.6 µm	9.5 ± 1.6	12.6 ± 2.4	10.6 ± 2.1	10.3 ± 1.7	8.9 ± 1.5	10.3 ± 2.3
zoospore cysts	7.9 ± 0.7	8.8 ± 0.8	9.1 ± 2.0	7.9 ± 0.7	8.2 ± 0.9	8.2 ± 2.1	7.5 ± 1.1	8.6 ± 0.9
Breeding system	sterile	sterile	**homothallic**	sterile	sterile	**homothallic**	**homothallic**	sterile
Oogonia	–	–	smooth-walled, **some slightly ornamented**	–	–	smooth-walled	**wavy to slightly verrucose goldenbrown wall**	–
mean diam			47.8 ± 4.0			48.2 ± 4.6	54.2 ± 3.8	
range of isolate means			43.0–49.9			46.7–49.2	51.6–55.6	
total range			32.0–58.6			18.4–58.7	39.4–64.3	
Oospores	–	–	99.3 % plerotic	–	–	100 % plerotic	95 % plerotic	–
mean diam			45.3 ± 4.1			43.7 ± 4.2	47.5 ± 3.7	
total range			29.1–54.9			30.1–54.5	33.9–57.6	
wall diam			2.2 ± 0.5			**1.7** ± 0.4	**2.9** ± 0.6	
oospore wall index			0.26 ± 0.05			0.22 ± 0.04	0.32 ± 0.05	
Abortion rate			22.7 % (2–50 %)			**41.5 %** (14–82 %)	**4.2 %** (0–13 %)	
Antheridia	**–**	**–**	paragynous, **mostly intricate stalks**	**–**	**–**	paragynous intricate stalks occasionally	paragynous, very rarely intricate stalks	**–**
size			18.3±3.6 × 10.3±2.7			15.2±3.1 × 7.8±1.7	14.9±2.8 × 11.6±1.8	
Hyphal swellings	–	infrequent, triangular	rare	–	rare	infrequent	–	**infrequent; 33.8 ± 9.5**
Hyphal aggregations	–	**common**	–	–	–	–	–	–

Table 3 (cont.)

	H. brevisporangia	*H. celeris*	*H. frigida*	*H. lateralis*	*H. lusitanica*	*H. macrosporangia*	*H. sinuata*	*H. thermoambigua*
Colonies on sV8A	faintly radiate, limited cottony mycelium	**uniform, limited cottony**	faint radiate to petaloid, limited aerial or cottony	stellate, limited aerial mycelium	petaloid-faintly petaloid, limited aerial mycelium	faint stellate, limited aerial, submerged edge	uniform, limited aerial mycelium	stellate-radiate or petaloid, limited aerial
Colonies on sCA	uniform, limited cottony mycelium	uniform, limited cottony	similar to sV8A	faintly petaloid, limited aerial mycelium	petaloid-faintly petaloid, limited aerial mycelium	uniform, limited aerial, submerged edge	faintly radiate, limited aerial mycelium	stellate-radiate or petaloid, limited aerial
Colonies on sPDA	uniform or petaloid, dense-felty appressed	faint petaloid – petaloid, felty, cottony margin	faint petaloid, felty-cottony, submerged edge	dense-felty, uniform	felty, uniform, ring of collapsed aerial mycelium	stoloniferous-petaloid, appressed-submerged	faintly petaloid, cottony	felty, petaloid
Maximum temperature	32.5	32.5	**25**	32.5	32.5	**27.5**	**27.5**	32.5
Optimum temperature	25	25	**15** (20)	25	**25 (20, 27.5)**	**15, (20), 25**	25	**25 (20, 27.5)**
Growth rate sV8A 20 °C	**18.5 ± 1.3**	**20.4 ± 0.7**	8.3 ± 2.3	10.3 ± 0.7	7.3 ± 0.6	4.2 ± 1.1	14.9 ± 0.3	5.2 ± 1.2
Growth rate sCA 20 °C	**16.7 ± 0.5**	**17.0 ± 0.1**	9.4 ± 0.8	12.0 ± 0.4	6.9 ± 0.8	5.1 ± 1.4	12.8 ± 0.1	5.2 ± 1.4
Growth rate sPDA 20 °C	**13.3 ± 1.4**	**15.7 ± 0.3**	5.7 ± 0.6	9.8 ± 0.3	6.7 ± 0.4	4.1 ± 1.1	**13.3 ± 0.4**	5.0 ± 2.1

[a] Numbers of isolates included in the growth tests: *H. thermoambigua* - 5; *H. lusitanica* - 5; *H. lateralis* - 4; *H. frigida* - 5; *H. sinuata* - 5; *H. macrosporangia* - 5; *H. brevisporangia* - 3; *H. celeris* - 3.
[b] Apex in all 8 new *Halophytophthora* species becoming pseudo-papillate during zoospore differentiation due to the shrinkage of the protoplasm away from the apex.
– = character not observed; n.a. = not available.

Table 4 Morphological characters and dimensions (µm), cardinal temperatures (°C) and temperature-growth relations (mm/d) of the seven known species of *Halophytophthora* s.str. Most discriminating characters are highlighted in **bold**.

	H. avicennae	*H. avicennae*	*H. batemanensis*	*H. fluviatilis*	*H. insularis*	*H. polymorphica*	*H. souzae*	*H. vesicula*
Source / no. of isolates	Gerrettson-Cornell & Simpson (1984) / n.a.	this study / 7	Gerrettson-Cornell & Simpson (1984)) / n.a.	Yang & Hong (2014) / 6	Jesus et al. (2019) / 3	Gerrettson-Cornell & Simpson (1984) / n.a.	Jesus et al. (2019) / 3	Anastasiou & Churchland (1969) / n.a.
Sporangia	ovoid, obpyriform, ob-clavate, botuliform, reniform, distorted)	obpyriform 56%, ovoid (limoniform, distorted, obturbinate)	ovoid, ellipsoid, limoniform	globose-ovoid, (limoni-form, obovoid, distorted)	limoniform, ovoid, obpyriform	ovoid, obpyriform, variable, asymetric, distorted	limoniform, ovoid, obpyriform	ovoid, obpyriform, (fusiform, distorted)
l×b mean	75 × 31	65.5±10.6 × 43.8±8.5	64 × 48	**38.4±5.8** × **28.8±4.4**	71.1 × 51.6	72 × 58	93.5 × 56.5	**117** × **59**
range of isolate means	n.a.	56.1–71.3 × 36.9–50.9	n.a.	n.a.	n.a.	n.a.	n.a.	n.a.
total range	44–121 × 18–44	43.0–98.8 × 28.2–74.3	33–96 × 26–81	28.3–58.2 × 20.1–41.0	38.9–105.3 × 28.2–80.9	44–102 × 33–84	52.5–162.5 × 37.5–77.5	47–192 × 24–100
l/b ratio	2.6 (1.6–4.8)	1.5 ± 0.2	1.3 (1.1–1.6)	1.3	1.4	1.3 (1.0–1.6)	1.7	2.0
apex[a]	non-papillate, some-times pointed or 2 apices	non-papillate, some-times pointed (9.2%) or 2 apices	non-papillate, some-times pointed or protuberant	non-papillate, often protuberant	non-papillate, pointed, sometimes 2 apices	non-papillate, sometimes protuberant or 2 apices	non-papillate, pointed, often 2 apices	papillate, sometimes bi-papillate
special features	sometimes lateral attachment or 1–2 vacuoles	4% lateral attachment, 0.8% with 1–2 vacuoles	sometimes lateral attachment	often basal plug, wide base, or rarely vacuoles	usually basal plug	often lateral attachment, hyphal beak, 1–3 vacuoles	usually basal plug, often curved	
external proliferation	common	rare	rare	common, lax or compound sympodium	common	rare	infrequent	common, lax sympodia

Table 4 (cont.)

	H. avicennae	*H. avicennae*	*H. batemanensis*	*H. fluviatilis*	*H. insularis*	*H. polymorphica*	*H. souzae*	*H. vesicula*
zoospore release	directly or through variable persistent vesicle; operculum-like structure not reported[b]	through semi-persistent vesicle; operculum-like structure not observed	directly or through elongated persistent vesicle; operculum-like structure not reported[b]	**directly, no vesicle**	through semipersistent globose or elongated vesicle with operculum-like structure	directly or through persistent vesicle; operculum-like structure not reported[b]	through semipersistent globose or elongated vesicle with operculum-like structure	through semipersistent vesicle and **dehiscence tube**; operculum-like structure frequent
exitpores	10 (9–13)	10.6 ± 1.5	9 (7–15)	n.a.	n.a.	10 (7–12)	n.a.	n.a.
zoospore cysts	c. 8	8.8 ± 1.0	c. 8	n.a.	11.2 (10–12.5)	n.a.	10.2 (8.7–12.5)	n.a.
Breeding system	sterile	sterile	sterile	**homothallic**	sterile	sterile	**homothallic**	**homothallic**
Oogonia	–	–	–	**smooth-walled**	–	–	**smooth-walled**	**smooth-walled**
mean diam				28.2±2.6			38.6	**46.3**
range of isolate means				n.a.			n.a.	n.a.
total range				23.4–35.1			25–45	32.1–59.7
Oospores	–	–	–	plerotic	–	–	plerotic, yellow-brown	plerotic
mean diam				25.2±2.1			38.3	42.2
Total range				21.8–29.3			25–45	29.7–49.4
wall diam				n.a.			3 (2.5–5.0)	2.5–5.0
oospore wall index				n.a.			n.a.	n.a.
Abortion rate				n.a.			n.a.	n.a.
Antheridia	**–**	**–**	**–**	paragynous, intricate	–	–	paragynous, some amphigynous?	paragynous, 1–3
size				< 5			< 5	(15–25) 20.5 × (8–13) 9
Hyphal swellings	–	–	–	common, limoniform	n.a.	–	n.a.	reniform or tuberous
Hyphal aggregations	n.a.	–	n.a.	n.a.	n.a.	**infrequent**	n.a.	n.a.
Colonies on V8A	petaloid, scanty aerial mycelium	petaloid-faintly petaloid, limited aerial mycelium	petaloid, submerged	faintly striate, limited aerial, submerged	n.a.	petaloid, scanty aerial mycelium	n.a.	n.a.
Colonies on CMA	Coralloid, scanty aerial to submerged	n.a.	petaloid, submerged	n.a.	n.a.	radiate, submerged	n.a.	rosaceous, submerged, limited aerial
Colonies on PDA	no growth	n.a.	no growth	n.a.	n.a.	no growth	n.a.	n.a.
Maximum temperature	n.a.	32.5	n.a.	**29**	**35**	n.a.	c. 30	n.a.
Optimum temperature	n.a.	20	n.a.	**25**	**25**	n.a.	**15**	n.a.
Growth rate V8A 25 °C	2.8 (25 °C)	4.1 ± 0.5	3.8 (25 °C)	2.8	n.a.	4.3 (25 °C)	n.a.	n.a.
Growth rate CMA 25 °C	0.8 (25 °C)	n.a.	0.9 (25 °C)	n.a.	n.a.	2.8 (25 °C)	n.a.	1–2

[a] Apex in all 7 known *Halophytophthora* species becoming pseudo-papillate during zoospore differentiation due to the shrinkage of the protoplasm away from the apex.
[b] Operculum-like structure reported by Jesus et al. (2019) but not mentioned in the original description by Gerrettson-Cornell & Simpson (1984).
– = character not observed; n.a. = not available.

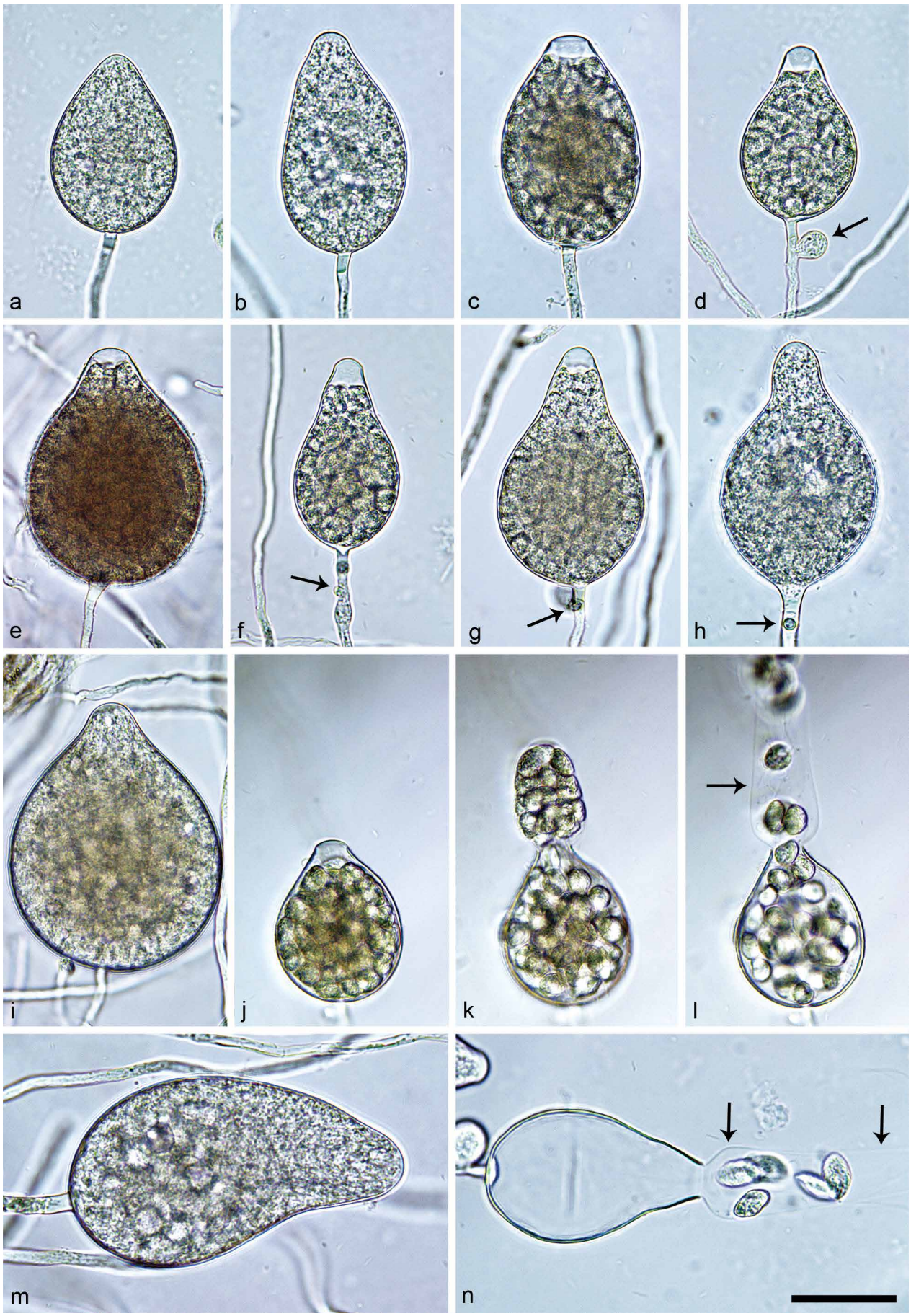

Fig. 5 Sporangia of *Halophytophthora brevisporangia* formed on saltwater V8 agar (sV8A) flooded with nonsterile 50 % seawater. — a–b. Non-papillate, with a conspicuous basal plug; a. ovoid; b. obpyriform; c–g. pseudo-papillate apex due to shrinkage of protoplasm before zoospore release; c. ovoid, d. obpyriform, with external proliferation (arrow); e. broad-ovoid with conspicuous basal plug; f–h. obpyriform, with external proliferation (arrows) and conspicuous basal plug; h. non-papillate; i. broad-ovoid, with non-papillate pointed apex; j–l. ovoid, becoming pseudo-papillate and then releasing zoospores through an elongated semi-persistent vesicle (arrow); m. elongated-obpyriform with non-papillate curved apex and a conspicuous basal plug; n. obpyriform, with a conspicuous basal plug and external proliferation, releasing zoospores through an elongated semi-persistent vesicle (arrows). — Scale bar = 30 µm, applies to a–n.

fully homozygous and the other eight isolates having between 1 and 25 heterozygous sites. In contrast to the nuclear genes, the mitochondrial *cox1*, *nadh1* and *rps10* genes contained no heterozygous sites.

Taxonomy

Morphological and physiological characters and morphometric data of the eight new *Halophytophthora* species and, for comparison, the seven known species of *Halophytophthora* s.str. are listed in Table 3, 4.

Halophytophthora brevisporangia T. Jung, C. Maia, G. Carella, M. Horta Jung, *sp. nov.* — MycoBank MB 838602; Fig. 5

Etymology. Name refers to the relatively short length of most sporangia.

Typus. Portugal, Parque Natural da Ria Formosa, Quelfes, isolated from a tidal pond in a coastal saltmarsh, *T. Jung*, 2015 (CBS H-24574 holotype, dried culture on sV8A, Herbarium CBS-KNAW Fungal Biodiversity Centre, CBS 147238 = BD662, ex-type culture). ITS and *cox1* sequences GenBank OK033641 and OK091206, respectively.

Sporangia, hyphal swellings and chlamydospores (Fig. 5) — Sporangia were not observed in solid agar but were abundantly produced in a mixture of distilled water and non-sterile seawater (1 : 1). They were produced terminally, mainly on unbranched sporangiophores (Fig. 5a–c, e, i, m) or in lax sympodia resulting from external proliferation (Fig. 5d, f–h, n). Sporangia were non-caducous and non-papillate becoming pseudo-papillate immediately before zoospore release due to shrinkage of protoplasm near the apex (Fig. 5c–g, j), often with a pointed apex (34 %; Fig. 5f–i). Sporangial shapes were mostly ovoid (86.0 %; Fig. 5a, c, e, i–l) and less frequently obpyriform or elongated obpyriform (11.5 %; Fig. 5c–d, f–h, m), distorted (1.0 %), ellipsoid (1.0 %) and obturbinate (0.5 %). Sporangia with two apices were not observed. A conspicuous basal plug was frequently formed (Fig. 5a–b, d–e, h, m–n) while lateral attachment of the sporangiophore occurred only occasionally. Sporangial dimensions averaged 57.6 ± 10.9 × 42.1 ± 8.8 µm with an overall range of 31.2–101.4 × 20.9–78.8 µm and a range of isolate means of 54.7–59.7 × 39.9–45.9 µm. The l/b ratio was 1.4 ± 0.1. Release of zoospores occurred through an exit pore of 9.8 ± 1.7 µm width into a semi-persistent elongated vesicle (Fig. 5j–l, n). Zoospore cysts measured 7.9 ± 0.7 µm. Hyphal swellings or chlamydospores were not observed.

Oogonia, oospores and antheridia — All four isolates of *H. brevisporangia* were self-sterile.

Colony morphology, growth rates and cardinal temperatures (Fig. 13, 15) — All isolates formed limited cottony mycelium on sV8A and sCA and dense-felty appressed mycelium on sPDA. Colonies showed faintly radiate and uniform patterns on sV8A and sCA, respectively, and were uniform or petaloid on sPDA (Fig. 13). All isolates tested shared the same optimum and maximum temperatures of 25 and 32.5 °C, respectively (Fig. 15). All isolates were not growing at 35 °C but resumed growth after being re-incubated at 20 °C. Therefore, the lethal temperature is > 35 °C. All isolates were fast growing with radial growth rates on sV8A at 20 and 25 °C of 18.5 ± 1.3 and 20.2 ± 2.1 mm/d, respectively (Fig. 15). On sCA and sPDA radial growth at 20 °C was 16.7 ± 0.5 and 13.3 ± 1.4 mm/d, respectively.

Additional specimens examined. Portugal, Sapal de Castro Marim / Rio Guadiana, Castro Marim, isolated from brackish water in the river estuary, *G. Carella & M. Horta Jung*, 2015; CBS 147239 = BD695; Parque Natural da Ria Formosa, Santa Luzia, isolated from a tidal channel in a coastal saltmarsh, *T. Jung*, 2015; BD644; Parque Natural da Ria Formosa, Quelfes, isolated from a tidal pond in a coastal saltmarsh, *T. Jung*, 2015; BD658.

Halophytophthora celeris T. Jung, C. Maia, G. Carella, M. Horta Jung, *sp. nov.* — MycoBank MB 838603; Fig. 6

Etymology. Name refers to the fast growth in culture (*celeris* Latin = fast).

Typus. Portugal, Parque Natural da Ria Formosa, Santa Luzia, isolated from a tidal channel in a coastal saltmarsh, *T. Jung*, 2015 (CBS H-24575 holotype, dried culture on sV8A, Herbarium CBS-KNAW Fungal Biodiversity Centre, CBS 147240 = BD885, ex-type culture). ITS and *cox1* sequences GenBank OK033645 and OK091210, respectively.

Sporangia, hyphal swellings and chlamydospores (Fig. 6) — Sporangia were not observed in solid agar but were readily produced in a mixture of distilled water and non-sterile seawater (1 : 1). Sporangia were non-papillate, often with a pointed apex (20.7 %; Fig. 6a, h), becoming pseudo-papillate immediately before releasing zoospores (Fig. 6b–f, i), non-caducous and formed usually terminally (Fig. 6a–b, d–e, g–l) on unbranched sporangiophores or sometimes intercalary (Fig. 6c) or on short lateral hyphae (Fig. 6f). External proliferation was only rarely observed. Sporangial shapes varied mainly between ovoid to broad-ovoid (60 %; Fig. 6a–d, f, h–l), obpyriform (30.7 %; Fig. 6g) and ovoid to obpyriform (7.3 %; Fig. 6e) whereas subglobose (1.3 %) and limoniform (0.7 %) sporangia were rare. Lateral attachment of the sporangiophore (13.3 %; Fig. 6a–b, f–h) and a conspicuous basal plug (Fig. 6a, e–g, i) sometimes protruding into the empty sporangium (Fig. 6l) were common, small hyphal beaks infrequent. Size of the sporangia averaged 60.5 ± 12.5 × 46.1 ± 10.4 µm with a total range of 29.4–92.8 × 20.8–78.0 µm, a range of isolate means of 56.2–64.6 × 43.9–47.3 µm and a l/b ratio of 1.3 ± 0.1. Zoospores were released through an exit pore with a diameter of 10.5 ± 1.6 µm and a semi-persistent elongated vesicle (Fig. 6j–l). Zoospore cysts averaged 8.8 ± 0.8 µm. Hyphal aggregations (Fig. 6m–n) were common while globose or triangular hyphal swellings (Fig. 6o) were occasionally formed. Chlamydospores were not observed.

Oogonia, oospores and antheridia — All isolates of *H. celeris* were self-sterile.

Colony morphology, growth rates and cardinal temperatures (Fig. 13, 15) — All isolates formed uniform colonies with sparse cottony mycelium on sV8A and sCA and dense-felty colonies with cottony margins and faintly petaloid to petaloid patterns on sPDA (Fig. 13). All three isolates included in the growth tests had similar optimum, maximum and lethal temperatures of 25, 32.5 and 35 °C, respectively (Fig. 15) and showed fast growth. Radial growth rates at 20 and 25 °C on sV8A were 20.4 ± 0.7 and 24.0 ± 0.4 mm/d, respectively (Fig. 15). Radial growth on sCA and sPDA at 20 °C was 17.0 ± 0.1 and 15.7 ± 0.3 mm/d, respectively.

Additional specimens examined. Portugal, Parque Natural da Ria Formosa, Santa Luzia, isolated from a tidal channel in a coastal saltmarsh, *T. Jung*, 2015; CBS 147241 = BD646, BD886.

Halophytophthora frigida T. Jung, C. Maia, G. Carella, M. Horta Jung, *sp. nov.* — MycoBank MB 838587; Fig. 7

Etymology. Name refers to the low optimum and maximum temperatures for growth.

Typus. Portugal, Parque Natural da Ria Formosa, Santa Luzia, isolated from a tidal pond in a coastal saltmarsh, *T. Jung*, 2015 (CBS H-24571 holotype, dried culture on sV8A, Herbarium CBS-KNAW Fungal Biodiversity Centre, CBS 147235 = BD655, ex-type culture). ITS and *cox1* sequences GenBank OK033652 and OK091217, respectively.

Sporangia, hyphal swellings and chlamydospores (Fig. 7a–h) — Sporangia were infrequently observed in solid agar but were abundantly produced in a mixture of distilled water and non-sterile seawater (1 : 1). They were usually formed terminally on mostly unbranched sporangiophores (Fig. 7a, c–h) or in lax sympodia of 2–3 sporangia although a few intercalary sporangia (Fig. 7b) could be observed in all isolates. Sporangia

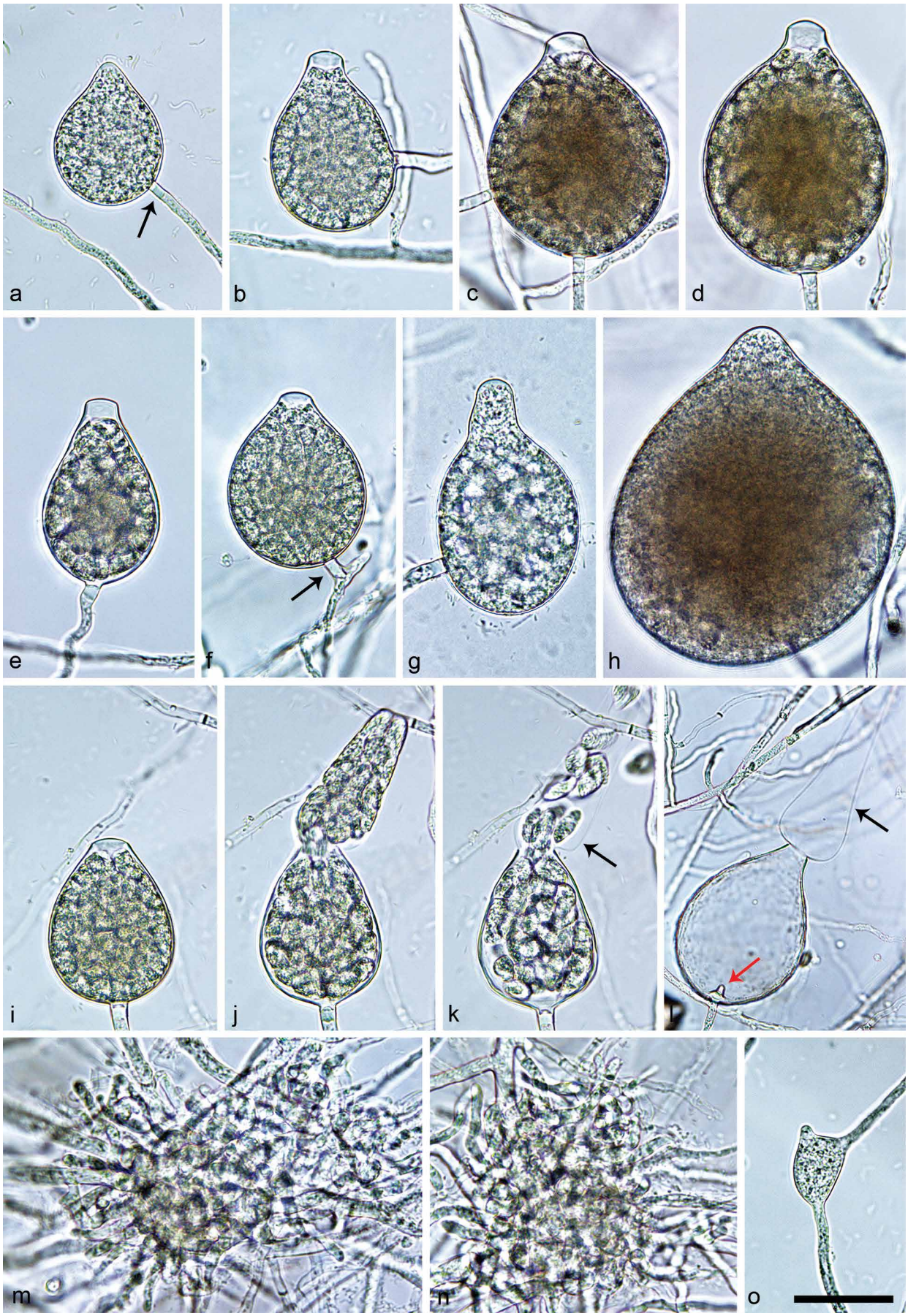

Fig. 6 Morphological structures of *Halophytophthora celeris*. — a–l. Sporangia formed on saltwater V8 agar (sV8A) flooded with nonsterile 50 % seawater, most of them with a conspicuous basal plug (a, d–g, i–k); a. ovoid with non-papillate pointed apex, laterally attached, with conspicuous basal plug (arrow); b–f. pseudo-papillate apex due to shrinkage of protoplasm before zoospore release; b. ovoid, laterally attached; c. broad-ovoid, intercalary; d. broad-ovoid; e. ovoid to obpyriform; f. ovoid, on a short lateral hypha (arrow); g. obpyriform, non-papillate, laterally attached; h. broad-ovoid with non-papillate pointed apex; i–k. ovoid, becoming pseudo-papillate and then releasing zoospores through an elongated semi-persistent vesicle (arrow); l. ovoid, after zoospore release with an elongated semi-persistent vesicle (black arrow) and a conspicuous basal plug protruding into the empty sporangium (red arrow); m–n. hyphal aggregations; o. triangular hyphal swelling. — Scale bar = 30 µm, applies to a–o.

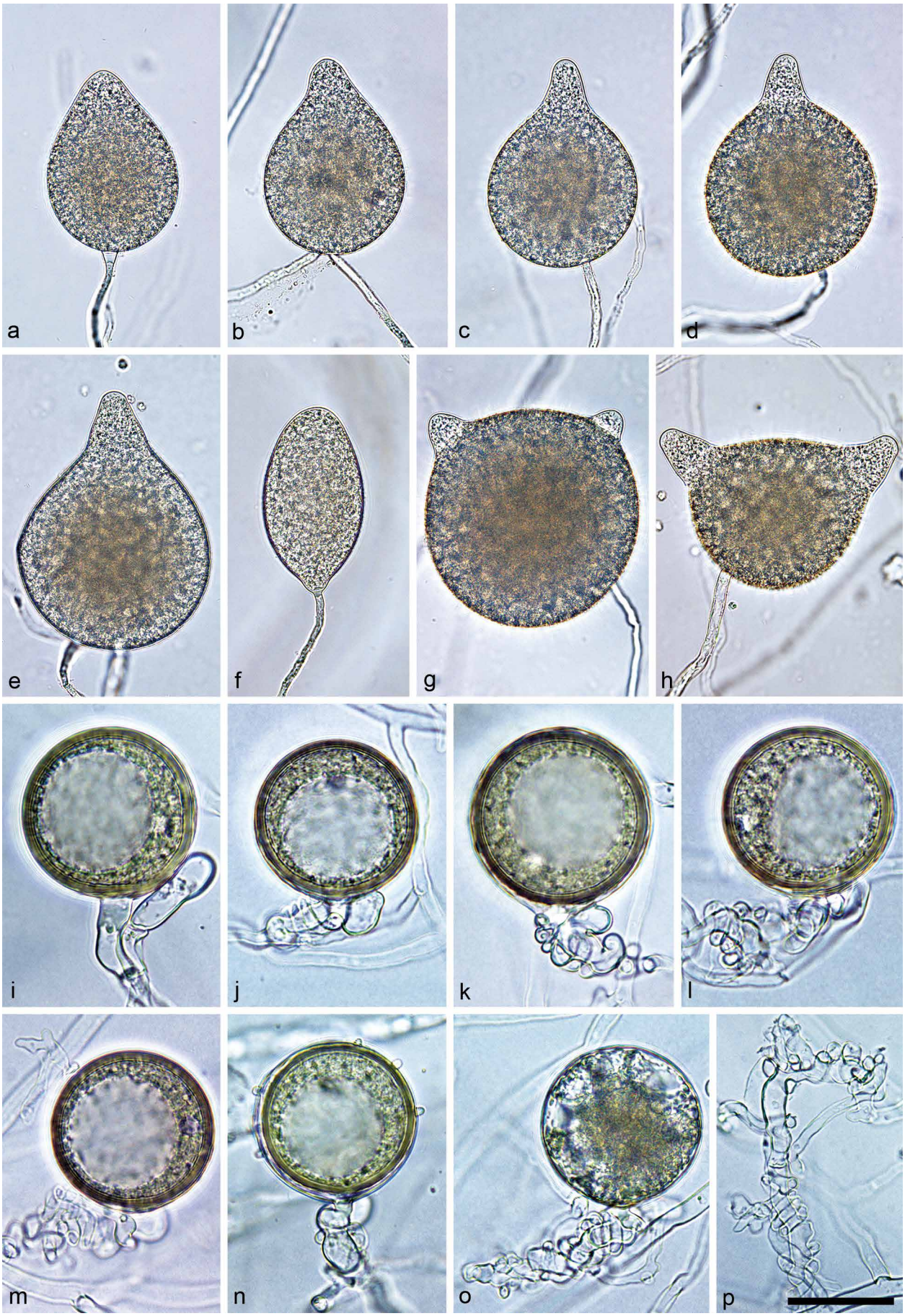

Fig. 7 Morphological structures of *Halophytophthora frigida*. — a–h. Sporangia formed on saltwater V8 agar (sV8A) flooded with nonsterile 50 % seawater; a. ovoid with non-papillate pointed apex; b. obpyriform with non-papillate pointed apex, intercalary inserted; c–h. non-papillate with pointed protruding apices and lateral attachment of the sporangiophores; c–e. broad-obpyriform; f. elongated-obpyriform with curved apex; g. globose with two apices; h. distorted with two apices; i–n. mature globose oogonia formed in single culture in sV8A, containing thick-walled plerotic oospores with large lipid globules, and paragynous antheridia; i–m. smooth-walled; j–m. antheridial stalks entangling the oogonial stalks (intricate); n. ornamented oogonial wall; o. aborted oogonium with intricate antheridial stalk; p. vegetative hyphae entangling each other. — Scale bar = 40 µm in a–h and 30 µm in i–p.

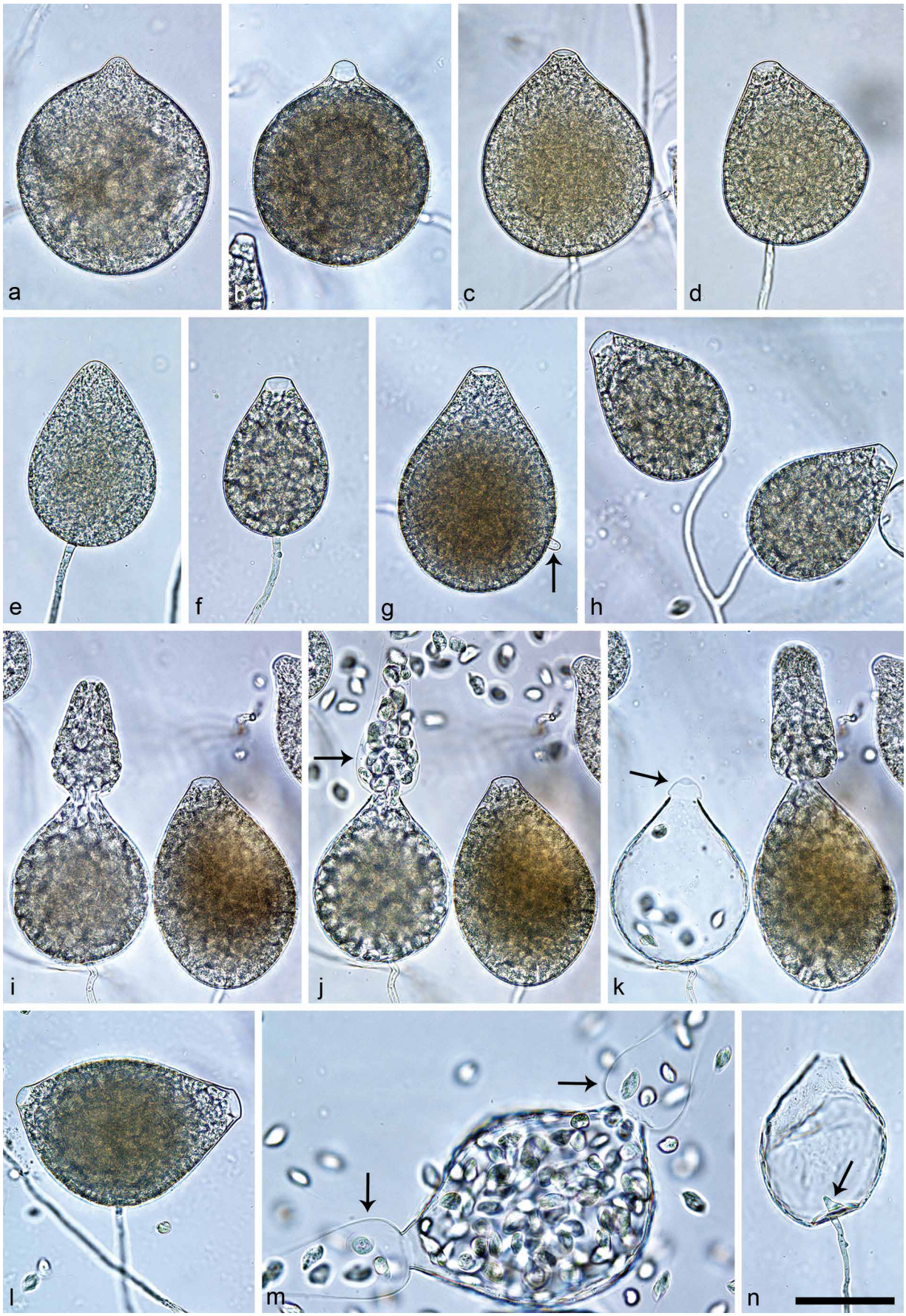

Fig. 8 Sporangia of *Halophytophthora lateralis* formed on saltwater V8 agar (sV8A) flooded with nonsterile 50% seawater. — a–b. Subglobose, laterally attached; a. non-papillate pointed apex; b. pseudo-papillate apex due to shrinkage of protoplasm before zoospore release; c. broad-ovoid, shallow semi-papillate; d. broad-ovoid, with pseudo-papillate apex before zoospore release, laterally attached; e–f. ovoid; e. non-papillate, laterally attached, with conspicuous basal plug; f. with pseudo-papillate apex before zoospore release; g. ovoid to obpyriform, shallow semi-papillate, laterally attached, with hyphal projection (arrow); h. lax sympodium of two ovoid, laterally attached sporangia with pseudo-papillate apices before zoospore release; i–k. ovoid to obpyriform sporangia releasing zoospores through elongated semi-persistent vesicles (arrows); k. shrinking vesicle (arrow) closing exit pore; l. limoniform with two pseudo-papillate apices before zoospore release; m. limoniform with two apices, releasing zoospores through elongated semi-persistent vesicles (arrows); n. ovoid with a conspicuous basal plug (arrow) protruding into the empty sporangium after zoospore release. — Scale bar = 40 µm, applies to a–n.

were non-papillate, usually with a pointed often protuberant apex (Fig. 7b–h), and non-caducous. Sporangial shapes were mainly obpyriform, broad-obpyriform and elongated obpyriform (83.1 %; Fig. 7b–f), ovoid (7.1 %; Fig. 7a) or globose to distorted with two apices (4.7 %; Fig. 7g–h) and, less frequently, obturbinate (1.8 %), limoniform (1.2 %), ellipsoid (0.6 %) or subglobose (0.3 %). Lateral attachment of the sporangiophore was common (15.7 %; Fig. 7d–h) and apices were occasionally curved (3.0 %; Fig. 7f). Sporangial dimensions of seven isolates averaged 80.4 ± 19.3 × 50.1 ± 13.8 µm, with an overall range of 32.4–150.7 × 18.8–98.1 µm and an isolate range of 72.7–85.7 × 44.5–57.1 µm. The l/b ratio was 1.6 ± 0.3. The zoospores, 9.1 ± 2.0 µm after encystment, were released through an exit pore of 9.5 ± 1.6 µm and a semi-persistent vesicle. Chlamydospores were not observed.

Oogonia, oospores and antheridia (Fig. 7i–o) — Gametangia were produced in single-culture in sV8A after 14–20 d. Mature oogonia were globose and mostly smooth-walled (Fig. 7i–m, o), although slightly ornamented oogonia were occasionally observed (Fig. 7n). Oogonial diameter was 47.8 ± 4.0 µm with an overall range of 32.0–58.6 µm and a range of isolate means of 43.0–49.9 µm. Oospores were plerotic (99.3 %) with a big reserve globule (ooplast), averaging 45.3 ± 4.1 µm (overall range 29.1–54.9 µm), with a wall diameter of 2.2 ± 0.5 µm and an oospore wall index of 0.26 ± 0.05. The abortion rate varied between isolates (2–50 %; Fig. 7o) with an average of 22.7 %. Antheridia were exclusively paragynous, measuring 18.3 ± 3.6 × 10.3 ± 2.7 µm, with intricate stalks commonly entangling the oogonial stalks (Fig. 7i–o). Vegetative hyphae were also frequently entangling each other (Fig. 7p).

Colony morphology, growth rates and cardinal temperatures (Fig. 13, 15) — There was variation in the colony morphology of the isolates tested. In one group the colonies on sV8A and sCA had a faintly radiate pattern with submerged margins and denser aerial mycelium in the centre or as a ring around the centre, while in the other group colonies on sV8A and sCA were faintly petaloid with limited aerial mycelium across the colonies. In both groups colonies on sPDA were faintly petaloid with irregular margins and felty to cottony aerial mycelium (Fig. 13). Both groups of colony patterns were present at the same sampling site. The optimum temperature for growth was generally low, 15 °C for four of the five isolates tested and 20 °C for the other isolate, while the maximum temperature was 25 °C for all isolates (Fig. 15). To verify the lethal temperature, all Petri dishes incubated for 1 wk at 27.5, 30, 32.5 and 35 °C were transferred to 20 °C. All Petri dishes from 27.5 and 30 °C resumed growth whereas those from 32.5 and 35 °C failed to grow, confirming 32.5 °C as the lethal temperature. Radial growth rates on sV8A at 15 and 20 °C were 9.0 ± 1.6 mm/d and 8.3 ± 2.3 mm/d, respectively (Fig. 15) whereas radial growth at 20 °C on sCA and sPDA was 9.4 ± 0.8 and 5.7 ± 0.6 mm/d, respectively.

Additional specimens examined. Portugal, Parque Natural da Ria Formosa, Santa Luzia, isolated from a tidal pond in a coastal saltmarsh, *T. Jung*, 2015; CBS 147236 = BD650, BD647, BD654; Parque Natural da Ria Formosa, Santa Luzia, isolated from a tidal channel in a coastal saltmarsh, *T. Jung*, 2015; BD641; Ria de Alvor, Alvor, isolated from seawater in a lagoon, *T. Jung & C. Maia*, 2015; BD675, BD676.

Halophytophthora lateralis T. Jung, C. Maia, G. Carella, M. Horta Jung, *sp. nov*. — MycoBank MB 838586; Fig. 8

Etymology. Name refers to the frequent lateral insertion of the sporangiophores to the sporangia.

Typus. Portugal, Parque Natural da Ria Formosa, Quelfes, isolated from a tidal pond in a coastal saltmarsh, *T. Jung*, 2015 (CBS H-24570 holotype, dried culture on sV8A, Herbarium CBS-KNAW Fungal Biodiversity Centre, CBS 147233 = BD657, ex-type culture). ITS and *cox1* sequences GenBank OK033655 and OK091220, respectively.

Sporangia, hyphal swellings and chlamydospores (Fig. 8) — Sporangia were not observed in solid agar but were abundantly produced in a mixture of distilled water and nonsterile seawater (1 : 1). Sporangia formed predominantly on unbranched sporangiophores or occasionally in lax sympodia (Fig. 8h) and were mostly ovoid (95.0 %, Fig. 8c–f, h–k, n) or rarely subglobose (2.0 %; Fig. 8a–b), limoniform or distorted with two apices (2.0 %; Fig. 8l–m) and ovoid to obpyriform (1.0 %; Fig. 8g). Sporangial apices were non-papillate (Fig. 8a, e) or shallow semipapillate (Fig. 8c, g), sometimes pointed (Fig. 8a), becoming pseudo-papillate due to the shrinkage of the protoplasm near the apex during zoospore differentiation (Fig. 8b, d, f, h–j, l). Lateral attachment of the sporangiophore was common (41.5 %, Fig. 8a–b, d, g–h) and short hyphal projections (Fig. 8g) and a conspicuous basal plug, protruding into the sporangium (Fig. 8n), were occasionally formed. Sporangial dimensions of four isolates averaged 75.9 ± 16.1 × 52.4 ± 12.5 µm, with an overall range of 41.6–122.0 × 22.8–100.3 µm, a range of isolate means of 67.7–89.5 × 45.4–63.6 µm and a l/b ratio of 1.5 ± 0.2. Limoniform to reniform zoospores were released through a wide exit pore (12.6 ± 2.4 µm) into a semi-persistent elongated vesicle (Fig. 8i–k, m) which after zoospore release shrinks relatively fast sometimes closing the empty sporangium again (Fig. 8k). In sporangia with two apices zoospores are often released through both apices via exit pores and vesicles (Fig. 8m). Zoospore cysts averaged 7.9 ± 0.7 µm. Hyphal swellings & chlamydospores were not observed.

Oogonia, oospores and antheridia — All isolates of *H. lateralis* were self-sterile.

Colony morphology, growth rates and cardinal temperatures (Fig. 14, 15) — Colonies on sV8A and sCA were stellate and faintly petaloid, respectively, with limited aerial mycelium whereas colonies on sPDA were dense-felty and uniform (Fig. 14). All four isolates included in the temperature tests had the same optimum and maximum growth temperature of 25 °C and 32.5 °C, respectively. The isolates did not grow at 35 °C and did not resume growth when transferred to 20 °C. Radial growth on sV8A at 20 and 25 °C was 10.3 ± 0.7 and 11.4 ± 0.9 mm/d, respectively (Fig. 15). On sCA and sPDA radial growth rates at 20 °C were, 12.0 ± 0.4 and 9.8 ± 0.3 mm/d, respectively.

Additional specimens examined. Portugal, Parque Natural da Ria Formosa, Almancil, isolated from a tidal pond in a coastal saltmarsh, *T. Jung*, 2015; CBS 147234 = BD680; Parque Natural da Ria Formosa, Quelfes, isolated from a tidal pond in a coastal saltmarsh, *T. Jung*, 2015; BD660, BD665.

Halophytophthora lusitanica T. Jung, C. Maia, G. Carella, M. Horta Jung, *sp. nov*. — MycoBank MB 838585; Fig. 9

Etymology. Name refers to the origin of the first isolates in Portugal (*lusitanica* Latin = from Lusitania which is the old Roman name for Portugal).

Typus. Portugal, Parque Natural da Ria Formosa, Almancil, isolated from a tidal pond in a coastal saltmarsh, *T. Jung*, 2015 (CBS H-24569 holotype, dried culture on sV8A, Herbarium CBS-KNAW Fungal Biodiversity Centre, CBS 147231 = BD686, ex-type culture). ITS and *cox1* sequences GenBank OK033663 and OK091228, respectively.

Sporangia, hyphal swellings and chlamydospores (Fig. 9) — Sporangia were not observed in solid agar but were abundantly produced in a mixture of distilled water and nonsterile seawater (1 : 1). Sporangial apices were mostly non-papillate or rarely shallow semipapillate (Fig. 9e) becoming pseudo-papillate due to the shrinkage of the protoplasm near the apex during zoospore differentiation (Fig. 9c, g, i). Sporangia were non-caducous and formed mostly terminally on unbranched sporangiophores or occasionally on short lateral hyphae (Fig. 9e). External proliferation close to the sporangial base was only rarely observed (Fig. 9o). Special features like lateral attachment of the sporangiophore (33.3 % of sporangia; Fig. 9a, h),

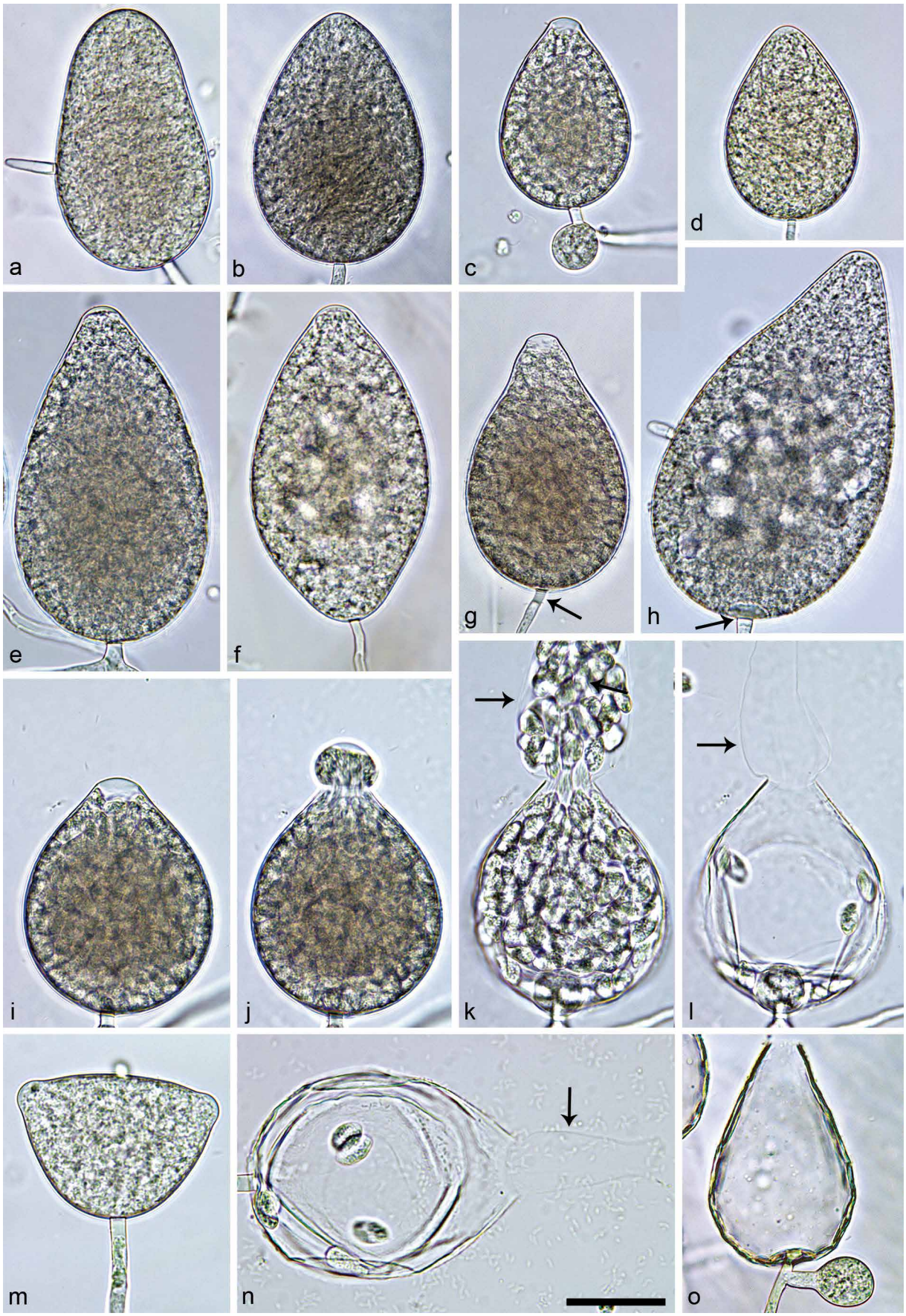

Fig. 9 Sporangia of *Halophytophthora lusitanica* formed on saltwater V8 agar (sV8A) flooded with nonsterile 50 % seawater. — a. Ellipsoid, non-papillate, laterally attached, with short hyphal projection; b. ovoid, non-papillate; c. ovoid, with pseudo-papillate apex due to shrinkage of protoplasm before zoospore release, and globose swelling close to sporangial base; d. ovoid with pointed apex; e. elongated ovoid, on a short lateral hypha with non-papillate to shallow semi-papillate apex; f. non-papillate, limoniform; g. obpyriform, with pseudo-papillate apex before zoospore release, and conspicuous basal plug (arrow); h. elongated obpyriform, non-papillate, laterally attached, with short hyphal projection; i–l. broad-ovoid, becoming pseudo-papillate and then releasing zoospores through an elongated semi-persistent vesicle (arrows); m. distorted with two non-papillate apices; n. broad-ovoid after release of most zoospores through an elongated semi-persistent vesicle (arrow); o. ovoid to obpyriform, after zoospore release, with conspicuous basal plug and external proliferation. — Scale bar = 30 µm, applies to a–o.

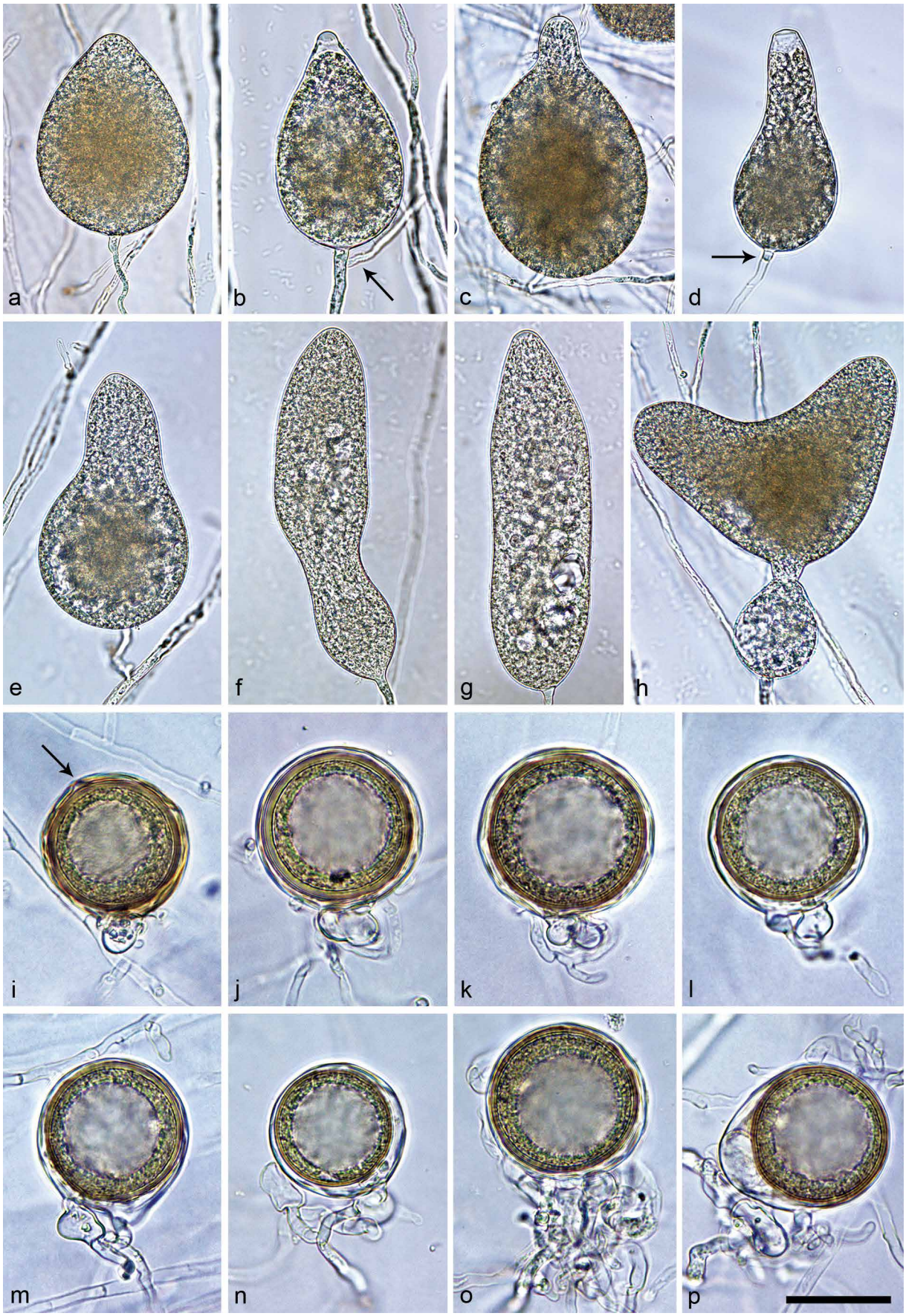

Fig. 10 Morphological structures of *Halophytophthora macrosporangia*. — a–h. Sporangia formed on saltwater V8 agar (sV8A) flooded with nonsterile 50 % seawater; a. ovoid, non-papillate; b. ovoid to obpyriform, with pseudo-papillate apex due to shrinkage of protoplasm before zoospore release, and external proliferation (arrow); c–e. elongated-obpyriform; c. non-papillate pointed apex, laterally attached; d. with pseudo-papillate apex before zoospore release, and conspicuous basal plug (arrow); e. non-papillate; f. elongated peanut-shaped to ampulliform, non-papillate, with small lipid globules; g. elongated-ellipsoid, non-papillate, with small lipid globules; h. distorted with two non-papillate apices and a subglobose swelling close to the sporangial base; i–p. mature, globose golden-brown oogonia formed in single culture in sV8A with mostly thick-walled (a–m, o–p) or rarely thin-walled (n), plerotic to nearly plerotic oospores containing large lipid globules, and paragynous antheridia; i. globose with slightly ornamented wall (arrow); j–o. globose, smooth-walled; o. antheridial stalk entangling the oogonial stalk; p. excentric, smooth-walled. — Scale bar = 40 µm in a–h and 30 µm in i–p.

short hyphal projections (Fig. 9e, h), a conspicuous basal plug (Fig. 9g–h, o) and a curved apex occurred in all isolates. Sporangial shapes were variable, ranging from obpyriform (54.0 %; Fig. 9g–h), ovoid to obpyriform (12.0 %; Fig. 9o) and ovoid, broad-ovoid or elongated ovoid (27.3 %, Fig. 9b–e, i–l, n) to ellipsoid (3.0 %; Fig. 9a), limoniform (1.0 %; Fig. 9f), obturbinate (1.0 %), ampulliform (0.7 %) and distorted shapes with two apices (1.0 %; Fig. 9m). Sporangia of six isolates averaged 84.0 ± 15.8 × 54.3 ± 10.6 µm, with an overall range of 40.5–162.5 × 25.4–86.3 µm, and a range of isolate means of 76.2–95.4 × 47.1–60.2 µm. The l/b ratio was 1.6 ± 0.3. Limoniform to reniform zoospores were released through an exit pore of 10.6 ± 2.1 µm width into a semi-persistent elongated vesicle (Fig. 9i–l, n); zoospores measuring 8.2 ± 0.9 µm after encystment. Hyphal swellings were sometimes formed close to the base of the sporangium (Fig. 9c). Chlamydospores were not observed.

Oogonia, oospores and antheridia — All six isolates of *H. lusitanica* were self-sterile.

Colony morphology, growth rates and cardinal temperatures (Fig. 14, 15) — All isolates formed petaloid to faintly petaloid colonies with limited aerial mycelium on sV8A and sCA and uniform felty colonies with an appressed ring of collapsed aerial mycelium on sPDA (Fig. 14). The optimum temperature varied between the isolates. Three of the five tested isolates had an optimum temperature on sV8A of 25 °C, while the remaining two isolates had their optimum at 20 and 27.5 °C, respectively, averaging at 25 °C. The maximum growth temperature of all isolates was 32.5 °C. No growth occurred after transferring isolates that were incubated for 1 wk at 35 °C to 20 °C. Radial growth rates on sV8A at 20 and 25 °C were 7.3 ± 0.6 and 7.5 ± 0.8 mm/d, respectively (Fig. 15). Radial growth on sCA and sPDA at 20 °C was 6.9 ± 0.8 and 6.7 ± 0.4 mm/d, respectively.

Additional specimens examined. Portugal, Rio Séqua, Tavira, isolated from brackish river water in the tidal zone near the estuary, *T. Jung*, 2015; CBS 147232 = BD628; BD632, BD634; Parque Natural da Ria Formosa, Almancil, isolated from a tidal pond in a coastal saltmarsh, *T. Jung*, 2015; BD679, BD681.

Halophytophthora macrosporangia T. Jung, C. Maia, G. Carella, M. Horta Jung, *sp. nov.* — MycoBank MB 838597; Fig. 10

Etymology. Name refers to the large size of the sporangia.

Typus. Portugal, Parque Natural da Ria Formosa, Santa Luzia, isolated from a tidal channel in a coastal saltmarsh, *T. Jung*, 2015 (CBS H-24573 holotype, dried culture on sV8A, Herbarium CBS-KNAW Fungal Biodiversity Centre, CBS 147290 = BD639, ex-type culture). ITS and *cox1* sequences GenBank OK033664 and OK091229, respectively.

Sporangia, hyphal swellings and chlamydospores (Fig. 10a–h) — Sporangia were not observed in solid agar but were slowly produced in a mixture of distilled water and non-sterile seawater (1 : 1). Sporangia were formed terminally, mostly on unbranched sporangiophores (Fig. 10a–d, f–h), or less frequently on short lateral hyphae (Fig. 10e). External proliferation occurred infrequently (Fig. 10b). Sporangia were non-papillate, sometimes with a pointed apex (Fig. 10b–c), becoming pseudo-papillate during zoospore differentiation due to the shrinkage of the protoplasm near the apex (Fig. 10b, d), and non-caducous. Sporangial shapes were diverse ranging from obpyriform or elongated obpyriform (55.7 %; Fig. 10c–e), ovoid (29.3 %; Fig. 10a) and ovoid to obpyriform (6.0 %; Fig. 10b) to subglobose (3.7 %) and much less frequently distorted with often two apices (2.0 %; Fig. 10h), peanut-shaped to ampulliform (2.7 %; Fig. 10f), elongated-ellipsoid (0.3 %; Fig. 10g) and obturbinate (0.3 %). Special features like a slightly laterally displaced attachment of the sporangiophore (16 %; Fig. 10c), small vacuoles (Fig. 10g), a conspicuous basal plug (Fig. 10d) or a swelling close to the sporangial base (Fig. 10h) were observed in all isolates. Sporangial dimensions averaged 97.5 ± 24.8 × 55.0 ± 14.8 µm, with an overall range of 58.0–186.7 × 32.3–106.3 µm, a range of isolate means of 76.8–118.9 × 42.9–67.4 µm and a l/b ratio of 1.8 ± 0.4. Zoospores were released through an exit pore with a mean diameter of 10.3 ± 1.7 µm and a semipersistent vesicle. Zoospore cysts measured 8.2 ± 2.1 µm. Chlamydospores were not produced.

Oogonia, oospores and antheridia (Fig. 10i–p) — Gametangia were produced in single-culture in sV8A after 14–20 d. Oogonia were mostly globose (Fig. 10i–o) and less frequently, excentric (Fig. 10p), mostly with smooth, sometimes slightly wrinkled walls (Fig. 10j–p) or rarely slightly ornamented (Fig. 10i). Oogonia had an average diameter of 48.2 ± 4.6 µm, with an overall range of 18.4–58.7 µm and an isolate range of 46.7–49.2 µm. Oospores were plerotic or nearly plerotic with a large ooplast and an average diameter of 43.7 ± 4.2 µm, an overall range of 30.1–54.5 µm, a wall diameter of 1.7 ± 0.4 µm and an oospore wall index of 0.22 ± 0.04. The abortion rate varied between isolates from 14 to 82 % averaging 41.5 %. Antheridia were exclusively paragynous with an average size of 15.2 ± 3.1 × 7.8 ± 1.7 µm. Antheridial stalks entangled the oogonial stalks occasionally (Fig. 10o).

Colony morphology, growth rates and cardinal temperatures (Fig. 14, 15) — All isolates produced colonies with wide submerged margins and limited aerial mycelium in the centre on sV8A and sCA, faintly stellate on sV8A and uniform on sCA whereas colonies on sPDA were stoloniferous to petaloid and appressed with submerged margins (Fig. 14). Regarding optimum temperature for growth, the five isolates tested showed considerable variation. The optimum temperature was 15 °C for each one isolate from Santa Luzia and Quelfes, 20 °C for another isolate from Quelfes and 25 °C for two other isolates from Santa Luzia. While the maximum growth temperature was 27.5 °C in all isolates there was also variation in the lethal temperature, which was 32.5 °C in two isolates and 35 °C in three isolates. Radial growth rates on sV8A at 20 and 25 °C were 4.2 ± 1.1 and 3.7 ± 0.3 mm/d (Fig. 15). Radial growth on sCA and sPDA at 20 °C was 5.1 ± 1.4 and 4.1 ± 1.1 mm/d.

Additional specimens examined. Portugal, Parque Natural da Ria Formosa, Santa Luzia, isolated from a tidal channel in a coastal saltmarsh, *T. Jung*, 2015; CBS 147291 = BD642, BD643, BD645; Parque Natural da Ria Formosa, Santa Luzia, isolated from a tidal pond in a coastal saltmarsh, *T. Jung*, 2015; BD649; Parque Natural da Ria Formosa, Quelfes, isolated from a tidal pond in a coastal saltmarsh, *T. Jung*, 2015; BD659, BD664.

Halophytophthora sinuata T. Jung, C. Maia, G. Carella, M. Horta Jung, *sp. nov*. — MycoBank MB 838590; Fig. 11

Etymology. Name refers to the sinuate-waved oogonial walls.

Typus. Portugal, Parque Natural da Ria Formosa, Santa Luzia, isolated from a tidal pond in a coastal saltmarsh, *T. Jung*, 2015 (CBS H-24572 holotype, dried culture on sV8A, Herbarium CBS-KNAW Fungal Biodiversity Centre, CBS 147237 = BD656, ex-type culture). ITS and *cox1* sequences GenBank OK033671 and OK091236, respectively.

Sporangia, hyphal swellings and chlamydospores (Fig. 11a–h) — Sporangia were not observed in solid agar but were slowly produced in a mixture of distilled water and non-sterile seawater (1 : 1). They were formed terminally, almost exclusively on unbranched sporangiophores (Fig. 11a–h). External sporangial proliferation occurred very rarely (Fig. 11h). Sporangia had non-papillate apices which were often pointed (Fig. 11b–g), becoming pseudo-papillate due to the shrinkage of the protoplasm near the apex during zoospore differentiation (Fig. 11c), and were non-caducous with sporangial shapes ranging from mostly obpyriform or elongated and often asymmetrically obpyriform (84.7 %; Fig. 11b–f) to elongated ovoid (6.3 %; Fig. 11a), distorted with two apices (5.0 %; Fig. 11g), ovoid to obpyriform (3.3 %; Fig. 11h), limoniform (0.3 %), ampulliform (0.3 %) and obturbinate (0.3 %). Lateral attachment of the sporangiophore

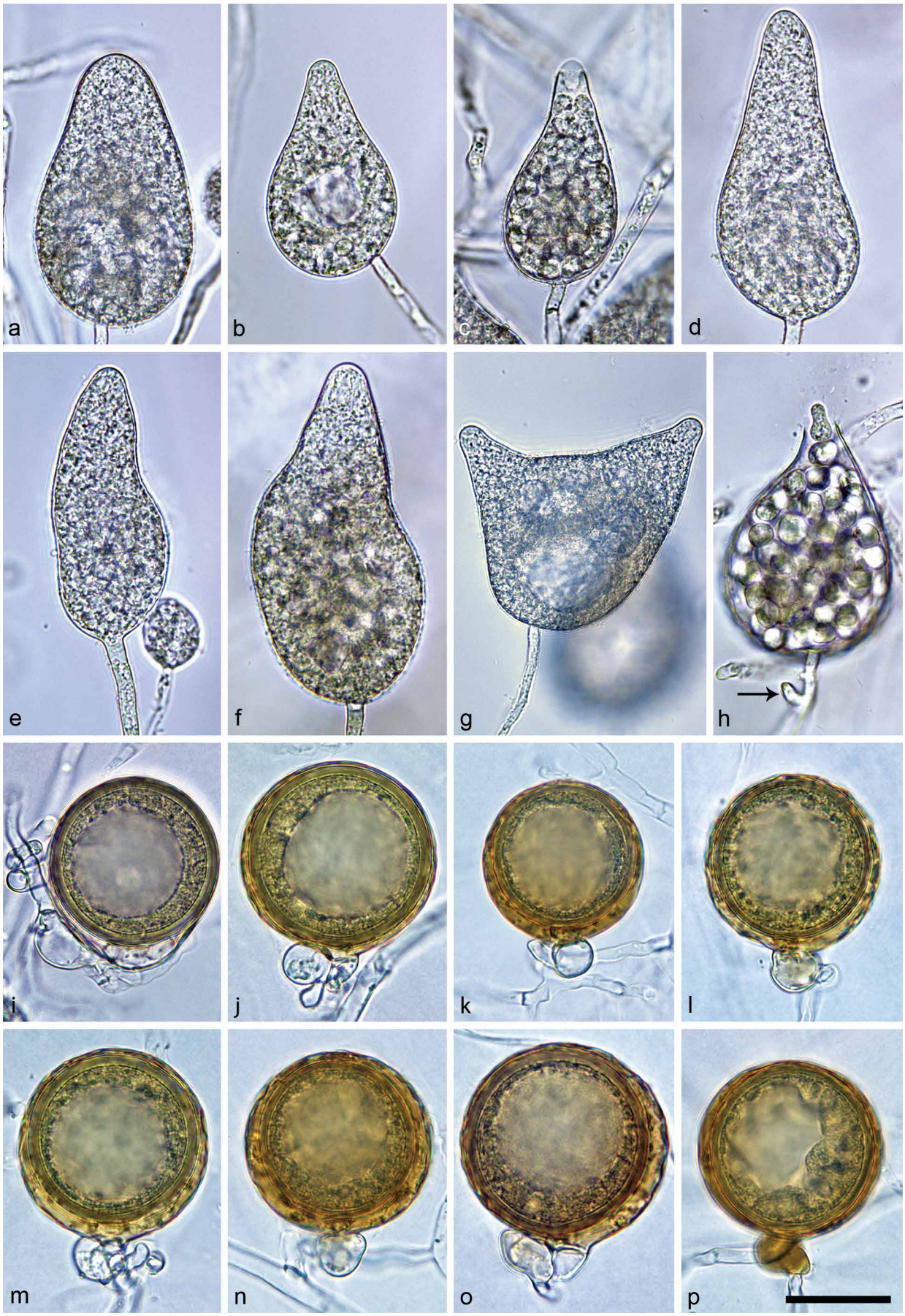

Fig. 11 Morphological structures of *Halophytophthora sinuata*. — a–h. Sporangia formed on saltwater V8 agar (sV8A) flooded with nonsterile 50 % seawater; a. elongated-ovoid, non-papillate; b. obpyriform, with non-papillate pointed apex and lipid globule, laterally attached; c. obpyriform, with pseudo-papillate apex due to shrinkage of protoplasm before zoospore release; d–f. elongated-obpyriform, slightly excentric, non-papillate with pointed apex; d, e. with conspicuous basal plug; g. distorted with two pointed non-papillate apices and lipid globules; h. ovoid to obpyriform, releasing zoospores directly without vesicle, with beginning external proliferation (arrow); i–p. mature, globose golden-brown oogonia formed in single culture in sV8A containing thick-walled, plerotic to nearly plerotic oospores with large lipid globules, and paragynous antheridia; i–j. smooth-walled; k–p. with sinuate-wavy to wrinkled walls; p. with golden-brown antheridium. — Scale bar = 30 µm, applies to a–p.

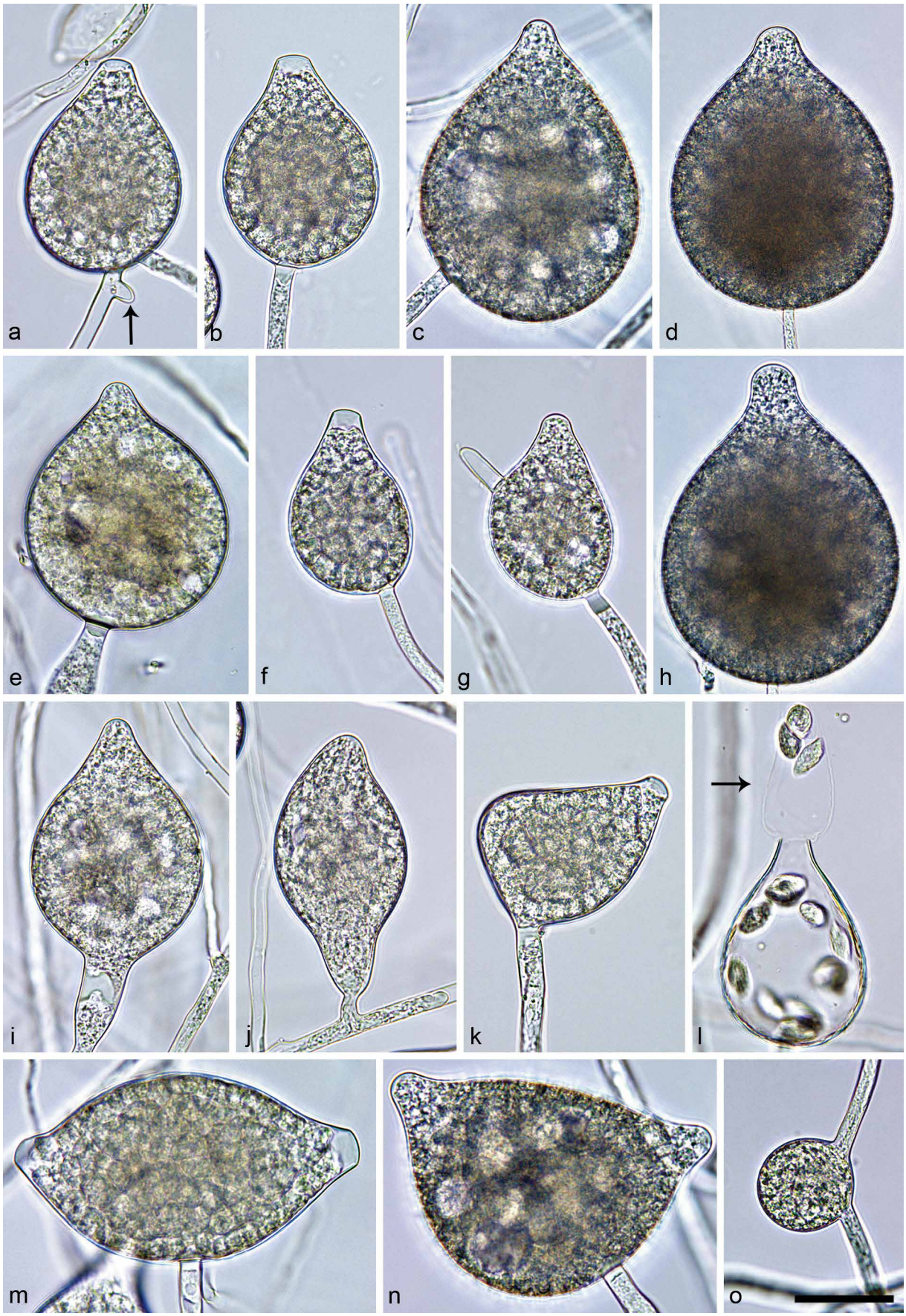

Fig. 12 Morphological structures of *Halophytophthora thermoambigua* formed on saltwater V8 agar (sV8A) flooded with nonsterile 50 % seawater. — a–n. Sporangia; a–b. ovoid, pseudo-papillate apex due to shrinkage of protoplasm before zoospore release; a. intercalary with beginning external proliferation (arrow); b. conspicuous basal plug; c–e. broad-ovoid with non-papillate pointed apex; c. laterally attached; e. laterally attached with conspicuous basal plug; f. obpyriform, pseudo-papillate apex before zoospore release, laterally attached; g. non-papillate pointed with hyphal projection, laterally attached; h. broad-obpyriform with non-papillate pointed apex; i. ovoid to obpyriform with non-papillate pointed apex, widening sporangiophore and conspicuous basal plug; j. limoniform with non-papillate curved apex, on short lateral hypha; k. distorted, laterally attached with conspicuous basal plug and pseudo-papillate apex before zoospore release; l. ovoid to obpyriform, releasing zoospores through elongated semi-persistent vesicle (arrow); m. limoniform with two pseudo-papillate apices before zoospore release; n. limoniform with two non-papillate pointed apices; o. intercalary globose hyphal swelling. — Scale bar = 30 µm, applies to a–o.

occurred in 31.3 % of the sporangia (Fig. 11b). One or more vacuoles were frequently observed (Fig. 11b, g). Sporangia averaged 74.1 ± 19.5 × 44.0 ± 12.6 µm, with an overall range of 28.1–129.2 × 19.8–89.5 µm and a range of isolate means of 56.9–82.1 × 32.5–51.4 µm. The l/b ratio was 1.7 ± 0.3. The zoospores were released through a narrow exit pore of 8.9 ± 1.5 µm width, either directly (Fig. 11h) or through a semi-persistent vesicle. After encystment, zoospores had an average diameter of 7.5 ± 1.1 µm. Hyphal swellings & chlamydospores were not observed.

Oogonia, oospores and antheridia (Fig. 11i–p) — Gametangia were abundantly produced in sV8A after 14–20 d. Mature oogonia were globose with usually sinuate wavy to wrinkled (Fig. 11j–p) or, more rarely, smooth walls (Fig. 11i) and a golden-brown colour. Size of the oogonia averaged 54.2 ± 3.8 µm with an overall range of 39.4–64.3 µm and a range of isolate means of 51.6–55.6 µm. Oospores were mostly plerotic or nearly plerotic (95 %; Fig. 11i–p), with a big lipid globule, a diameter of 47.5 ± 3.7 µm (overall range 33.9–57.6 µm), a wall diameter of 2.9 ± 0.6 µm and an oospore wall index of 0.32 ± 0.05. With 4.2 % (isolate range 0–13 %) abortion rate was low. Antheridia were exclusively paragynous (Fig. 11i–p), sometimes golden-brown (Fig. 11p), averaging 14.9 ± 2.8 × 11.6 ± 1.8 µm. Antheridial stalks almost never entangled the oogonial stalks (Fig. 11i–p).

Colony morphology, growth rates and cardinal temperatures (Fig. 14, 15) — All isolates of *H. sinuata* had similar patterns on all three agar media. Colonies had limited aerial mycelium on sV8A and sCA and were cottony on sPDA. Colony patterns were uniform on sV8A, uniform to faintly radiate on sCA and uniform to faintly petaloid on sPDA (Fig. 14). All five isolates tested had the same optimum, maximum, and lethal temperatures, 25 °C, 27.5 °C and 32.5 °C, respectively. On sV8A radial growth at 20 and 25 °C was 14.9 ± 0.3 and 17.9 ± 0.6 mm/d (Fig. 15). Radial growth rates, on sCA and sPDA at 20 °C were 12.8 ± 0.1 and 13.3 ± 0.4 mm/d, respectively.

Additional specimens examined. Portugal, Parque Natural da Ria Formosa, Santa Luzia, isolated from a tidal channel in a coastal saltmarsh, *T. Jung*, 2015; CBS 147292 = BD943, BD640, BD941, BD942, BD944.

Halophytophthora thermoambigua T. Jung, C. Maia, G. Carella, M. Horta Jung, *sp. nov.* — MycoBank MB 838582; Fig. 12

Etymology. Name refers to the limited effect of temperature on growth rates and the variability of optimum temperatures between isolates.

Typus. Portugal, Parque Natural da Ria Formosa, Santa Luzia, isolated from a tidal pond in a coastal saltmarsh, *T. Jung*, 2015 (CBS H-24568, holotype, dried culture on sV8A, Herbarium CBS-KNAW Fungal Biodiversity Centre, CBS 147229 = BD651, ex-type culture). ITS and *cox1* sequences GenBank OK033680 and OK091244, respectively.

Sporangia, hyphal swellings and chlamydospores (Fig. 12) — Sporangia were infrequently observed on solid agar but were abundantly produced in a mixture of distilled water and non-sterile seawater (1 : 1). Sporangial apices were non-papillate, usually pointed and often protuberant (Fig. 12c–e, g–j, n), becoming pseudo-papillate due to the shrinkage of the protoplasm near the apex during zoospore differentiation (Fig. 12a–b, f, k, m); frequently two or rarely three apices (Fig. 12m–n). Sporangia were non-caducous and formed mostly terminally on unbranched sporangiophores (Fig. 12b–i, k, m–n) and less frequently intercalary (Fig. 12a) or on short lateral hypha (Fig. 12j). External proliferation was only infrequently observed (Fig. 12a). Lateral attachment of the sporangiophore (38.4 %, Fig. 12c, e, c, f–g, k, n) and a conspicuous basal plug were common (Fig. 12b, e, g, i, k, m–n) while other special features such as short hyphal projections (Fig. 12g), widening of the sporangiophore (Fig. 12i) and a curved apex (Fig. 12f, j–k) occurred occasionally. Shapes were mostly obpyriform (50.4 %; Fig. 12f–h), ovoid to broad-ovoid (33.1 %; Fig. 12a, d), ovoid to obpyriform (7.3 %; Fig. 12b–c, e, i, l) and less frequently limoniform to asymmetrically limoniform (Fig. 12j, m–n), ellipsoid, ampulliform and distorted (Fig. 12k). Sporangial dimensions of nine isolates of *H. thermoambigua* averaged 75.3 ± 15.7 × 48.1 ± 9.7 µm with an overall range of 43.4–185.3 × 25.3–83.9 µm and a range of isolate means of 69.2–83.2 × 40.3–57.1 µm and a length/breadth (l/b) ratio of 1.6 ± 0.3. Zoospores were differentiated inside the sporangium and released through an exit pore of 10.3 ± 2.3 µm width and a semi-persistent apically rupturing vesicle (Fig. 12l). Zoospore cysts averaging 8.6 ± 0.9 µm. Hyphal swellings (33.8 ± 9.5 µm) were infrequently produced (Fig. 12o). Chlamydospores were not observed.

Oogonia, oospores and antheridia — All nine isolates of *H. thermoambigua* were self-sterile.

Colony morphology, growth rates and cardinal temperatures (Fig. 14, 15) — All isolates produced stellate to radiate colonies with limited aerial mycelium on sV8A and sCA, respectively, and felty petaloid colonies on sPDA (Fig. 14). *Halophytophthora thermoambigua* showed a flat temperature-growth curve (Fig. 15). The five isolates had optimum growth temperatures of 20, 25 and 27.5 °C, respectively. The maximum growth temperature was 32.5 °C in all isolates. None of the isolates grew at 35 °C, and they did not resume growth after being re-incubated at 20 °C. Radial growth on sV8A at 20 and 25 °C was 5.2 ± 1.2 and 5.6 ± 1.0 mm/d, respectively (Fig. 15). Radial growth rates on sCA and sPDA at 20 °C were 5.2 ± 1.4 and 5.0 ± 2.1 mm/d, respectively.

Additional specimens examined. Portugal, Rio Séqua, Tavira, isolated from brackish river water in the tidal zone near the estuary, *T. Jung*, 2015; CBS 147230 = BD637; BD631; Parque Natural da Ria Formosa, Santa Luzia, isolated from a tidal pond in a coastal saltmarsh, *T. Jung*, 2015; BD652, BD653; Ribeira de Odelouca, Silves, isolated from brackish river water in the tidal zone near the estuary, *T. Jung*, 2014; BD91, BD93; Ria de Alvor, Alvor, isolated from seawater in a lagoon, *T. Jung & C. Maia*, 2015; BD668, BD673, BD674; Sapal de Castro Marim / Rio Guadiana, Castro Marim, isolated from brackish water in the river estuary, *G. Carella & M. Horta Jung*, 2015; BD698.

Notes — Across the 8 759 character alignment of LSU, ITS, *Btub*, *hsp90*, *rpl10*, *tigA*, *cox1*, *nadh1* and *rps10* the Clade 6 species *H. brevisporangia*, *H. celeris*, *H. frigida*, *H. lateralis*, *H. lusitanica*, *H. macrosporangia*, *H. sinuata*, *H. thermoambigua* and *H.* sp. thermoambigua-like differ from each other and from the other Clade 6 species *H. polymorphica* at 82–501 positions and contain 55–61, 32–36, 50–51, 68–69, 53–71, 76–82, 52–63, 23–70 and 29–32 unique polymorphisms, respectively. *Halophytophthora lateralis* differs in ITS from the ex-type isolate of *H. vesicula* at 39 positions. In addition, unique combinations of morphological and physiological characters allow to distinguish the eight new species from each other and from the seven known *Halophytophthora* species. The most discriminating features are highlighted in bold in Table 3 and 4. For the known *Halophytophthora* species morphological and physiological information were taken from the original descriptions (Anastasiou & Churchland 1969, Gerrettson-Cornell & Simpson 1984, Yang & Hong 2014, Jesus et al. 2019). In addition, seven isolates of *H. avicennae* from Portugal were examined in this study. Having a homothallic breeding system *H. frigida*, *H. macrosporangia* and *H. sinuata* can easily be separated from the sterile *H. avicennae*, *H. batemanensis*, *H. brevisporangia*, *H. celeris*, *H. insularis*, *H. lateralis*, *H. lusitanica*, *H. polymorphica* and *H. thermoambigua*. *Halophytophthora sinuata* differs from the other five homothallic species, *H. fluviatilis*, *H. frigida*, *H. macrosporangia*, *H. souzae* and *H. vesicula*, by having on average the largest oogonia with mostly sinuate-wavy oogonial walls and a high proportion of asymmetric sporangia. Furthermore, it shows over the whole range between 10 and 27 °C much

faster growth than *H. frigida* and *H. macrosporangia* (Fig. 14). *Halophytophthora frigida* is unique in forming both smooth-walled and slightly ornamented oogonia and mostly intricate antheridial stalks. It also differs from all other homothallic *Halophytophthora* species except of *H. souzae* by its low optimum temperature of 15 to 20 °C and from *H. souzae* by producing markedly larger oogonia. *Halophytophthora macrosporangia* is separated from all other homothallic *Halophytophthora* species except of *H. souzae* by its large sporangia and from the latter species by having on average larger oogonia and a lower maximum temperature for growth. *Halophytophthora frigida*, *H. macrosporangia* and *H. sinuata* are also distinguished from each other by having different colony morphologies on all three agar media tested (Fig. 12, 13). The sterile *H. brevisporangia* and *H. celeris* differ from the other new sterile species from Portugal, *H. lateralis*, *H. lusitanica* and *H. thermoambigua*, by having on average smaller sporangia with lower l/b ratios, different colony morphologies on all three agar media and faster growth between 10 and 27 °C. (Fig. 12–14). *Halophytophthora celeris* can be distinguished from *H. brevisporangia* by its faster growth between 10 and 32.5 °C and by forming hyphal aggregations (Fig. 14). *Halophytophthora lateralis*, *H. lusitanica* and *H. thermoambigua* have different colony morphologies on all three agar media (Fig. 12). Furthermore, unlike *H. lateralis* both *H. thermoambigua* and *H. lusitanica* have no clear optimum temperature for growth (Fig. 14). The latter two species can be separated by the slower growth of *H. thermoambigua* between 10 and 32.5 °C, and the high proportion of laterally attached sporangia and the predominance of ovoid sporangia in *H. lateralis* (Fig. 14). Finally, *H. lateralis* differs from the homothallic *H. vesicula* by being sterile.

Colony morphologies, growth rates, morphological characters and morphometric data from different studies can only be compared with caution due to differences in the preparation of agar media and the different methods of producing and measuring morphological structures. For instance, the l/b ratio of the sporangia from seven *H. avicennae* isolates from Portugal in the present study was 1.5 compared to 2.6 in the original description from Australia (Gerrettson-Cornell & Simpson 1984). Another example are the operculum-like structures which become visible after opening of the sporangial apex for zoospore release and were first reported for *Calycofera operculata* (previously *Phytophthora operculata* and *Halophytophthora operculata*) (Pegg & Alcorn 1982, Ho & Jong 1990). Jesus et al. (2019) observed operculum-like structures also in isolates of *H. avicennae*, *H. batemanensis*, *H. polymorphica* and *H. vesicula* although these were not reported in the original descriptions by Anastasiou & Churchland (1969) and Gerrettson-Cornell & Simpson (1984). Also in the present study, despite of studying high numbers of sporangia per isolate and species, operculum-like structures could not be observed in any of the eight new *Halophytophthora* species or the seven isolates of *H. avicennae* from Portugal.

Portuguese isolates of *H. thermoambigua*, *H. lateralis* and *H. frigida*, previously informally named *Halophytophthora* sp. 1, *Halophytophthora* sp. 3 and *Halophytophthora* sp. 4, respectively, were demonstrated to host a diverse assembly of eight putative novel mycoviruses from the order *Bunyavirales* (Botella et al. 2020). The virus-infected *Halophytophthora* isolates did not show obvious phenotypic differences compared to non-infected isolates.

Geographical distribution and diversity of Halophytophthora species

The distribution of the eight new *Halophytophthora* species, *H. avicennae*, *Halophytophthora* sp. thermoambigua-like, and *Halophytophthora* sp. Portugal_9 (of which the only isolate died during long-term storage), and the exact location of the seven sampled marine and brackish water sites along the Algarve coast in Portugal are given in Table 5. *Halophytophthora thermoambigua* was most widespread (6 sites) followed by *H. avicennae* (5 sites). Both species were isolated from all three ecosystem types, i.e., brackish river estuaries, brackish to marine tidal ponds or channels in saltmarshes and a marine lagoon. *Halophytophthora brevisporangia* and *H. lusitanica* were found at three sites in a river estuary and in saltmarshes while *H. frigida* occurred in the marine lagoon at Ria de Alvor and the saltmarsh in Santa Luzia. The remaining three new species, *H. celeris*, *H. lateralis* and *H. sinuata*, were each isolated from one or two saltmarsh sites. *Halophytophthora* sp. thermoambigua-like and *Halophytophthora* sp. Portugal_9 were recovered from each one site. Within-site diversity ranged from two *Halophytophthora* species in brackish water of the Ribeira de Odelouca estuary, 3–5 *Halophytophthora* taxa in tidal saltmarsh ponds in Quelfes and Almancil, the lagoon of Ria de Alvor and the Rio Séqua and Rio Guadiana estuaries, to six *Halophytophthora* species plus *Halophytophthora* sp. thermoambigua-like in a tidal pond and a neighbouring tidal channel in the saltmarsh at Santa Luzia (Table 5). Noteworthy, six *Phytophthora* species, i.e., *P. condilina*, *P. gonapodyides*, *P. plurivora*, *P. inundata*, *P. pseudocryptogea* and the undescribed *P.* sp. Clade06a New PT, were also occasionally isolated (Table 1, 5).

Table 5 Geographical distribution of *Halophytophthora* spp. in marine and brackish-water ecosystems along the Algarve coast in Portugal.

Site[a]	Geographical coordinates	Ecosystem, water type	*Halophytophthora* spp.[b]
Ribeira de Odelouca, Silves	N37 12.284, W8 29.484	Estuary, brackish	AVI, THE
Rio Séqua, Tavira	N37 7.930, W7 39.367	Estuary, brackish	AVI, LUS, THE[c]
Rio Guadiana, Castro Marim	N37 14.476, W7 25.585	Estuary, brackish	AVI, BRE, LUS, PT9, THE[d]
PN da Ria Formosa, Santa Luzia	N37 05.346, W7 40.261	Tidal pond and channel in saltmarsh; marine	BRE, CEL, FRI, MAC, SIN, THE, THE-like
PN da Ria Formosa, Quelfes	N37 01.835, W7 49.104	Tidal pond in saltmarsh; marine	BRE, LAT, MAC[e]
PN da Ria Formosa, Almancil	N37 01.030, W7 59.619	Tidal pond in saltmarsh; brackish	AVI, LAT, LUS, THE[f]
Ria de Alvor, Alvor	N37 08.538, W8 35.606	Lagoon; marine	AVI, FRI, THE[g]

[a] PN = Parque Natural.
[b] AVI = *Halophytophthora avicennae*, BRE = *H. brevisporangia*, CEL = *H. celeris*, FRI = *H. frigida*, LAT = *H. lateralis*, LUS = *H. lusitanica*, MAC = *H. macrosporangia*, PT9 = *Halophytophthora* sp. Portugal_9, SIN = *H. sinuata*, THE = *H. thermoambigua*, THE-like = *Halophytophthora* sp. thermoambigua-like.
[c] *Phytophthora plurivora* and *P. pseudocryptogea* also isolated.
[d] *P. plurivora* also isolated.
[e] *P. gonapodyides* and *P. condilina* also isolated.
[f] *P. inundata*, *P. pseudocryptogea* and *P.* sp. Clade06a New PT also isolated.
[g] *P. condilina* and *P. inundata* also isolated.

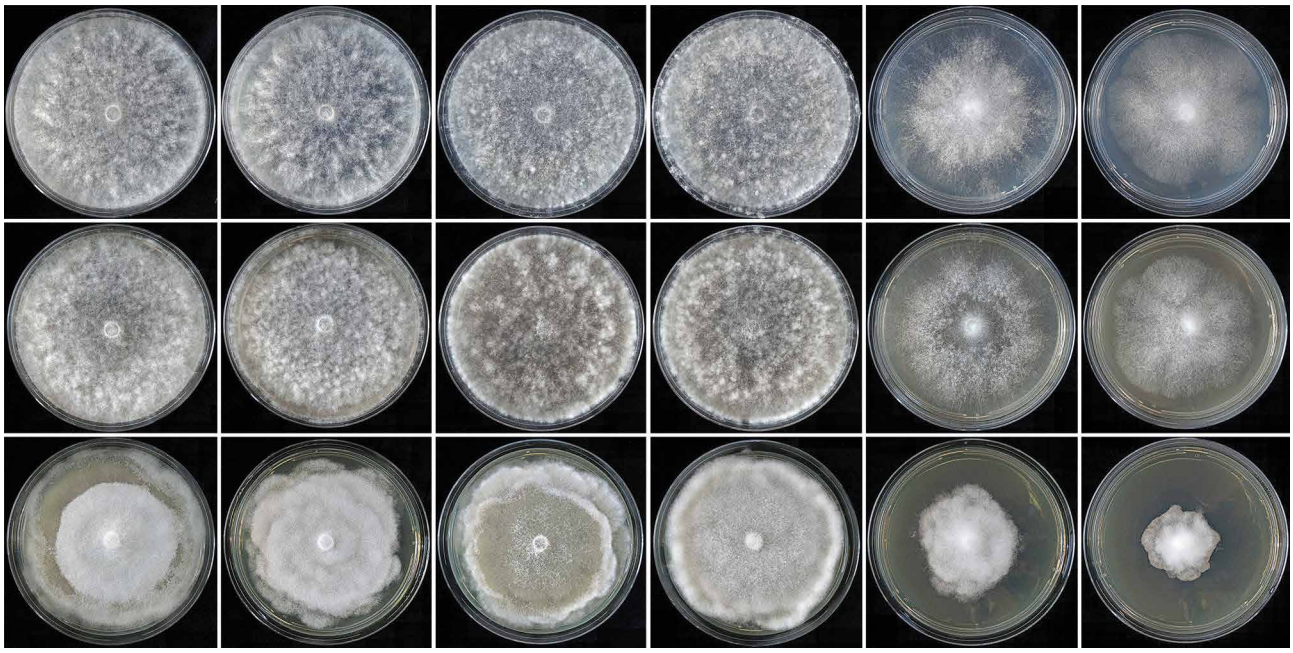

Fig. 13 Colony morphology of *Halophytophthora brevisporangia* (BD662 and BD695), *H. celeris* (BD646 and BD885) and *H. frigida* (BD650 and BD655) (from left to right) after 7 d growth at 20 °C on sV8A, sCA and sPDA (from top to bottom).

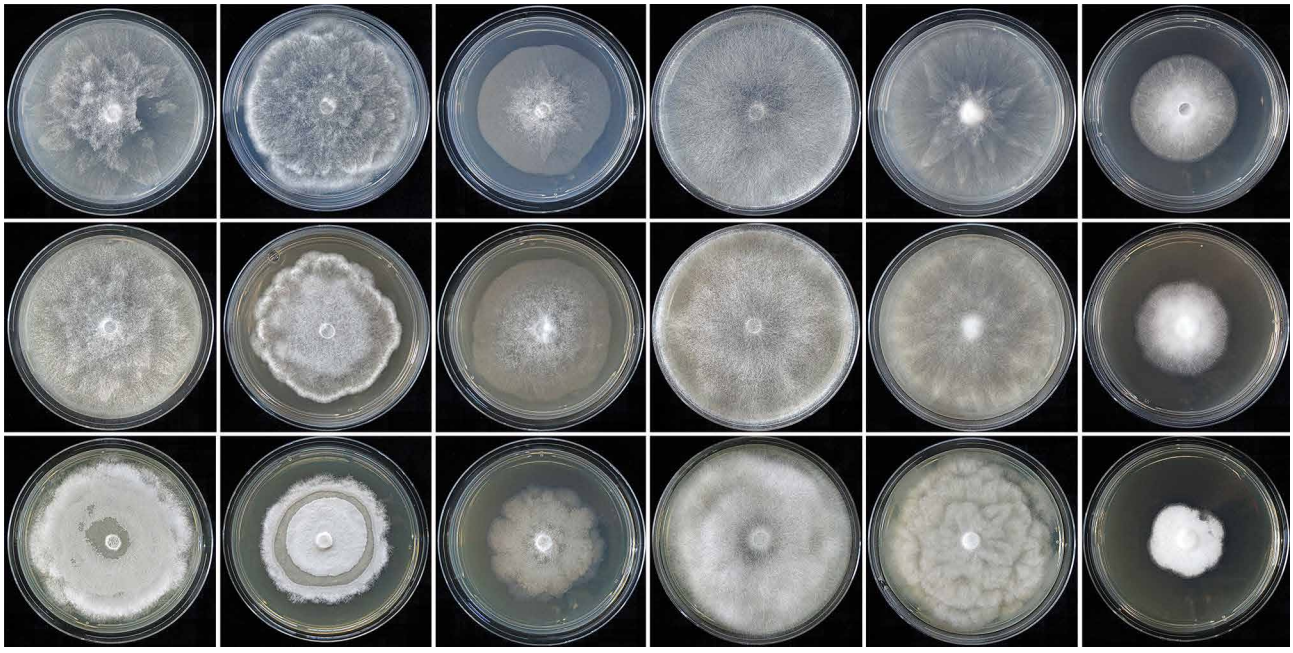

Fig. 14 Colony morphology of *Halophytophthora lateralis* (BD680), *H. lusitanica* (BD628), *H. macrosporangia* (BD642), *H. sinuata* (isolate BD656), *H. thermoambigua* (isolate BD637) and *H.* sp. thermoambigua-like (isolate BD652) (from left to right) after 7 d growth at 20 °C on sV8A, sCA and sPDA (from top to bottom).

DISCUSSION

To resolve the polyphyletic nature of the genus *Halophytophthora* (Lara & Belbahri 2011, Nigrelli & Thines 2013, Jung et al. 2017d) 10 previous *Halophytophthora* species were transferred to the genera *Calycofera*, *Phytopythium*, *Salisapilia* and *Salispina* (Hulvey et al. 2010, Thines 2014, Li et al. 2016, Bennett et al. 2017a, 2018, Bennet & Thines 2019). As a consequence of these reorganisations, seven described species, *H. avicennae*, *H. batemanensis*, *H. fluviatilis*, *H. insularis*, *H. polymorphica*, *H. souzae* and *H. vesicula* (Yang & Hong 2014, Jung et al. 2017d, Bennet & Thines 2019, Jesus et al. 2019) and the informally designated *Halophytophthora* sp. Zostera (Govers et al. 2016) and *Halophytophthora* sp. 1–4 (Nigrelli & Thines 2013, Man in 't Veld et al. 2019) remained in *Halophytophthora* s.str.

The oomycete survey performed with a single sampling date at seven sites in marine and brackish water of tidal ponds and channels in saltmarshes, lagoon ecosystems and two river estuaries distributed along an 80 km stretch of the Algarve coast in the South of Portugal unveiled an unprecedented bounty of 10 previously unknown *Halophytophthora* taxa plus *H. avicennae*, originally described from New South Wales and also reported from Brazil (Gerrettson-Cornell & Simpson 1984, Jesus et al. 2016), and six *Phytophthora* species. Based on differences in morphology and temperature-growth relations and a multigene phylogeny, eight new *Halophytophthora* species from Portugal are described here as *H. brevisporangia*, *H. celeris*, *H. frigida*, *H. lateralis*, *H. lusitanica*, *H. macrosporangia*, *H. sinuata* and *H. thermoambigua* thus doubling the number of described species in *Halophytophthora* s.str.

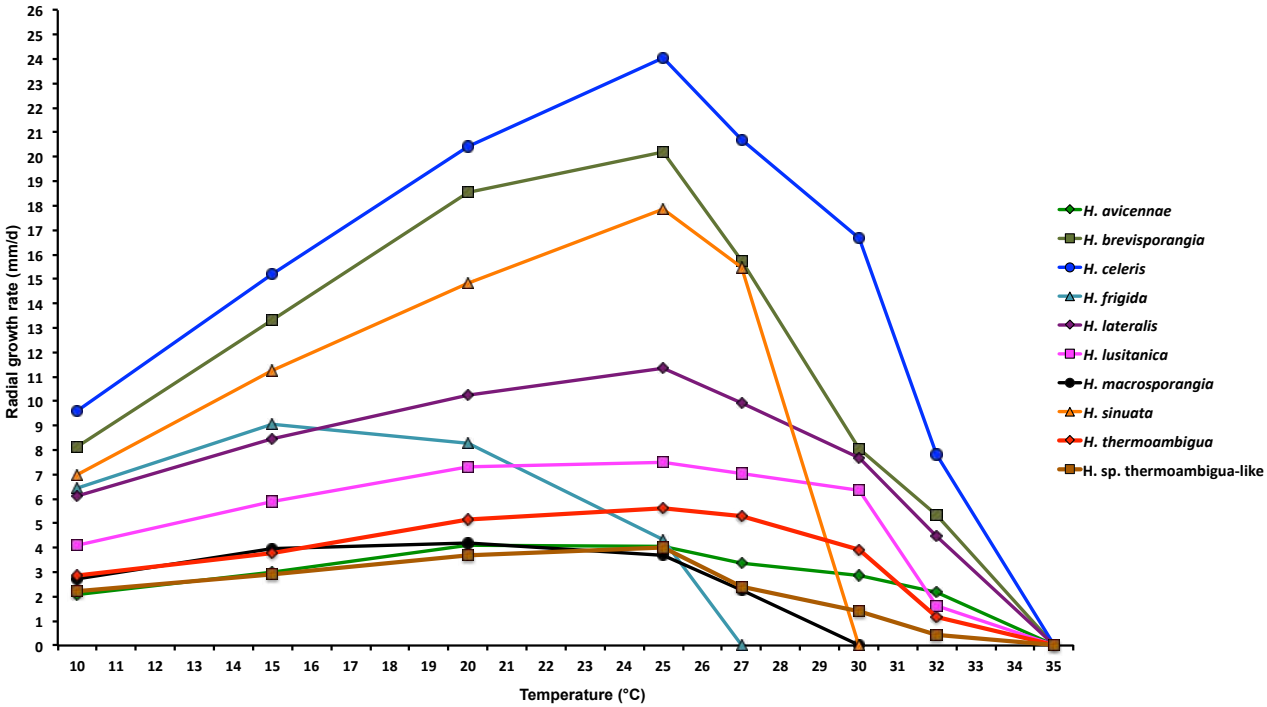

Fig. 15 Mean radial growth rates of *Halophytophthora avicennae* (three isolates), *H. brevisporangia* (three isolates), *H. celeris* (three isolates), *H. frigida* (five isolates), *H. lateralis* (four isolates), *H. lusitanica* (five isolates), *H. macrosporangia* (five isolates), *H. sinuata* (five isolates), *H. thermoambigua* (five isolates) and *H.* sp. thermoambigua-like (two isolates) on sV8A at different temperatures.

The phylogenetic analyses of separate LSU and ITS datasets, comprising all described *Halophytophthora* species, the 10 new *Halophytophthora* taxa from Portugal and all relevant and distinctive sequences available from GenBank, provided for the first time a comprehensive phylogeny of the genus *Halophytophthora* s.str. with a structure of ten clades which are designated as Clades 1–10. Except of *Halophytophthora* sp. Portugal_9 which constituted Clade 10, all new *Halophytophthora* taxa from the Algarve coast resided in Clade 6 together with *H. polymorphica* and *H. vesicula*. In the phylogenetic analyses of a concatenated nine-loci (ITS, LSU, *Btub*, *hsp90*, *rpl10*, *tigA*, *cox1*, *nadh1*, *rps10*) dataset *H. brevisporangia*, *H. celeris*, *H. frigida*, *H. lateralis*, *H. lusitanica*, *H. macrosporangia*, *H. polymorphica*, *H. sinuata*, *H. thermoambigua* and *H.* sp. thermoambigua-like formed two distinct strongly supported sub-clades 6a and 6b. In the LSU analysis *Halophytophthora* s.str. clustered in sister position to *Phytophthora* with *Nothophytophthora* residing in a basal position to this cluster. In contrast, a recent phylogenetic analysis of a comprehensive three-loci (LSU, ITS, *cox1*) dataset placed *Halophytophthora* s.str. in a basal position to the sister genera *Nothophytophthora* and *Phytophthora* reflecting better the closer similarities in morphology, lifestyles and habitats between *Phytophthora* and *Nothophytophthora* as compared to *Halophytophthora* (Jung et al. 2017d). '*Halophytophthora*' *exoprolifera* belongs to an undescribed genus basal to the *Halophytophthora-Nothophytophthora-Phytophthora* cluster supporting a previous phylogeny (Jung et al. 2017d). For the cryptic species *H. porrigovesica* only a 18S ribosomal RNA gene sequence (GU994168) and an ITS sequence (GU258844) of isolate P15166 from Thailand could be retrieved from GenBank and an *rps10* sequence of the Japanese ex-type isolate CBS 125230 from http://oomycetedb.cgrb.oregonstate.edu (Foster et al. 2021). BLAST® searches for these three sequences showed that all closest hits belong to *Phytophthora*. ML and BI analyses using a 1 373 characters dataset including 69 ITS sequences of *H. porrigovesica* and representative species from all phylogenetic clades of *Halophytophthora* and *Phytophthora*, and other genera in the *Peronosporaceae*, *Pythiaceae* and *Salisapiliaceae* demonstrated that *H. porrigovesica* belongs to *Phytophthora* Clade 9 (see Appendix; alignment and trees deposited at Dryad: https://doi.org/10.5061/dryad.gf1vhhmr2). Besides many freshwater and a few terrestrial species *Phytophthora* Clade 9 also includes several species from marine and brackish-water habitats, i.e., *P. estuarina* and *P. rhizophorae* (Li et al. 2016). Many ITS and LSU sequences retrieved from GenBank for isolates from marine and brackish-water ecosystems along the coasts of North America, Brazil, the Philippines and the North Sea could not be assigned to any of the known *Halophytophthora* species or the new *Halophytophthora* species from Portugal. Most likely, these isolates constitute multiple undescribed species in *Halophytophthora* Clades 1, 2, 6, 8 and 9.

Halophytophthora diversity at the individual marine sites in Portugal was high, ranging from two species in the brackish water upstream of the Ribeira de Odelouca estuary to seven species in the saltmarsh at Santa Luzia. With the two known species *H. avicennae* and *H. polymorphica*, the two new species *H. insularis* and *H. souzae*, and another unknown species, erroneously identified as *H. vesicula*, *Halophytophthora* diversity in tropical mangrove ecosystems along the Perequê river in Brazil was nearly as high as in Portugal (Jesus et al. 2016, 2019). In contrast, oomycete surveys in brackish and marine water ecosystems in British Columbia, the South-eastern USA and the Caribbean, New South Wales, Singapore, the Philippines and Japan showed lower diversity of *Halophytophthora* s.str. than in Portugal and Brazil (Fell & Master 1975, Nakagiri et al. 1994, 2001, Tan & Pek 1997, Nakagiri 2000, Hulvey et al. 2010, Bennett et al. 2018, Bennett & Thines 2019, 2020). However, differences between the various surveys might have been strongly biased by the use of different isolation and sampling methods. For instance, in the North Sea in total three *Halophytophthora* taxa, all of them unknown to science, were obtained during various oomycete surveys (Nigrelli & Thines 2013, Govers et al. 2016, Man in 't Veld et al. 2019). However, these surveys were focussed on direct isolations from necrotic *Z. marina* seeds and leaves and *in situ* baiting tests would most likely obtain a wider range of *Halophytophthora* species from the North Sea. Interestingly, in the south-eastern USA, the

Caribbean, Southeast Asia and Japan the genera *Salisapilia* and *Salispina* seem to be more common than *Halophytophthora* s.str. (Fell & Master 1975, Nakagiri et al. 1994, 2001, Tan & Pek 1997, Nakagiri 2000, Hulvey et al. 2010, Bennett et al. 2018, Bennett & Thines 2019, 2020). In contrast, *Salisapilia* or *Salispina* species could not be isolated from any of the seven sites sampled in this study in Portugal or from the mangrove sites along the Perequê river in Brazil (Jesus et al. 2016, 2019). Also in Chesapeake Bay in Maryland and the North Sea *Salisapilia* species seem to be rare and there is only one record of *S. sapolensis* from a *Zostera* leaf at the German island of Sylt (Man in 't Veld et al. 2019).

Three of the eight new *Halophytophthora* species, *H. frigida*, *H. macrosporangia* and *H. sinuata*, have a homothallic breeding system with exclusively paragynous antheridia like *H. fluviatilis*, *H. souzae* and *H. vesicula* (Anastasiou & Churchland 1969, Yang & Hong 2014, Jesus et al. 2019). Since an amphigynous antheridial insertion, as observed in many *Phytophthora* species and in *Nothophytophthora amphigynosa* (Erwin & Ribeiro 1996, Jung et al. 2017a, c) has never been observed in any known species of the genera *Halophytophthora* and *Phytopythium* (De Cock et al. 2015) this morphological character most likely evolved for the first time in the common ancestor of *Phytophthora* and *Nothophytophthora*, *Protophytophthora* (Jung et al. 2017d). Homothallic species are mainly inbreeding rather than outcrossing (Erwin & Ribeiro 1996, Brasier et al. 2003, Jung et al. 2011). Consequently, the main evolutionary role of the oospores in *H. frigida*, *H. macrosporangia* and *H. sinuata* is most likely the survival of unsuitable environmental conditions rather than the creation of genetic diversity. Intriguingly, these three homothallic species have comparably low maximum temperatures for growth (25 – < 30 °C) and, hence, cannot spread and grow when shallow tidal ponds heat up in the sun during low tide. Therefore, they most likely survive low tides via oospores formed in plant debris or in infected living plant tissues, either submerged or temporarily exposed to the air and drying. In contrast, due to their relatively high maximum temperatures for growth (32 – < 35 °C) the five sterile new *Halophytophthora* species, *H. brevisporangia*, *H. celeris*, *H. lateralis*, *H. lusitanica* and *H. thermoambigua*, are better adapted to remain active in shallow warm tidal ponds and channels during low tides. The combination of high cardinal temperatures and a sterile or silent breeding system, enabling allocation of most resources to continuous asexual reproduction and spread via zoospores, is a typical feature of primarily aquatic *Phytophthora* species and considered as an adaptation to a mainly saprotrophic lifestyle as litter decomposers and opportunistic pathogens of riparian vegetation (Brasier et al. 2003, Jung et al. 2011).

In general, *Halophytophthora* species, like species from the related genera *Salisapilia*, *Salispina*, *Phytopythium* and *Calycofera*, play a key role as decomposers of plant litter in tropical and subtropical mangrove ecosystems and saltmarshes (Fell & Master 1975, Pegg & Alcorn 1982, Gerrettson-Cornell & Simpson 1984, Newell et al. 1987, Ho & Jong 1990, Ho et al. 1991, 1992, Newell & Fell 1992, 1995, Nakagiri et al. 1994, 2001, Raghukumar et al. 1995, Tan & Pek 1997, Leaño et al. 1998, 2000, Marano et al. 2016, Jesus et al. 2016, 2019, Bennett et al. 2017a, b, Bennett & Thines 2020, Su et al. 2020). Accordingly, also the eight new *Halophytophthora* species and *H. avicennae* most likely have, at least partially, a saprophytic lifestyle in the coastal ecosystems in Portugal. However, marine oomycetes are also known as serious plant pathogens. Species from early diverging oomycete genera, including *Anisolpidium* (*Anisolpidiaceae*, *Anisolpidiales*), *Eurychasma* (*Eurychasmales*, previously *Saprolegniales*), *Olpidiopsis* (*Olpidiopsidaceae*, *Olpidiopsidales*), *Ectrogella* s.lat. (*Olpidiopsidales* or *Anisolpidiales*), *Pontisma* (*Pontismataceae*, *Lagenidiales*) and *Sirolpidium* (*Sirolpidiacae*, *Lagenidiales*), are common pathogens of a wide range of algal groups (Sparrow 1960, West et al. 2006, Gachon et al. 2009, 2017, Badis et al. 2019, Buaya et al. 2019, 2021, Garvetto et al. 2020). Marine *Halophytophthora* and *Phytophthora* species are occasionally found associated with diseases of higher plants, and the low number of such reports most likely reflects the scarcity of marine phytopathological studies rather than the true importance of these genera as plant pathogens. In severely declining mangrove stands of Queensland an unidentified *Halophytophthora* species resembling *H. vesicula* was causing stem cankers and root rot of *Avivennia marina* trees (Pegg et al. 1980). In the early 1930s, a large-scale loss of up to 90 % of the marine foundation species *Z. marina* on both sides of the North Atlantic was attributed to the so-called 'wasting disease' associated with *Labyrinthula zosterae* (*Labyrinthulomycetes*, *Straminipila*). Later studies, however, have casted doubt on the primary role of *Labyrinthula* in the decline of eelgrass (Vergeer & Den Hartog 1994, Brakel et al. 2014, Martin et al. 2016). Recent isolations of *Phytophthora* and *Halophytophthora* species from necrotic seeds and leaves of declining eelgrass in the North Sea and at Chesapeake Bay on the US Atlantic coast raised the question whether *Phytophthora* and *Halophytophthora* species are involved as causal agents in the global seagrass decline (Man in 't Veld et al. 2011, 2019, Govers et al. 2016). Both *Halophytophthora* sp. Zostera, which is most likely identical to *H. lateralis*, and *P. gemini* were isolated from almost all *Z. marina* seeds collected at the island Sylt in the North Sea, and severely reduced seed germination rate in a pathogenicity trial (Govers et al. 2016). Interestingly, three of the eight new *Halophytophthora* species from Portugal, *H. lusitanica*, *H. lateralis* and *H. thermoambigua*, were recently isolated from necrotic *Z. marina* leaves at the Atlantic coast of Norway (T. Jung, I. Milenković, T. Corcobado & V. Talgø, unpubl. data). The potential involvement of these and other *Halophytophthora* and *Phytophthora* species in eelgrass decline is currently being investigated in Norway and Portugal. In the Netherlands, *P. inundata* was recently isolated from leaves of the halophytic *Aster tripolium* and *Salicornia europaea* (Man in 't Veld et al. 2019). In the three saltmarshes sampled in Parque Natural da Ria Formosa in Portugal during the present study, scattered and patch mortality of halophytic plants, including *Salicornia* and *Sarcocornia* spp., has been observed. It remains unclear whether this mortality was caused by the harsh environmental conditions, characterised by periodical flooding and drying out and continuous, often strong winds, or by pathogen infections which might have been triggered by environmental stress. To clarify the potential involvement of the eight new *Halophytophthora* species in eelgrass decline and the mortality of halophytic saltmarsh plants in Portugal their pathogenicity to *Z. marina*, *Salicornia ramomissima* and *Sarcocornia* spp. is currently being tested. In addition, leaf litter decomposition trials with the seagrasses *Cymodocea nodosa* and *Z. marina* (Santschi et al. 2017, Aram & Rizzo 2019) are underway to get first insights into the ecological role and lifestyle of all new *Halophytophthora* species in the marine and brackish-water ecosystems along the Algarve coast.

The co-occurrence of 10 *Halophytophthora* taxa in these ecosystems raises the question whether some of them had been introduced from overseas, e.g., with water, sediments, and biofilm discharged from big ships' ballast water tanks which were demonstrated to contain high concentrations of bacteria and viruses (Ruiz et al. 2000a, b, Drake et al. 2007) and most likely also provide suitable habitats for the transport of oomycetes. More oomycete surveys in yet under-surveyed regions of the world and population genetic or phylogenomic analyses of global populations are needed to unveil the true diversity of oomycetes in marine ecosystems and clarify the origin of these

Halophytophthora species as has been done recently for the widespread plant pathogens *P. cinnamomi* and *P. ramorum* (Jung et al. 2021, Shakya et al. 2021).

Acknowledgements The authors are grateful to the Portuguese Science and Technology Foundation (FCT) for co-financing with Portuguese national funds the European BiodivERsA project 'RESIPATH: Responses of European Forests and Society to Invasive Pathogens' (BIODIVERSA/0002/2012), and to the Czech Ministry for Education, Youth and Sports and the European Regional Development Fund for financing the Project 'Phytophthora Research Centre' (Reg. No. CZ.02.1.01/0.0/0.0/15_003/0000453). Cristiana Maia acknowledges FCT and the European Social Fund (FSE) for her Ph.D. grant (SFRH/BD/136277/2018). We also thank the Institute for the Conservation of Nature and Forestry (ICNF) for logistic support during the fieldwork in Portugal. DNA sequencing was partly supported by the Italian Ministry of Education, University and Research (MIUR) funded project 'Metagenomic strategies to assess genetic diversity in soil-borne *Phytophthora* species'. Aneta Bačová, Henrieta Ďatková and Milica Raco (all Mendel University in Brno) are acknowledged for technical support.

Declaration on conflict of interest The authors declare that there is no conflict of interest.

REFERENCES

Anastasiou CJ, Churchland LM. 1969. Fungi on decaying leaves in marine habitats. Canadian Journal of Botany 47: 251–257.

Aram K, Rizzo DM. 2019. Phytophthora ramorum and Phytophthora gonapodyides differently colonize and contribute to the decomposition of green and senesced Umbellularia californica leaves in a simulated stream environment. Forests 10: 434.

Badis Y, Klochkova TA, Strittmatter M, et al. 2019. Novel species of the oomycete Olpidiopsis potentially threaten European red algal cultivation. Journal of Applied Phycology 31: 1239–1250.

Bennett RM, Cock AWAM, Lévesque A, et al. 2017a. Calycofera gen. nov., an estuarine sister taxon to Phytopythium, Peronosporaceae. Mycological Progress 16: 947–954.

Bennett RM, Devanadera MK, Dedeles GR, et al. 2018. A revision of Salispina, its placement in a new family, Salispinaceae (Rhipidiales), and description of a fourth species, S. hoi sp. nov. IMA Fungus 9: 259–269.

Bennett RM, Nam B, Dedeles GR, et al. 2017b. Phytopythium leanoi sp. nov. and Phytopythium dogmae sp. nov., Phytopythium species associated with mangrove leaf litter from the Philippines. Acta Mycologia 52: 1103.

Bennett RM, Thines M. 2019. Revisiting Salisapiliaceae. Fungal Systematics and Evolution 3: 171–184.

Bennett RM, Thines M. 2020. An overview on Philippine estuarine oomycetes. Philippine Journal of Systematic Biology 14: 1–14.

Blair JE, Coffey MD, Park S-Y, et al. 2008. A multi-locus phylogeny for Phytophthora utilizing markers derived from complete genome sequences. Fungal Genetics and Biology 45: 266–277.

Botella L, Janoušek J, Maia, C, et al. 2020. Marine oomycetes of the genus Halophytophthora harbor viruses related to Bunyaviruses. Frontiers in Microbiology 11: 1467.

Botella L, Jung T. 2021. Multiple viral infections detected in Phytophthora condilina by total and small RNA sequencing. Viruses 13: 620.

Brakel J, Werner FJ, Tams V, et al. 2014. Current European Labyrinthula zosterae are not virulent and modulate seagrass (Zostera marina) defense gene expression. PLoS One 9: e92448.

Brasier CM, Cooke DEL, Duncan JM, et al. 2003. Multiple new phenotypic taxa from trees and riparian ecosystems in Phytophthora gonapodyides – P. megasperma ITS Clade 6, which tend to be high-temperature tolerant and either inbreeding or sterile. Mycological Research 107: 277–290.

Buaya AT, Ploch S, Inaba S, et al. 2019. Holocarpic oomycetes parasitoids of red algae are not Olpidiopsis. Fungal Systematics and Evolution 4: 21–31.

Buaya AT, Scholz B, Thines M. 2021. Sirolpidium bryopsidis, a parasite of green algae, is probably conspecific with Pontisma lagenidioides, a parasite of red algae. Fungal Systematics and Evolution 7: 223–231.

Caballol M, Štraus D, Macia H, et al. 2021. Halophytophthora fluviatilis pathogenicity and distribution along a Mediterranean-subalpine gradient. Journal of Fungi 7: 112.

Cooke DEL, Drenth A, Duncan JM, et al. 2000. A molecular phylogeny of Phytophthora and related oomycetes. Fungal Genetics and Biology 30: 17–32.

De Cock AWAM, Lodhi AM, Rintoul TL, et al. 2015. Phytopythium: molecular phylogeny and systematics. Persoonia 34: 25–39.

Dick MW. 1990. Keys to Pythium. University of Reading Press, Reading, UK.

Drake LA, Doblin MA, Dobbs FC. 2007. Potential microbial bioinvasions via ships' ballast water, sediment, and biofilm. Marine Pollution Bulletin 55: 333–341.

Edler D, Klein J, Antonelli A, et al. 2021. raxmlGUI 2.0: A graphical interface and toolkit for phylogenetic analyses using RAxML. Methods in Ecology and Evolution 12: 373–377.

Erwin DC, Ribeiro OK. 1996. Phytophthora diseases worldwide. APS Press, St. Paul, Minnesota.

Fell JW, Master IM. 1975. Phycomycetes (Phytophthora spp. nov. and Pythium sp. nov.) associated with mangrove (Rhizophora mangle) leaves. Canadian Journal of Botany 53: 2908–2922.

Foster ZSL, Albornoz FE, Fieland VJ, et al. 2021. A new oomycete metabarcoding method using the rps10 gene. bioRxiv: 2021.09.22.460084.

Gachon CMM, Strittmatter M, Badis Y, et al. 2017. Pathogens of brown algae: culture studies of Anisolpidium ectocarpii and A. rosenvingei reveal that the Anisolpidiales are uniflagellated oomycetes. European Journal of Phycology 52: 133–148.

Gachon CMM, Strittmatter M, Müller DG, et al. 2009. Detection of differential host susceptibility to the marine oomycete pathogen Eurychasma dicksonii by real-time PCR: not all algae are equal. Applied and Environmental Microbiology 75: 322–328.

Garbelotto MM, Lee HK, Slaughter G, et al. 1997. Heterokaryosis is not required for virulence of Heterobasidion annosum. Mycologia 89: 92–102.

Garvetto A, Perrineau M-M, Dressler-Allame M, et al. 2020. 'Ectrogella' parasitoids of the diatom Licmophora sp. are polyphyletic. Journal of Eukaryotic Microbiology 67: 18–27.

Gerrettson-Cornell L, Simpson J. 1984. Three new marine Phytophthora species from New South Wales. Mycotaxon 19: 453–470.

Govers LL, Man in ´t Veld WA, Meffert JP, et al. 2016. Marine Phytophthora species can hamper conservation and restoration of vegetated coastal ecosystems. Proceedings of the Royal Society B: Biological Sciences 283: 20160812.

Ho HH, Chang HS, Hsieh SY. 1991. Halophytophthora kandeliae, a new marine fungus from Taiwan. Mycologia 83: 419–424.

Ho HH, Chang HS, Huang SH. 2003. Halophytophthora elongata, a new marine species from Taiwan. Mycotaxon 85: 417–422.

Ho HH, Jong SC. 1990. Halophytophthora, gen. nov., a new member of the family Pythiaceae. Mycotaxon 36: 377–382.

Ho HH, Nakagiri A, Newell SY. 1992. A new species of Halophytophthora from Atlantic and Pacific subtropical islands. Mycologia 84: 548–554.

Hopple JS, Vilgalys R. 1994. Phylogenetic relationships among coprinoid taxa and allies based on data from restriction site mapping of nuclear rDNA. Mycologia 86: 96–107.

Hüberli D, Hardy GEStJ, White D, et al. 2013. Fishing for Phytophthora from Western Australia's waterways: A distribution and diversity survey. Australasian Plant Pathology 42: 251–260.

Hulvey J, Telle S, Nigrelli L, et al. 2010. Salisapiliaceae – a new family of oomycetes from marsh grass litter of southeastern North America. Persoonia 25: 109–116.

Jesus AL, Marano AV, Gonçalves DR, et al. 2019. Two new species of Halophytophthora from Brazil. Mycological Progress 18: 1411–1421.

Jesus AL, Marano AV, Jerônimo GH, et al. 2016. The genus Halophytophthora (Peronosporales, Straminipila) in Brazil: first descriptions of species. Brazilian Journal of Botany 39: 729–739.

Jung T, Blaschke H, Neumann P. 1996. Isolation, identification and pathogenicity of Phytophthora species from declining oak stands. European Journal of Forest Pathology 26: 253–272.

Jung T, Burgess TI. 2009. Re-evaluation of Phytophthora citricola isolates from multiple woody hosts in Europe and North America reveals a new species, Phytophthora plurivora sp. nov. Persoonia 22: 95–110.

Jung T, Chang TT, Bakonyi J, et al. 2017a. Diversity of Phytophthora species in natural ecosystems of Taiwan and association with disease symptoms. Plant Pathology 66: 194–211.

Jung T, Cooke DEL, Blaschke H, et al. 1999. Phytophthora quercina sp. nov., causing root rot of European oaks. Mycological Research 103: 785–798.

Jung T, Horta Jung M, Cacciola SO, et al. 2017b. Multiple new cryptic pathogenic Phytophthora species from Fagaceae forests in Austria, Italy and Portugal. IMA Fungus 8: 219–244.

Jung T, Horta Jung M, Scanu B, et al. 2017c. Six new Phytophthora species from ITS Clade 7a including two sexually functional heterothallic hybrid species detected in natural ecosystems in Taiwan. Persoonia 38: 100–135.

Jung T, Horta Jung M, Webber JF, et al. 2021. The destructive tree pathogen Phytophthora ramorum originates from the Laurosilva forests of East Asia. Journal of Fungi 7: 226.

Jung T, Pérez-Sierra A, Durán A, et al. 2018. Canker and decline diseases caused by soil- and airborne Phytophthora species in forests and woodlands. Persoonia 40: 182–220.

Jung T, Scanu B, Bakonyi J, et al. 2017d. Nothophytophthora gen. nov., a new sister genus of Phytophthora from natural and semi-natural ecosystems. Persoonia 39: 143–174.
Jung T, Stukely MJC, Hardy GEStJ, et al. 2011. Multiple new Phytophthora species from ITS Clade 6 associated with natural ecosystems in Australia: evolutionary and ecological implications. Persoonia 26: 13–39.
Katoh K, Standley DM. 2013. MAFFT multiple sequence alignment software version 7: Improvements in performance and usability. Molecular Biology and Evolution 30: 772–780.
Kroon LPNM, Bakker FT, Van den Bosch GBM, et al. 2004. Phylogenetic analysis of Phytophthora species based on mitochondrial and nuclear DNA sequences. Fungal Genetics and Biology 41: 766–782.
Kumar S, Stecher G, Li M, et al. 2018. MEGA X: Molecular evolutionary genetics analysis across computing platforms. Molecular Biology and Evolution 35: 1547–1549.
Lamour K (ed). 2013. Phytophthora: A global perspective. CABI, Wallingford, UK.
Lamour KH, Finley L. 2006. A strategy for recovering high quality genomic DNA from a large number of Phytophthora isolates. Mycologia 98: 514–517.
Lara E, Belbahri L. 2011. SSU rRNA reveals major trends in oomycete evolution. Fungal Diversity 49: 93–100.
Leaño EM, Jones EBG, Vrijmoed LLP. 2000. Why are Halophytophthora species well adapted to mangrove habitats? In: Hyde KD, Ho WH, Pointing SB (eds), Aquatic mycology across the Millennium. Fungal Diversity 5: 131–151.
Leaño EM, Vrijmoed LLP, Jones ERG. 1998. Physiological studies on Halophytophthora vesicula (straminipilous fungi) isolated from fallen mangrove leaves from Mai Po, Hong Kong. Botanica Marina 41: 411–419.
Li GJ, Hyde KD, Zhao RL, et al. 2016. Fungal diversity notes 253–366: taxonomic and phylogenetic contributions to fungal taxa. Fungal Diversity 78: 1–237.
Man in 't Veld WA, Rosendahl KC, Brouwer H, et al. 2011. Phytophthora gemini sp. nov., a new species isolated from the halophilic plant Zostera marina in the Netherlands. Fungal Biology 115: 724–732.
Man in 't Veld WA, Rosendahl KCHM, Van Rijswick PCJ, et al. 2019. Multiple Halophytophthora spp. and Phytophthora spp. including P. gemini, P. inundata and P. chesapeakensis sp. nov. isolated from the seagrass Zostera marina in the Northern hemisphere. European Journal of Plant Pathology 153: 341–357.
Marano AV, Jesus AL, De Souza JI, et al. 2016. Ecological roles of saprotrophic Peronosporales (Oomycetes, Straminipila) in natural environments. Fungal Ecology 19: 77–88.
Martin DL, Chiari Y, Boone E, et al. 2016. Functional, phylogenetic and host-geographic signatures of Labyrinthula spp. provide for putative species delimitation and a global-scale view of seagrass wasting disease. Estuaries and Coasts 39: 1403–1421.
Martin FN, Tooley PW. 2003. Phylogenetic relationships among Phytophthora species inferred from sequence analysis of mitochondrially encoded cytochrome oxidase I and II genes. Mycologia 95: 269–284.
Muehlstein LK, Porter D, Short FT. 1988. Labyrinthula sp., a marine slime mold producing symptoms of wasting disease in eelgrass, Zostera marina. Marine Biology 99: 465–472.
Nakagiri A. 2000. Ecology and biodiversity of Halophytophthora species. In: Hyde KD, Ho WH, Pointing SB (eds), Aquatic mycology across the Millennium. Fungal Diversity 5: 153–164.
Nakagiri A, Ito T, Manoch L, et al. 2001. A new Halophytophthora species, H. porrigovesica, from subtropical and tropical mangroves. Mycoscience 42: 33–41.
Nakagiri A, Newell SY, Ito T. 1994. Two new Halophytophthora species, H. tartarea and H. masteri, from intertidal decomposing leaves in saltmarsh and mangrove regions. Mycoscience 35: 223–232.
Newell SY, Fell JW. 1992. Distribution and experimental responses to substrate of marine oomycetes (Halophytophthora spp.) in mangrove ecosystems. Mycological Research 96: 851–856.
Newell SY, Fell JW. 1995. Do halophytophthoras (marine Pythiaceae) rapidly occupy fallen leaves by intraleaf mycelial growth? Canadian Journal of Botany 73: 761–765.
Newell SY, Miller JD, Fell JW. 1987. Rapid and pervasive occupation of fallen mangrove leaves by a marine zoosporic fungus. Applied and Environmental Microbiology 53: 2464–2469.
Nigrelli L, Thines M. 2013. Tropical oomycetes in the German Bight – Climate warming or overlooked diversity? Fungal Ecology 6: 152–160.
Pegg KG, Alcorn JL. 1982. Phytophthora operculata sp. nov., a new marine fungus. Mycotaxon 16: 99–102.
Pegg KG, Gillespie NC, Forsberg LI. 1980. Phytophthora sp. associated with mangrove death in Central Coastal Queensland. Australasian Plant Pathology 9: 6–7.
Raghukumar S, Sathe-Pathak V, Sharma S, et al. 1995. Thraustochytrid and fungal component of marine detritus. 111. Field studies on decomposition of leaves of the mangrove Rhizophora apiculata. Aquatic Microbial Ecology 9: 117–125.
Rahman MZ, Uematsu S, Coffey MD, et al. 2014. Re-evaluation of Japanese Phytophthora isolates based on molecular phylogenetic analyses. Mycoscience 55: 314–327.
Reeser PW, Sutton W, Hansen EM, et al. 2011. Phytophthora species in forest streams in Oregon and Alaska. Mycologia 103: 22–35.
Robideau GP, De Cock AW, Coffey MD, et al. 2011. DNA barcoding of oomycetes with cytochrome c oxidase subunit I and internal transcribed spacer. Molecular Ecology Resources 11: 1002–1011
Ronquist F, Huelsenbeck JP. 2003. MrBayes 3: Bayesian phylogenetic inference under mixed models. Bioinformatics 19: 1572–1574.
Ruiz GM, Fofonoff PW, Carlton JT, et al. 2000b. Invasion of coastal marine communities in North America: Apparent patterns, processes, and biases. Annual Review of Ecology and Systematics 31: 481–531.
Ruiz GM, Rawlings TK, Dobbs FC, et al. 2000a. Global spread of microorganisms by ships. Nature 408: 49–50.
Santschi F, Gounand I, Harvey E, et al. 2017. Leaf litter diversity and structure of microbial decomposer communities modulate litter decomposition in aquatic systems. Functional Ecology 32: 522–532.
Shakya SK, Grünwald NJ, Fieland VJ, et al. 2021. Phylogeography of the wide-host range panglobal plant pathogen Phytophthora cinnamomi. Molecular Ecology 30: 5164–5178.
Sparrow FK. 1960. Aquatic Phycomycetes. The University of Michigan Press, Ann Arbor, USA.
Stöver BC, Müller KF. 2010. TreeGraph 2: Combining and visualizing evidence from different phylogenetic analyses. BMC Bioinformatics 11: 7.
Su CJ, Hsieh SY, Chiang MWL, et al. 2020. Salinity, pH and temperature growth ranges of Halophytophthora isolates suggest their physiological adaptations to mangrove environments. Mycology 11: 256–262.
Sullivan BK, Trevathan-Tackett SM, Neuhauser S, et al. 2018. Host-pathogen dynamics of seagrass diseases under future global change. Marine Pollution Bulletin 134: 75–88.
Tan TK, Pek CL. 1997. Tropical mangrove leaf litter fungi in Singapore with an emphasis on Halophytophthora. Mycological Research 101: 165–168.
Thines M. 2014. Phylogeny and evolution of plant pathogenic oomycetes – a global overview. European Journal of Plant Pathology 38: 431–447.
Vergeer LHT, Den Hartog C. 1994. Omnipresence of Labyrinthulaceae in seagrasses. Aquatic Botany 48: 1–20.
West JA, Klochkova TA, Kim GH, et al. 2006. Olpidiopsis sp., an oomycete from Madagascar that infects Bostrychia and other red algae: Host species susceptibility. Phycological Research 54: 72–85.
White TJ, Bruns T, Lee S, et al. 1990. Amplification and direct sequencing of fungal ribosomal RNA genes for phylogenetics. In: Gelfand DH, Sninsky JJ, Innes MA, et al. (eds), PCR protocols: a guide to methods and applications: 315–322. Academic Press, San Diego, California, USA.
Yang X, Hong C. 2014. Halophytophthora fluviatilis sp. nov. from freshwater in Virginia. FEMS Microbiology Letters 352: 230–237.

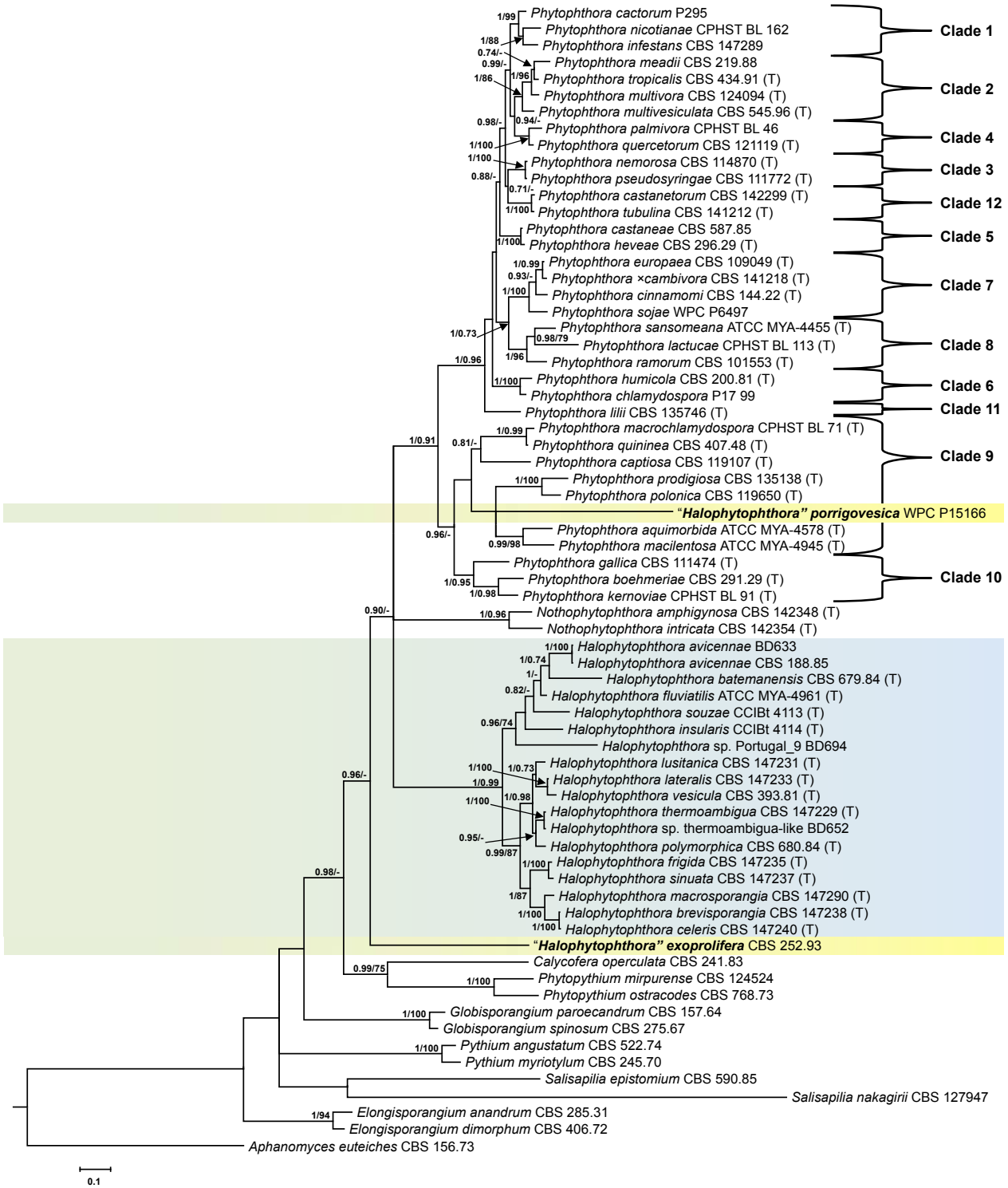

Appendix Fifty percent majority rule consensus phylogram derived from Bayesian inference analysis of an ITS dataset of '*Halophytophthora*' *porrigovesica* isolate WPC P15166 from Thailand, representative species from all phylogenetic Clades of *Phytophthora* and *Halophytophthora* s.str., and representative species from related genera in the *Peronosporaceae*, *Pythiaceae* and *Salisapiliaceae*. Bayesian posterior probabilities and ML bootstrap values (in %) are indicated but not shown below 0.70 and 70 %, respectively. *Aphanomyces euteiches* was used as outgroup taxon. Scale bar indicates 0.1 expected changes per site per branch.